

The impact of hydropower development on silt and clay loads in the Mekong Delta

F.A. Cornelje

The impact of hydropower development on silt and clay loads in the Mekong Delta

by

F.A. Cornielje

in partial fulfilment of the requirements for the degree of

Master of Science
Civil Engineering

at the Delft University of Technology,
to be defended publicly on Thursday December 20, 2023 at 01:00 PM.

Student number:	5407141
Thesis committee:	Dr. ir. A. Blom, Dr. ir. C.J. Sloff, Dr. T.A. Bogaard,
	TU Delft, chair TU Delft, supervisor TU Delft

Cover Image: ESA (2007)

An electronic version of this thesis is available at <http://repository.tudelft>

Preface

This thesis concludes my Master of Science in Water Management at Delft University of Technology. The subject has provided a great opportunity to discover my interests in the field of water.

I noticed during my BSc International Land and Water Management at Wageningen University and Research that I had a strong preference for large-scale water-related projects abroad. This has made the choice for the TU Delft logical.

For my thesis I chose a subject which required understanding and combining different aspects to turn a large-scale complicated problem into something tangible. I thoroughly enjoyed devising an approach and combining different kinds of data.

I would like to thank my graduation committee for their supervision and help during my graduation project. The chair of the committee, Astrid Blom, for not only advising me on the report structure and planning, but also for the motivational words when I was a bit unsure about the period after graduation. My daily supervisor Kees Sloff for always being full of passion and enthusiasm during our meetings, which made it easy for me to stay driven and inspired. Thom Bogaard for the sharp comments regarding the reliability and utility of data, which has given the research more depth.

Finally, I would like to thank my family for their unconditional support throughout my life and studies. You have always been my biggest supporters in every choice I made.

Floor Cornielje
Delft, December 20th 2023

Summary

The hydropower development in the Mekong Basin affects the silt and clay concentrations in the river which has ecological as well as socio-economic effects on the Mekong Delta and its inhabitants. Therefore, the first objective of this research was to obtain a better understanding of the effect of hydropower development on the silt and clay load in the Mekong Delta.

Subsequently, the objective was to determine possible sediment management strategies to mitigate the impacts on the silt and clay load in the Mekong Delta.

A conceptual model was developed and applied to analyse these impacts. By means of a sediment balance model with distributed sediment yield and individual trapping efficiencies of dams the annual sediment load has been determined.

This research has shown that the annual silt and clay load downstream has decreased from 140 Megaton \pm 40 [Mt] before hydropower development to 26 \pm 9 Mt in 2020. Including future hydropower dam projects, this could further decrease to 4-8 \pm 3-5 Mt in 2040. Approximately 4% of this sediment load will deposit in the Mekong Delta and therefore it is predicted that the clay and silt deposition will be close to zero in the future.

By 2040, approximately 75% of the total trapped sediment load is trapped in mainstream dams even though they account for 16% of the total dams. The majority (50%) will get trapped in Chinese dams that account for 9% of the total number of dams. This means that almost all sediment coming from China is trapped and will not reach the Mekong Delta. Around 80-85% of the future sediment load that will reach the delta has its source in the 3S region.

This reduction has implications for the sustainability of ecosystems and the productivity of the Mekong Delta. Clay and silt are nutrient rich alluvial sediments that support the ecosystems in the floodplains and delta. These nutrients are crucial for the soil fertility vital for rice cultivation and for various biological processes for fish. Today, nearly 80% of the 20 million people living in the Mekong Delta depend on the river system for their livelihood. However, the rice cultivation is expected to decrease significantly and by 2040, the loss of fisheries could cost close to \$23 billion.

Thus, the computed reduction displayed that sediment management strategies are inevitable to maintain the productivity of the Mekong Delta in the future. Therefore, two sediment management strategies were reviewed in this research: cancelling planned dams and reservoir sluicing. Reservoir sluicing is passing incoming sediment-laden water through the reservoir by discharging high flows to enable sediment to move past the dam without depositing.

The analysis of these two strategies showed that the maximum sediment load increase is 1-3 Mt as a result of cancelling planned dams and 2-3 Mt due to reservoir sluicing. This means a very small increase for the deposition in the Mekong Delta (4% deposits). Therefore, the sediment load increase was considered unsatisfactory, suggesting that these strategies are not providing the solution for the Mekong Basin.

The results indicate that effective sediment management strategies are urgently needed and that more research is needed into the effects of other strategies on the silt and clay load in the Mekong Delta.

Table of contents

Preface	iii
Summary.....	iv
1. Introduction.....	8
1.1 Context	8
1.2 Problem analysis.....	10
1.3 Research question	13
1.4 Methodology	13
1.5 Reading guide.....	13
2. Literature Review.....	14
2.1 Origin of clay and silt in the Mekong	14
2.1.1 Clay.....	14
2.1.2 Silt.....	16
2.2 Transport of silt and clay.....	17
2.3 Fine sediment deposition in the LMB region	18
2.4 Significance of clay and silt for the Mekong Delta.....	18
2.5 Trapping Efficiency model development.....	20
3. Conceptual model.....	21
3.1 Model purpose	21
3.2 Model design.....	21
3.2.1 Model assumptions.....	22
3.2.2 Model characteristics.....	22
3.2.3 Model input.....	23
3.2.4 Determining Trapping Efficiency.....	23
3.2.5 Sediment Load calculation.....	25
4. Results - Model Application to the Mekong Basin	26
4.1 Model characteristics	26
4.1.1 Model extent.....	26
4.1.2 Division into sub-basins	27
4.2 Model input	27
4.2.1 Expected future dams.....	27
4.2.2 Sub-basin discharge	27
4.2.3 Catchment area of dams	29
4.2.4 Active volume of dams	29

4.2.5 Sub-basin areas	29
4.2.6 Specific Sediment Yield.....	29
4.3 Determining Trapping Efficiency	30
4.3.1 Approach 1: TE calculation with Brune Model	30
4.3.2 Approach 2: Defined Trapping Efficiencies	30
4.4 Sediment Load calculation	30
4.4.1 Sediment load of sub-basins.....	30
4.4.2 Downstream Sediment load.....	31
4.5 Model verification.....	32
4.5.1 Data validation	32
4.5.2 Sensitivity analysis	34
4.6 Model result - Dam impact on silt and clay loads	39
4.6.1 Impact of Mekong Basin	39
4.6.2 Impact per sub-basin	40
4.6.3 Impact per country	44
5. Strategies for Sediment Load increase	46
5.1 Overview of different strategies	46
5.2.1 Strategy 1: Cancelling planned dams	47
5.2.2 Strategy 2: Reservoir sluicing	48
6. Results – Strategy application to the Mekong Basin.....	51
6.1 Results - Strategy 1: Cancelling planned dams.....	51
6.2 Results - Strategy 2: Reservoir sluicing.....	53
6.2.1 Brune Model	54
6.2.2 Defined TE Model	55
7. Discussion.....	57
7.1 Discussion - Dam impact on silt and clay loads.....	57
7.2 Discussion – Two strategies to mitigate the impact on silt and clay loads	58
7.2.1 Discussion strategy 1: Cancelling planned dams	58
7.2.2 Discussion strategy 2: Reservoir sluicing.....	58
8. Conclusion	60
9. Recommendations	62
Bibliography	63
Appendix A. Dam information	72
Appendix B. Sub-basin information.....	83
Appendix C. Extension of Results – Dam impact on silt and clay loads	84

Appendix D. Rainfall interpolation	90
Appendix E. Sensitivity analysis of models	93
Appendix F. Strategy analyses	106
Appendix G. Threshold of motion.....	132

1. Introduction

1.1 Context

With a total length of 4,800 km and a drainage area of 795,000 km², the Mekong is one of the world's greatest rivers (Van Zalinge et al., 2003). The river arises on the Tibetan Plateau in China as the Lancang River and flows via Myanmar to Lao PDR, from where it is called the Mekong. Here the Mekong enters the Lower Mekong Basin (LMB) and flows through Thailand, Cambodia and Vietnam, where it forms a large delta into the East Sea (Figure 1) (Orr et al., 2012).

The Upper Mekong Basin (UMB) in China and Myanmar is characterized by a high-altitude continental and temperate climate, whereas the climate in the LMB region is classified as tropical monsoonal (MRC, 2023a). Therefore, the LMB region has a dry and wet season resulting in high flow variability over the year. During the dry season from December to May, the discharge does not exceed 5000 m³/s, whereas the wet season discharge can reach up to 40,000 m³/s at Kratie (Figure 1) (MRC, 2005). Generally, 75% of the Mekong's annual discharge of 475 km³ flows through the delta during the wet season between July and October (Hecht et al., 2019; MRC, 2019).

The Mekong Delta is one of the world's largest deltas with an area of nearly 60,000 km² (Anthony et al., 2015) and is approximately 10,000 years old which means it is considered relatively young (Kondolf et al., 2018). Like any other delta, it forms as a result of downstream transportation of sediment that deposits when the river reaches the sea young (Li et al., 2017). These sediment depositions make it a very productive region within the Mekong River Basin (Kondolf et al., 2018).

Due to a long history of extensive alterations in the Mekong River Basin, the morphodynamics in the delta cannot be regarded as fully natural. Levees along the main channel were built centuries ago (around 1700), which were regularly overtapped and lower areas far from these channels were permanently submerged. Nowadays, these regions play an important environmental and hydrological role as they function as floodwater retention areas and natural water purification systems (MRC, 2005). Furthermore, these regions serve an economic purpose as the Mekong Delta is one of the world's largest rice production and most productive fishery regions (Kondolf et al., 2018; Manh et al., 2014).

The historical, agricultural and social development between 1890 and 1990 was dominated by draining vast areas in order to expand the rice cultivation. This has resulted in the delta currently being one of the world's largest rice production regions. Farmers in the delta can yield up to 5 tonnes per hectare (irrigated) compared to 3.9 tonnes in other Asia-Pacific regions (MRC, 2005). This high yield is a result of the huge floodplains and wetlands, high local flow variability (Manh et al., 2014) and the crucial role the Mekong has by delivering mineral and nutrient rich alluvial sediments during the monsoon season (MRC, 2005). Approximately 90% of the country's rice exports, worth 2.85 billion USD in 2015, and 55% of the country's rice production are attributed to this comparatively small region (Tan Yen et al., 2019).

Also, the Mekong Delta is responsible for approximately 18% of the global supply of freshwater fish, thereby establishing itself as the largest inland fishery in the world. Globally, the top four countries for freshwater fish consumption are Vietnam, Thailand, Lao PDR and Cambodia, where people eat between 24.5 and 34.5 kg of fish annually, which is more than triple the amount of the Dutch (Nederlands Visbureau, 2022). Therefore, the fish available in the Mekong River is crucial for ensuring food security in the area, especially as main protein source (Baran et al., 2015; Manh et al., 2014; Pukinskis, 2013).

Also, there is a big economic component as the annual economic value of the fish catch in the Mekong Delta is estimated to be between 2.2 and 3.9 billion USD (Baran et al., 2015). Today, nearly 80% of the 20 million people living in the delta depend on the river system for their livelihood (Orr et al., 2012).



Figure 1: Map of the Mekong Basin

1.2 Problem analysis

Damming has become the primary anthropogenic disruption to rivers globally in the last century as a result of the development of human society (Wang X. et al., 2022). These dams not only provide access to electricity which is fundamental for regional socio-economic development, it also expands irrigation possibilities which are important for food security (MRC, 2023c). Furthermore, it allows adapting to climate change by providing water management during floods and droughts (MRC, 2023c) and can be helpful for navigation (Wang X. et al., 2022).

The first hydroelectric dam in the Mekong Basin was taken into operation in 1965, but large scale hydropower development began when the Chinese *Manwan* hydroelectric dam was implemented in 1996 (Kondolf et al., 2018; Li et al., 2017). Since then, the hydropower industry has increased tremendously to 131 operational dams. The current hydropower capacity of 69,000 megawatt (MW) (Stimson, 2023) is already much higher than estimated maximum potential by ICEM (2010). However, due to the high hydropower generation potential and an approximated yearly increasing energy demand of 6-7%, more dams are planned for the coming decades on both the main river and its tributaries (MRC, 2023c; Orr et al., 2012; Stimson, 2023). According to MRC (2023c), the LMB region alone could financially benefit over \$160 billion by 2040 due to hydropower dams.

In the Mekong Basin, two different types of dams are built: *run-of-river* dams and *reservoir* dams (Figure 2) (Pukinskis, 2013). *Run-of-river* dams are structures that use a canal or penstock to direct water flow towards a turbine. They are characterized by little to no storage capacity, which means that these dams generate a constant flow of electricity (base load) and some operational flexibility for daily variations. *Reservoir* dams are large systems that store water in a reservoir, generating electricity by releasing water. These dams offer, just like run-of-river dams, a base load, but depending on the demands of the river system these dams have the flexibility to respond to a water peak load (IHA, 2022).

The benefits of hydropower also come with downsides.

The construction of dams changes the water and sediment conditions in the river (Tang et al., 2023). It alters physical parameters such as water level, water flux and flow velocity which impacts ecosystems in the downstream regions and wetlands (Wang X. et al., 2022).

Dam construction levels out flood variation and alters downstream flow causing modifications to the hydrological conditions of river estuaries (Wang X. et al., 2022).

Hydropower development is expected to change the hydrology of the Mekong River by reducing and delaying wet season flows and increasing dry season flows (Hecht et al., 2019). If all planned dams are constructed, dry season flows at Kratie (Figure 1) are expected to increase by 25–160% and flood peaks are expected to decrease by 5–24% (Kondolf et al., 2018).

Dampening of floods and increasing low flows is a severe change in hydrological regime that has effect on the environmental flows (eFlows) in the river (Hoque et al., 2022). According to the Brisbane Declaration (2007), “environmental flows are the quantity, timing, duration, frequency and quality of flows required to sustain freshwater, estuarine, and near shore ecosystems and the human livelihoods and well-being that depend on them”. The ecological function and species diversity of near shore ecosystems are both highly dependent on the eFlows. However, due to hydropower dams the quantity and timing of both the dry and wet season flows are expected to change (Hecht et al., 2019; Hoque et al., 2022).

The absence of floodwater may affect soil fertility and soil quality, whereas an increase in low flows may decrease the possibility of salt water intrusion in the delta (Mezger et al., 2021). The latter may seem favourable, but salt water intrusion is highly important for multiple estuary ecosystems. These degradations affect floodplain agriculture and fisheries which are important sources of community livelihood (Hoque et al., 2022).

Furthermore, hydropower development is altering the sediment transport in a river (Manh et al., 2014). When a river's flow velocity decreases upstream of a dam, the system changes from a natural 'river' to an artificial 'lake', which causes the sediment transported from upstream to deposit in the reservoir by gravitational force (McCully, 1996; Wang X. et al., 2022). The percentage of trapped sediment is called the trapping efficiency and depends on multiple factors varying from the capacity of the dam to the size of the sediment (Kondolf et al., 2013; Kummu et al., 2010). Due to longer residence times in *reservoir* dams, more sediment tends to settle in these types of dams compared to *run-of-river* dams (Binh et al., 2019; Pukinskis, 2013). This sediment trapping does not only affect dam operation by decreasing the storage capacity and damaging mechanical components (Hydro, 2017), it also creates a variety of negative environmental impacts (Anthony et al., 2015). The vast majority of the total sediment load in the Mekong is transported as suspended load, which comprises mostly of both clay and silt (Anthony et al., 2015; Walling, 2009). These are nutrient rich alluvial sediments that support the ecosystems in the floodplains, delta and fisheries. By 2040, the loss of fisheries could cost close to \$23 billion, whereas mangrove, wetland, and forest loss could cost up to \$145 billion (MRC, 2023c). Furthermore, the only mechanism that can mitigate the effects of sea level rise is the deposition of fluvial sediment on the delta plains (Bussi et al., 2021).

Sediment transport can be divided into two groups based on its origin: bed material load and wash load. Bed material load interacts with the local bed surface sediment and wash load is always supplied in suspension (Blom, 2021; Czuba et al., 2011). Bed material load can be transported both as bedload and as suspended load, whereas the wash load is always transported as suspended load. In the Mekong River, the suspended load commonly consists of clay and silt (Walling, 2009).

In terms of transportation rate, the suspended and wash load generally has a higher transportation rate compared to bedload transportation. This is because suspended load particles are smaller and lighter, allowing them to be more easily transported by the flowing water. This explains why fine sediments like silt and clay have a small response time, which means that a decrease in these sediments has an immediate impact on the system (Wagner et al., 2015). As a result, the satellite observations show that the colour of the Mekong is changing from brown to blue which indicates that the silt concentrations in the Mekong have reduced drastically (Dauphin & Patel, 2020).

The average annual total sediment load at the mouth of the Mekong, before the construction of dams, was estimated to be 145-160 Mt/year (Thi Ha et al., 2018). However, the Mekong is currently experiencing sediment starvation (Manh et al., 2014) because the construction of all planned dams (Figure 2) has been estimated to reduce the sediment delivery to the delta by 60% to 96% (Kondolf et al., 2018). Kummu et al. (2010) estimated this to range between 51%-69%, whereas Kondolf et al. (2014) predicted this to be 96%. This implies that a reduction is expected but that the downstream impact of constructing all hydropower dams is not completely understood yet.

Thus, the hydropower dams in the Mekong Basin trap silt and clay particles onto which important nutrients are attached for the fisheries and rice production. This means that the amount of available nutrients in the river and thus delta decrease which impacts ecosystems in the floodplains and delta.

The effect of dams on the annual sediment load at the city Kratie was examined more often, but the effect on the monthly silt and clay loads in the Mekong Delta has not been researched before. The focus on monthly loads makes it easier to analyse possible sediment management strategies that mitigate the effect on silt and clay concentrations in the Delta.

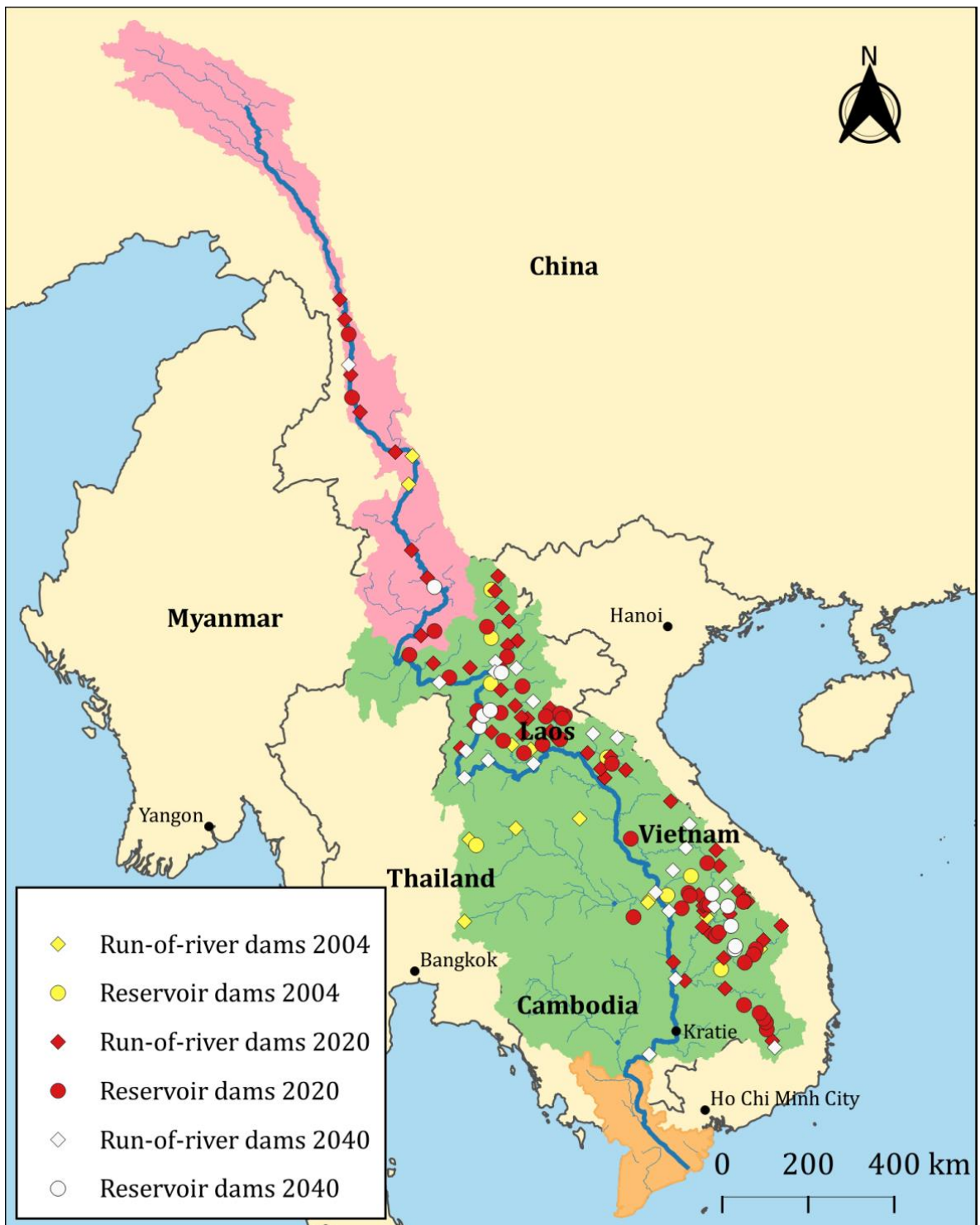


Figure 2: Location of run-of-river dams and reservoir dams for different years in the Mekong Basin

1.3 Research question

The main objective is to determine the effect of hydropower dams in the Mekong Basin on the silt and clay loads in the Mekong Delta and to establish strategies to mitigate negative impacts on silt and clay loads in the Mekong Delta. In order to meet this objective, the following research question is proposed:

What is the influence of hydropower dams in the Mekong Basin on the silt and clay loads in the Mekong Delta and what are possible strategies to mitigate the effects on these loads in the Mekong Delta?

To answer this question, the following sub-questions are significant:

- What is the effect of hydropower dams in the Mekong Basin on the silt and clay loads in the Mekong Delta?
- What are possible strategies to mitigate the effect on the silt and clay loads in the Mekong Delta?

1.4 Methodology

In order to answer both sub-questions, a generic conceptual model is established with the help of predefined models from literature. This model can be defined as a sediment balance model with distributed sediment yield and individual trapping efficiencies of dams. The first question is answered by applying this model to the Mekong Basin and the second question is answered by defining strategies for the Mekong Basin and applying strategies to the system with the help of the conceptual model.

1.5 Reading guide

A literature overview of the Mekong Basin is given in chapter 2 in order to summarize all relevant processes that play a role in the sediment dynamics in the Mekong. This includes the significance, origin, transport and deposition of silt and clay. Also, a brief overview is given of previous model development.

The content of the conceptual model is described in chapter 3 and the result of the application of the model to the Mekong Basin is given in chapter 4. Subsequently, the strategies are explained in chapter 5 and the results of applying strategies in chapter 6. The discussion of both sub-questions is given in chapter 7 and finally, the conclusions and recommendations which follow from the results are explained in chapter 8 and 9 respectively.

2. Literature Review

In this chapter a description of the Mekong Basin is given, containing the significance, source, transportation and net deposition of silt and clay in the Mekong Basin. It is important to understand these aspects in order to learn the relevance of this research, to establish a conceptual model and to be able to apply the model for mitigation measures. Also, a model development overview is provided.

2.1 Origin of clay and silt in the Mekong

Sediments are inorganic materials that are formed through the natural processes of weathering and erosion of rocks and soils (Pukinskis, 2013). The average diameter of a sediment particle is called the grain size and typically 3 types of grain size classes are categorized: clay, silt and sand. According to the USDA grain size classification, clay has a grain size smaller than 2 µm, silt between 2 and 50 µm and sand between 50 and 2000 µm (Figure 3) (Corral-Pazos-de-Provens et al., 2022). This implies that this study includes all sediment that has a smaller particle size than 50 µm.

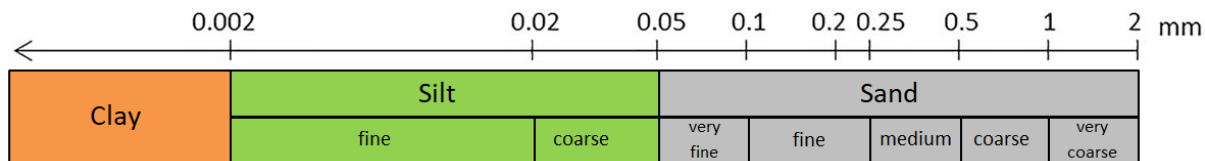


Figure 3: USDA grain size classification (Corral-Pazos-de-Provens et al., 2022)

2.1.1 Clay

Liu et al. (2004) performed isotope research in order to investigate the origin of clay in the Mekong Basin.

Clay contains essentially clay minerals which are generally formed by the chemical weathering of feldspar (Behrami et al., 2021; Lee, 2023). The soils found in the upper reach of the UMB are lithosol soils which contain the clay minerals illite and chlorite. Borehole samples collected at the Mekong River mouth in the East Sea contained 52% of these minerals. This means that more than half of the clay particles at the Mekong River mouth have their origin in this reach and thus in the Tibetan Plateau (Figure 4) (Figure 5) (Liu et al., 2004).

This can be explained by the many glaciers on the plateau that produce large amounts of sediment through glacial movement. In one of the glacier catchments of the Mekong, the Ming Yong glacier, the annual sediment yield was estimated to be 1104 t/km² (Lu et al., 2022), whereas the global average is 131 t/km² (Flemming, 2011).

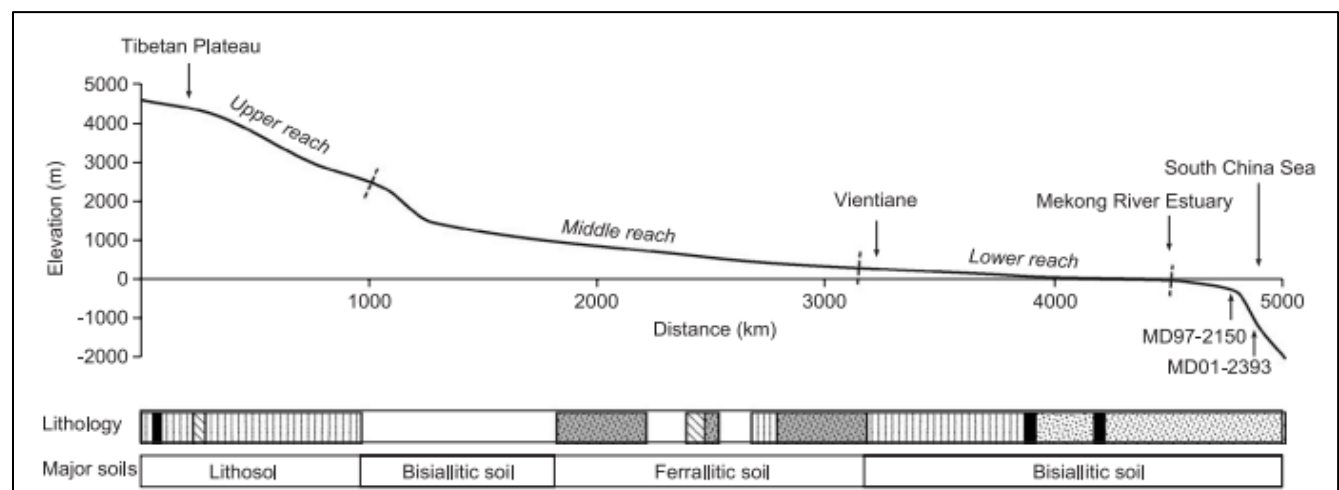


Figure 4: Profile of the Mekong river area with its major soil types and bore hole sample locations (Liu et al., 2004)

One of the soils found in middle reach of the UMB is ferralitic soil (Figure 4). The main clay mineral in ferralitic soil is kaolinite, of which 26% was found in the soil samples. Therefore, it can be concluded a quarter of the clay in the Mekong has its source in the middle reach and thus in the regions Three Rivers Area and the Lancang basin (Figure 5) (Liu et al., 2004) (MRC, 2023b).

Bisialitic soil can be found in both the middle reach of the UMB and the lower reach of the Mekong Basin. The main clay mineral of bisialitic soil is smectite, of which 22% was found in the samples (Liu et al., 2004).

When the above mentioned outcomes are combined, it can be concluded that at least 75% of the clay in the Mekong has its origin in the UMB region. The remaining clay has its source in the lower reach of the Mekong Basin that consist of five physiographic regions: the Northern Highlands, Khorat Plateau, the Eastern Highlands (Annamite Range and Bolaven Plateau), the Lowlands and the Southern Uplands (Kontum Massif and Volcanic Uplands)(Figure 5) (Carling, 2009). The 3S (Se Kong, Se San and Sre Pok) basins that are situated in the Southern uplands are estimated to be a major contributing source of sediment in the Lower Mekong Basin (LMB) (Shrestha et al., 2016)

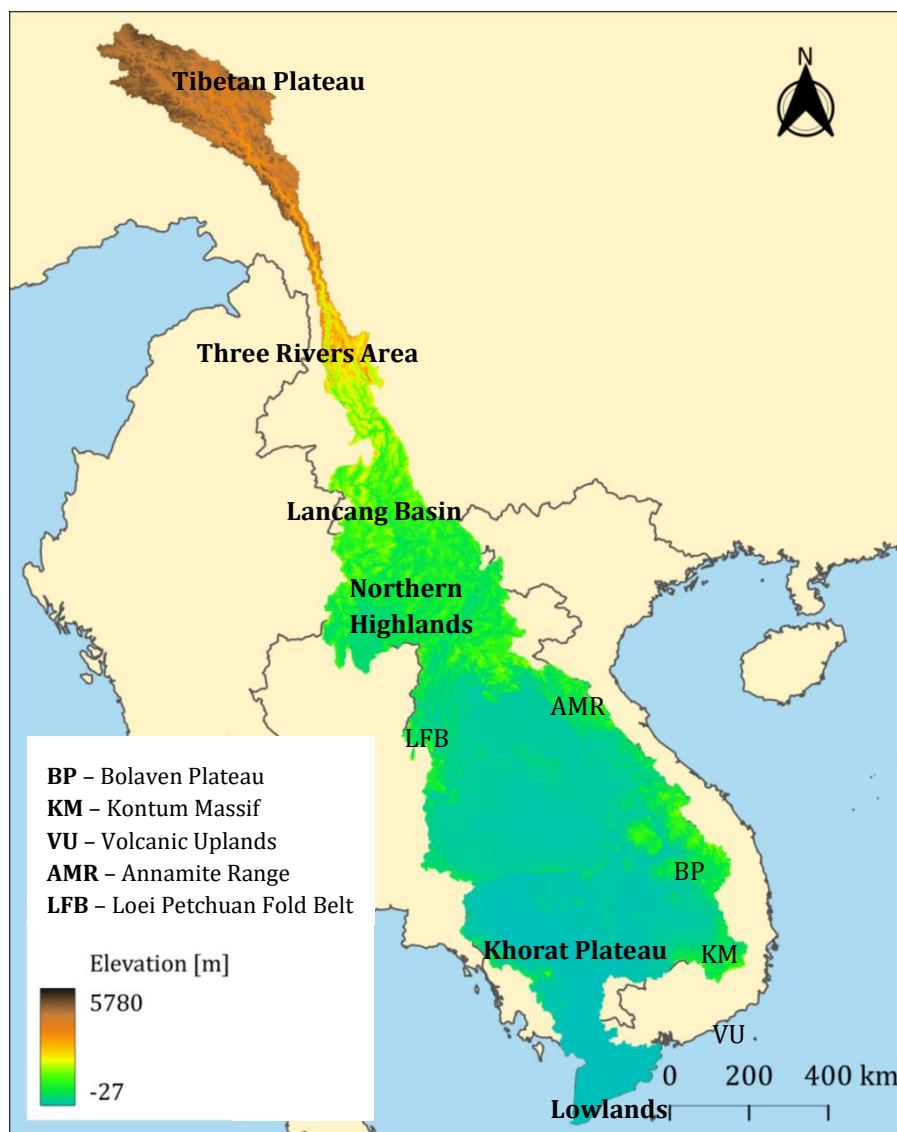


Figure 5: Topography and physiographic zones of the Mekong Basin (MRC, 2023b)

2.1.2 Silt

Long-term, high-energy processes are necessary for the formation of silt. The main process is abrasion through transport, which is the scraping or wearing down by friction of quartz. This includes fluvial comminution, aeolian attrition and glacial erosion (Wright et al., 1998). Fluvial comminution is the process by which the size of solid particles is reduced as a result of water movement across the streambed (Yang L., 2015), whereas the process of erosion that occurs during particle collision and wind-borne particle transportation is known as aeolian attrition (Lancaster et al., 2013). In the process of glacial erosion, ice removes quartz grains from a mountainside or landscape and carries the removed material downstream (Koppes, 2022; Schubert, 1964).

Even though the research by Liu et al. (2004) focused on clay mineralogical research, it should be mentioned that minor amounts of quartz clay size fractions were found in the researched bore hole samples (Liu et al., 2004). Gravity core research by Xue (2014) confirms this by establishing that the majority of the sediment reaching the East Sea can be categorized into clayey silt (Figure 6). This indicates that it is very likely that silt has a similar source pattern as the one identified for clay (Liu et al., 2004)

The literature research showed that it is very likely that half of the silt and clay in the Mekong has its source on the Tibetan Plateau and approximately a quarter has its origin in the Three Rivers Area and Lancang Basin. This means that the areas of intermediate and low relief in the LMB region produce less silt and clay compared to higher regions in the north (Walling, 2009).

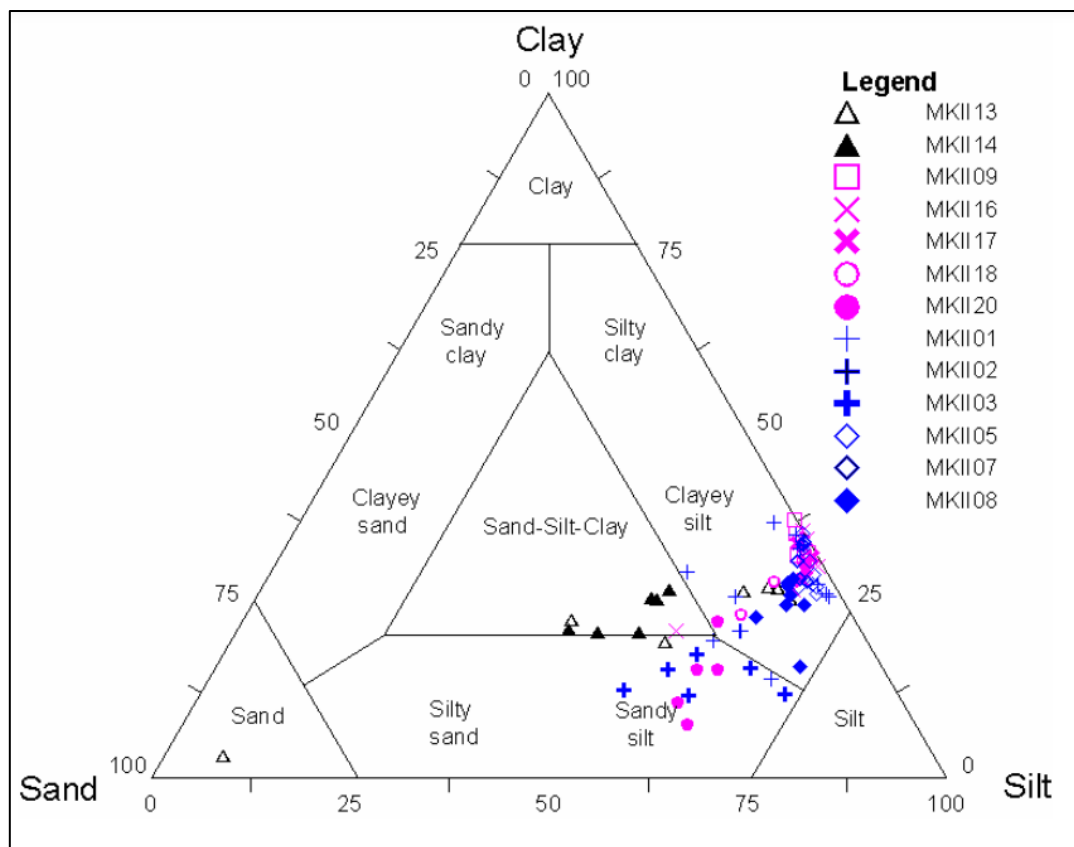


Figure 6: Ternary plot of sediment grain size with the results of the Gravity core research (Xue, 2014)

2.2 Transport of silt and clay

On the Tibetan Plateau, silt and clay are transported by glacial meltwater. The transport can be supraglacial (from the melting of ice), subglacial (at the bed) or englacial (within the glacier). Transportation varies spatially and has strong seasonal and diurnal variabilities. According to Lu et al. (2022), the discharge and Suspended Sediment Concentration (SSC) are higher from February to July and lower from August to January in the Ming Yong glacier. This seasonal variation suggests that clay and silt are stored during the low flow season and transported when flow is increasing (Lu et al., 2022).

Outside glacial areas, silt and clay enter the Mekong River via slope wash, gullies, and debris flows (Carling, 2009).

Sediment transport in the river can be divided into two distinct groups based on origin: bed material load and wash load (Figure 7). As the name suggests, bed material load has its origin in bed material and wash load is always supplied in suspension (Blom, 2021; Czuba et al., 2011).

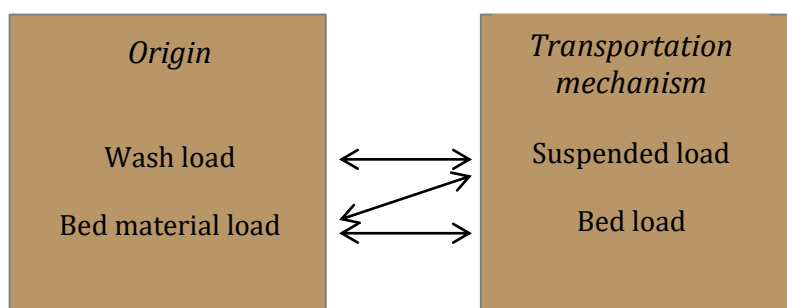


Figure 7: Classification of sediment transport (Fondriest Environmental, 2014)

Bed material load can be transported both as bedload and as suspended load (Figure 7). Bedload transportation is the movement of particles along the bottom of waterways by rolling, sliding, or bouncing. This type of transport mechanism is affecting the channel slope and bed surface texture (Blom, 2021) and accounts for approximately 5-20% of total sediment transport (Anthony et al., 2015). In general, larger and heavier particles are more likely to sink to the bottom as the effect of gravity on these particles exceeds the effect of upward forces by turbulence (Appendix G) (Bayoudh et al., 2019; Fondriest Environmental, 2014)

The portion of particles that are kept above the bed by tiny upward currents (turbulence) created by water flow is the suspended load. However, suspended load can become bedload during low or no flow. The suspended load affects, just like the bed load, the channel slope and bed surface texture (Blom, 2021). The majority of the year, the suspended sediment in the Mekong commonly has a smaller diameter than 63 µm (i.e. silt and clay) and approximately 45% of this is smaller than 2 µm (i.e. clay) (Walling, 2009).

Even though using the term ‘suspended sediment load’ seems logical, it is relevant to mention that not the transport mechanism, but rather the sediment properties are decisive in this research. The main sediment property that is essential is the ability to transport nutrients and minerals downstream (Section 2.4). Sand does not have a nutrient holding capacity, but may become suspended when discharges are high enough (Hurst, 1929; Wagner et al., 2015).

The wash load consists of sediment with a diameter typically less than 2 µm and is barely found in the river bed material (Southard, 2006). Unlike the suspended load, wash load will not settle when there is low flow. Therefore, it has no interaction with the bed sediment and thus has no effect on the channel slope and bed surface texture (Blom, 2021). Silt and clay regularly make up the wash load in channels, except when these sediments enter floodplains and reservoir. In these

low energy zones the deposition rate exceeds the entrainment rate (Fondriest Environmental, 2014).

The supply from upstream and the local hydrodynamics both affect how much sediment the river can carry. The latter determines a river's ability to transport sediment and is largely dependent on the flow rate. When the upstream supply is insufficient to meet the downstream demand, erosion, sedimentation, and morphological changes occur that can alter the characteristics of a river (Beierle et al., 2002).

2.3 Fine sediment deposition in the LMB region

Sediment deposition in the Mekong River occurs in reservoirs, floodplains along the entire length of the river and the delta (Wright L. D., 1985).

As a Mekong reaches its delta, the velocity decreases and the river widens due to the less steep topography and the opposing influence of the tide. Consequently, a significant amount of sediment that originates from the upper region of the basin is deposited. Sediment is gathered in various areas of the delta at varying speeds, mostly determined by the elevation, flow patterns of the river, tide, the specific design of river channels and the arrangement of vegetation (Wright L. D., 1985). The Mekong Delta is situated in both Vietnam and Cambodia and therefore often the division between the Vietnamese part of the Mekong Delta (VMD) and the Cambodian floodplains is made.

The VMD is made up of many floodplain sections with sizes ranging from 0.5 to 5 km² that have undergone significant modifications by humans compared to the Cambodian floodplains (Manh et al., 2014). In the VMD, the sediment that gets deposited ranges from 1% to 6% of the annual load at the city Kratie (Figure 1) (Manh et al., 2014).

The annual SL deposition in the Cambodian floodplains is significantly higher than the deposited load in the VMD. Here, it varies between 19% and 23% of the total yearly load at Kratie (Manh et al., 2014).

Upstream of the Cambodian floodplains is the Tonle Sap Lake (TSL) (Figure 1) that has an area of 2,700 km² covering 7.5% of Cambodia's surface (Campbell et al., 2009). The annual floods' rising and high stages cause water to flow into the TSL, but during the falling stage and subsequent dry season, this flow is reversed. This process turns the TSL into a massive buffer that holds floodwater and sediment during the flood season and raises the Mekong's discharge during the dry season. Approximately 8% of the annual SL at Kratie transports in and out of the TSL (Manh et al., 2014).

2.4 Significance of clay and silt for the Mekong Delta

There are two ways of transporting nutrients in a river: particulate and dissolved.

Dissolved nutrient transport is the movement of nutrients in dissolved or solubilized form (Harrington & Harrington, 2014). Different essential nutrients for various organisms like compounds of nitrogen such as ammonia and nitrate are largely dissolved in water (Tang et al., 2023).

This is in contrast to particulate nutrient transport, in which nutrients are attached to or incorporated into larger particles or solid particles that are suspended in water (Harrington & Harrington, 2014). Phosphorus mainly occurs in particulate form because more than 90% of the total phosphorus in a river is attached to sediment (Tang et al., 2023).

Sediments in rivers play an important role in transporting and storing inorganic nutrients like phosphorus and potassium. Since clean water typically has low levels of dissolved nutrients, the

majority of a river's nutrient content comes from nutrients attached or bound to sediments (Baran et al., 2015).

Clay and silt particles transport nutrients in river through adsorption which is the adhesion of ions or molecules to the surface of a solid material. There are several reasons why silt and clay are effective in transporting nutrients (Nathan, 2017).

Firstly, clay and silt particles both have a large surface area relative to their size. This extensive surface area increases the number of sites available for chemical interactions which enables the absorption of nutrients (Efretuei, 2016).

Secondly, clay particles carry a negative charge on their surface which can attract and hold onto positively charged nutrient ions (cations), such as magnesium (Mg^{2+}), potassium (K^+), and calcium (Ca^{2+}) which are essential plant and crop nutrients (NCDA&CS, 1999).

Additionally, clay has a high Cation Exchange Capacity (CEC), which is the ability to exchange cations with the surrounding water (Efretuei, 2016). Because of this characteristic, clay can absorb and hold onto these positive nutrient ions, preventing their immediate uptake by aquatic organisms and from converting them into forms that could be more easily lost from the system (Nathan, 2017).

Silt particles often carry a negative charge as well because these particles can contain clay minerals and other charged particles. Generally, the CEC of sediment increases with clay content which explains why silts can also have a higher CEC (Figure 8) (Nathan, 2017; NCDA&CS, 1999). Silt particles can also contain organic matter that may contribute to nutrient absorption as organic molecules can interact with certain nutrients (Efretuei, 2016).

Furthermore, these particles can act as a filter leading to trapping nutrients from the water. This filtration contributes to nutrient retention and an increase of nutrient availability in aquatic environments (NCDA&CS, 1999).

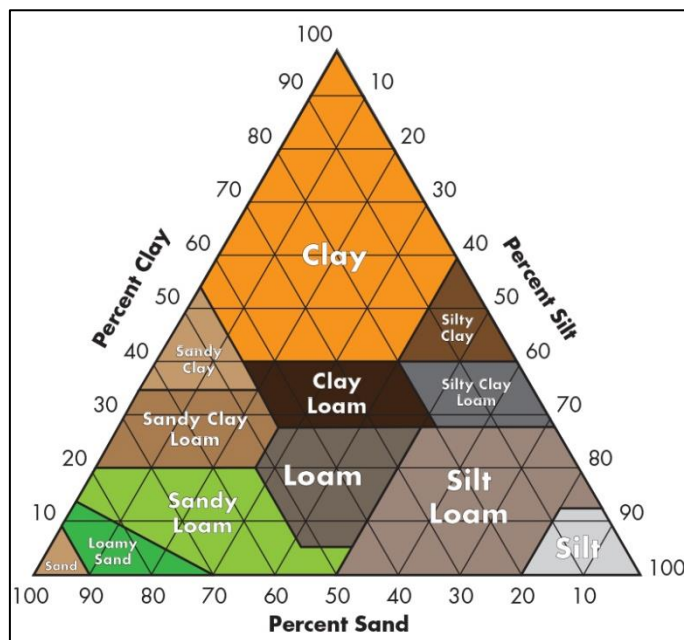


Figure 8: Soil Texture Triangle (OER Commons, 2019)

Small negatively charged ions (anions) like chloride (Cl^-) or nitrate (NO_3^-) are dispersed in water and are moved with the water flow. Larger anions or those with a higher affinity for solid particles may attach themselves to suspended sediment particles in water such as sediment, organic matter or microorganisms. They can absorb onto the surface of sediment particles as a

result of electrostatic forces as they are attracted to positively charged surfaces of e.g. silt and clay particles leading to adsorption (Wang J. S. et al., 2009).

Clay and silt can be suspended in water which allows them to transport absorbed nutrients downstream. When flow decreases, these particles may settle and deposit the associated nutrients onto the riverbed or delta (Nathan, 2017). In the Mekong Basin, fertility of its floodplains and delta mainly rely on nutrients connected to sediments (Baran et al., 2015). During the monsoon season, the Mekong delivers great amount of mineral and nutrient rich alluvial sediments to the floodplains and delta (MRC, 2005). These nutrients are crucial for the soil fertility necessary for rice cultivation.

The presence of sediments and the nutrients they carry also affect various biological processes for fish. This includes their nutrition through photosynthesis and predator-prey relationships, their ability to reproduce (since different species select particular spawning grounds based on the presence of sediment) and their ability to migrate (because sediments can cause movement) (Baran et al., 2015).

2.5 Trapping Efficiency model development

After Brown (1944) and Churchill (1948), Brune (1953) developed one of the first methods after to calculate the percentage of transported sediment into a dam reservoir that is deposited in that reservoir (Annandale et al., 2016), with a term called the Trapping Efficiency (TE) (Mulu & Dwarakishb, 2015; Tan et al., 2019). The TE depends on multiple factors varying from the capacity of the dam to the size of the sediment (Kondolf et al., 2013; Kummu et al., 2010). The Brune model was further advanced for different reservoir types and regions and has become one of the most widely adopted models for assessing the TE. The last decades, more modifications of this method appeared, especially for river catchments. (Tan et al., 2019).

Vörösmarty et al. (2003) was the first to apply the Brune method on basin-scale to predict the sediment TE of large reservoirs. This method is able to roughly estimate the TE of sub-basins resulting in a first indication of the SL downstream. However, the TE of singular dams is not calculated in this model, which means that the method is not able to predict the effect of dam cascades (multiple dams in a row). Furthermore, this model only takes dams with a larger maximum storage capacity than 0.5 km³ into account, meaning that the TE of many reservoir and run-of-river dams cannot be predicted. Moreover, the model does not consider mainstream dams and does not give the option to calculate the TE for a certain type of sediment size (Vörösmarty et al., 2003). Therefore, this model is not suitable for the purpose of this research.

Kummu et al. (2010) applied a modification of the Vörösmarty et al. (2003) model such that mainstream dams, dams with smaller active storages and dam cascades are considered. Nevertheless, it does not take into account the variation in TE for different sediment sizes even though in some researches this is preferable knowledge. Since the model by Kummu et al. (2010) includes more essential facets, it was used as a base for this conceptual model.

3. Conceptual model

In this chapter the conceptual model is explained by describing the model purpose and model design.

3.1 Model purpose

The goal was to set up a generic model. A generic model is a predefined, non-specific model that can be used as a template for specific applications (Eleven, 2013). With only small modifications or step substitutions such a model is widely applicable (Murray-Smith, 2012).

Due to global hydropower development in river basins the sediment loads downstream are decreasing (Bogen & Bønsnes, 2001; Kondolf et al., 2014). However, the magnitude of the reduction of sediment load is frequently unknown, which explains the need for an accessible approach to determine a first estimate of the downstream sediment load.

Subsequently, it is important to conduct an initial assessment regarding sediment management approaches such that sediment loads can be increased again.

Therefore, the main objective of this conceptual model is to determine the effect of hydropower dams in a river basin on sediment load downstream and to establish possible strategies to mitigate these effects.

3.2 Model design

The model consists of four components: Model Characteristics, Model Input, Determining Trapping Efficiency and Sediment Load Calculation (Figure 9). Each component contains different segments which are explained in this section as well as the model assumptions.

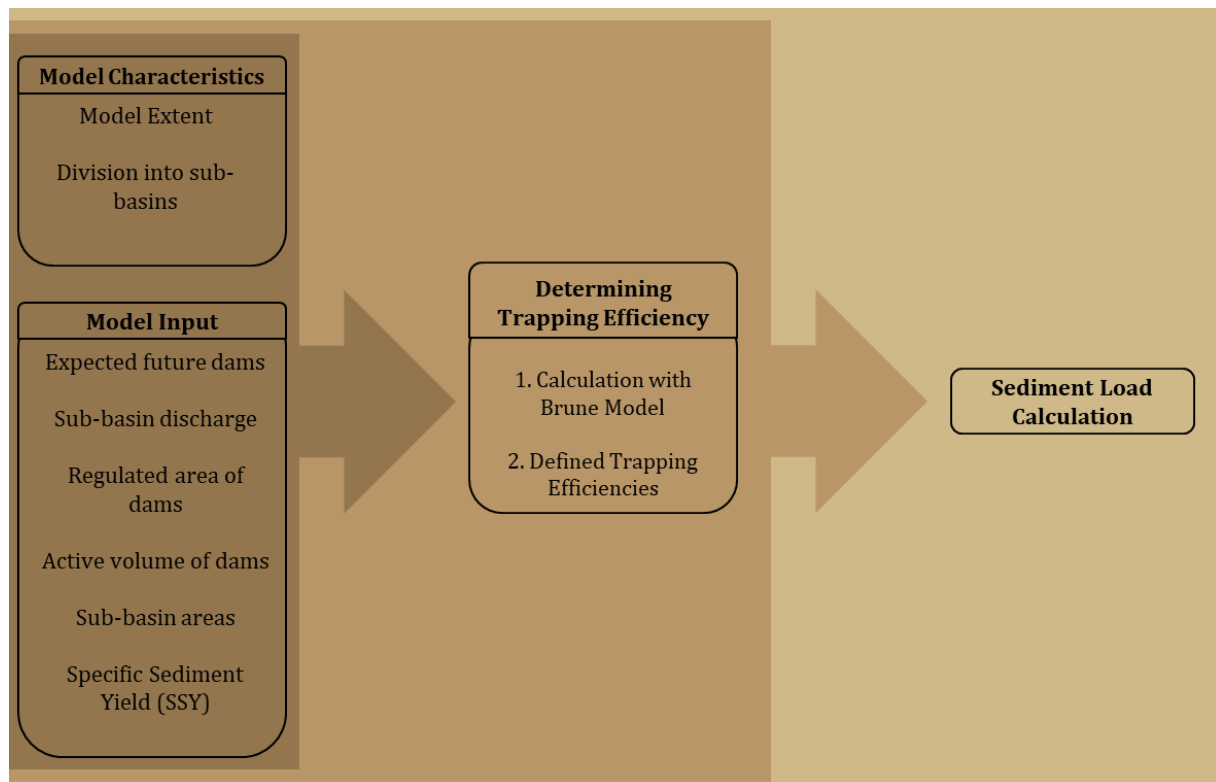


Figure 9: Methodological Framework

3.2.1 Model assumptions

A model is a simplified version of reality and therefore assumptions are necessary. In this model four main assumptions were made:

1. **No change in hydrological regime.** The dry season flows are significantly increasing whereas the wet season flows are decreasing in the Mekong Basin as a result of hydropower development (Section 1.2) (Lu & Chua, 2021; Räsänen et al., 2017). The sediment and nutrient transport is expected to be affected by this changing hydrological regime because there is an empirical relation between the sediment load and the discharge in the Mekong basin (Räsänen et al., 2017; Sok et al., 2020). In other words, the sediment transportation pattern of the river changes due to hydropower development but the exact effect is unknown. Therefore, it was assumed that there is no change in hydrological regime that impacts the sediment transport.
2. **No storage component.** When sediment is transported through a river, it often spends more time in storage than in transport which means that sediment delivery timescales are controlled by the time spent in storage (Huffman et al., 2022). This means that sediment can partly remain behind on floodplains along a river and may be transported again after some time. However, it is unknown how much sediment is stored annually in the Mekong River and also for how long the sediment is stored (Räsänen et al., 2017). Because of this large uncertainty, it has not been included in the model.
3. **No dam opening.** Throughout the year, reservoirs are filled and emptied several times for multiple reasons, but most often for electricity generation. When water is suddenly released, a peak of sediment enters the river (Annandale et al., 2016). However, this has not been considered in the model because it is unknown how often dams are opened and if so, for how long.
4. **No hysteresis.** At the beginning of the wet season water tends to hold more sediment as the availability of sediment is higher, meaning that more sediment is transported (Malutta et al., 2020). This phenomenon is called *hysteresis* and is not considered when calculating the SL because the extent of additional sediment transportation in these months is unknown.

3.2.2 Model characteristics

Model extent

It is advised to choose the model extent in such a way that the most downstream location in the model is not affected by external factors such as in or outflow of other rivers or lakes, tidal influences, sand mining activities or extensive irrigation applications.

Division into sub-basins

To be able to calculate sediment load, the river basin needs to be divided into sub-basins based on river tributaries.

3.2.3 Model input

Expected future dams

In order to determine the effect of hydropower dams on the downstream sediment load, it is essential to start with defining a baseline. The baseline describes the period before any hydropower dam development, meaning the undisturbed sediment concentrations.

Different reference years are preferred in order to calculate the change in sediment load over a specific period and for every reference year, a clear distinction between operational and planned dams is needed. The calculated sediment load can be compared to the baseline sediment load.

Sub-basin discharge (Q_{sub})

The discharge in the sub-basins can be determined in numerous ways. When observed discharge data is available within sub-basins, this is the preferred approach as this tends to be the closest to reality. Other ways can be trying to model the discharge with a distributed hydrological model such as SWAT or by estimating the discharge based on rainfall data. Depending on the desired approach, both monthly ($Q_{sub,month}$) and annual discharges ($Q_{sub,year}$) can be used.

Catchment area of dams ($A_{c.dam}$)

The catchment area of a dam is sometimes stated in datasheets. However, if it is not given, the area can be estimated by drawing a sub-area upstream of the hydropower dam in (e.g.) ArcGIS or QGIS. This holds for tributary as well as mainstream dams. In other words, the area upstream of a dam up to other dams is considered the catchment area of a dam.

Active volume of dams (C_R)

The active volume (C_R) of a dam is often general information which is displayed in dam databases. Dams can be divided based on their active volume; dams with reservoirs that have a small active storage are often referred to as a run-of-river dams, whereas dams with reservoirs that have a large active storage are often called reservoir dams.

Sub-basin areas (A_{sub})

The sub-basin areas (A_{sub}) can be calculated in programs such as ArcGIS or QGIS.

Specific Sediment Yield (SSY)

The annual Specific Sediment Yield (SSY) of sub-basins [t/km^2] is defined as the quantity of sediment that is exported from a specific drainage basin (Van Campenhout et al., 2022). Sometimes the SSY is established in a previous study but when it still needs to be determined it can be calculated with the suspended sediment concentration (SSC) and water discharge, or be estimated by geomorphic attributes of the sub-basins.

3.2.4 Determining Trapping Efficiency

The effect of the hydropower dams on the sediment load was determined using the Trapping Efficiency (TE) of each operational dam in a specific reference year. Two different approaches are applied to establish the TE: calculation of TE with the Brune model and Defined Trapping Efficiencies.

Approach 1: TE calculation with Brune Model

The empirical method was developed by Brune (1953) and was chosen over other methods such as Brown or Churchill because it is a widely used model and provides plausible estimates of long-term, mean TE (Kummu et al., 2010). This analysis works primarily on upstream discharges and dam reservoir size, all basically volumetric data and data coming from Digital Elevation Model (DEM) analysis.

The TE of each hydropower dam is calculated using an altered Brune model. The Brune curves were modified by the USDA-NRCS to create curves for three different types of sediments based upon the reservoir dimensionless timescale (τ_R). Depending on desired sediment size the formulas are chosen (Table 1) (Sun et al., 2022).

Table 1: TE formulas for different sediment curves and dimensionless timescales (Sun et al., 2022)

	$\tau_R > 1$	$1 > \tau_R > 0.02$	$\tau_R < 0.02$
Upper curve (sand-gravel)	100	$100 - (0.485 \ln(\tau_R) ^{2.99})$	$124 - (6.59 \ln(\tau_R) ^{1.52})$
Median curve (mixture)	97	$97 - (1.275 \ln(\tau_R) ^{2.47})$	$128 - (11.51 \ln(\tau_R) ^{1.304})$
Lower curve (clay-silt)	94	$94 - (3.38 \ln(\tau_R) ^{1.92})$	$94 - (3.38 \ln(\tau_R) ^{1.92})$

$$\tau_R = \frac{C_R}{Q_R} \quad (3.1)$$

$$Q_R = Q_{sub} \cdot \frac{A_{c,dam}}{A_{sub}} \quad (3.2)$$

τ_R	Dimensionless timescale [-]
C_R	Active volume of reservoir [km^3]
Q_R	Regulated reservoir discharge [km^3]
Q_{sub}	Sub-basin discharge [km^3]
$A_{c,dam}$	Catchment area dam [km^2]
A_{sub}	Sub-basin area [km^2]

Approach 2: Defined Trapping Efficiencies

The timing and duration of dam opening is often highly uncertain. Hence, in Equation 3.2 it was assumed that only the precipitation that falls in $A_{c,dam}$ flows through the dams. This results in an underestimation of the regulated reservoir discharge (Q_R) and thus in a large uncertainty in the calculated TEs.

To check if this has an effect, predefined TEs can be applied to the dams which can be based on multiple characteristics:

- *Discharge.* When flow in a river is influenced by dry and wet seasons, the magnitude of the TEs can be based on discharges. Due to lower flow velocities in the reservoirs during dry season, the settling distance for the sediment is also lower (Equation 3.9). Therefore, more sediment tends to settle and is thus trapped in the reservoir, leading to a higher TE compared to the wet season.
- *Dam type.* *Reservoir* dams have a larger active volume compared to *run-of-river* dams often leading to a larger reservoir length. This causes the settling distance to be smaller than the reservoir length, leading to a larger TE in *reservoir* dams (Equation 3.9).
- *Location.* If a dam is located on the mainstream river, more sediment tends to pass the dam, but due to a higher discharge mainstream dams tend to have a lower TE compared to a tributary dam.

3.2.5 Sediment Load calculation

Sediment load of sub-basins (SL_{sub})

This step is closely related to defining a baseline (Section 3.2.3).

The sediment load of a sub-basin can be calculated by using the pre-mentioned SSY and the area of a sub-basin (A_{sub}). By multiplying these two, the annual sediment load of each sub-basin (t/year) ($SL_{sub,year}$) is calculated. As the hydropower dams are not considered in this calculation, the sum of all these loads can be considered the baseline.

Downstream Sediment load (SL)

The annual SL of each sub-basin ($SL_{sub,year}$) can be scaled to monthly SL according to the discharge distribution if an empirical relation is established in the basin (Equation 3.3) (Figure 10).

$$SL_{sub,month} = SL_{sub,year} \cdot \frac{Q_{sub,month}}{Q_{sub,year}} \quad (3.3)$$

$SL_{sub,month}$ Monthly Sediment Load in sub basin [Mt]

$SL_{sub,year}$ Yearly Sediment Load in sub basin [Mt]

$Q_{sub,month}$ Monthly Discharge in sub basin [km^3]

$Q_{sub,year}$ Yearly Discharge in sub basin [km^3]

With the downstream sediment load, the trapped sediment load can be calculated (Equation 3.4). Consequently, it can be computed how much sediment passes the dam and if this is done for each successive dam, the downstream sediment load is determined.

$$SL_{trapped,dam} = SL_{sub} \cdot \frac{A_{c,dam}}{A_{sub}} \cdot TE \quad (3.4)$$

$SL_{trapped,dam,month}$ Monthly trapped sediment in dam [Mt]

$SL_{sub,month}$ Monthly Sediment Load in sub basin [Mt]

$A_{c,dam}$ Catchment area dam [km^2]

A_{sub} Sub-basin area [km^2]

TE Trapping efficiency [-]

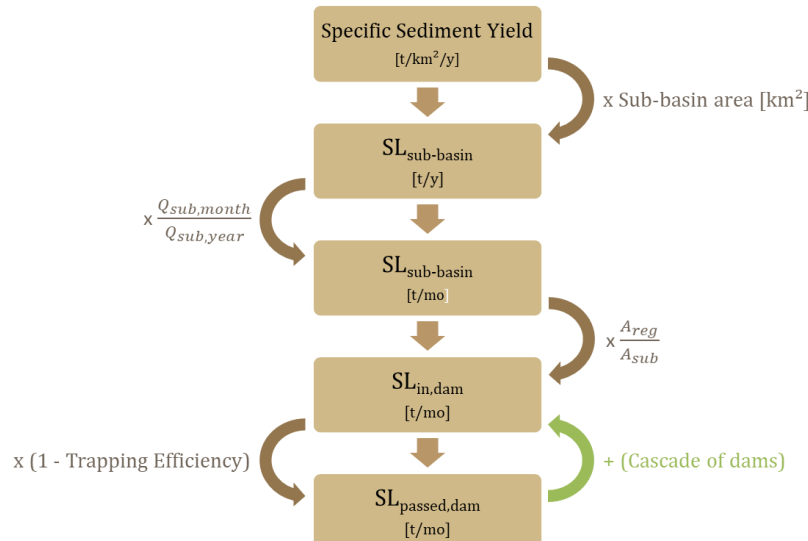


Figure 10: Calculation of the downstream sediment load

4. Results - Model Application to the Mekong Basin

4.1 Model characteristics

4.1.1 Model extent

Kratie is the most downstream city in the model because it is the most downstream location unaffected by tidal influence and the Tonle Sap Lake systems' buffering of the flood wave (Figure 11) (Sok et al., 2020). Furthermore, previous research has computed the loads up to Kratie as well, which makes comparison easy.

In order calculate the sediment load for the Mekong Delta, a rule of thumb was used: a minimum of 1% and a maximum of 6% of the sediment load at Kratie deposits in the delta. Therefore, the average of approximately 4% was applied (Manh et al., 2014).

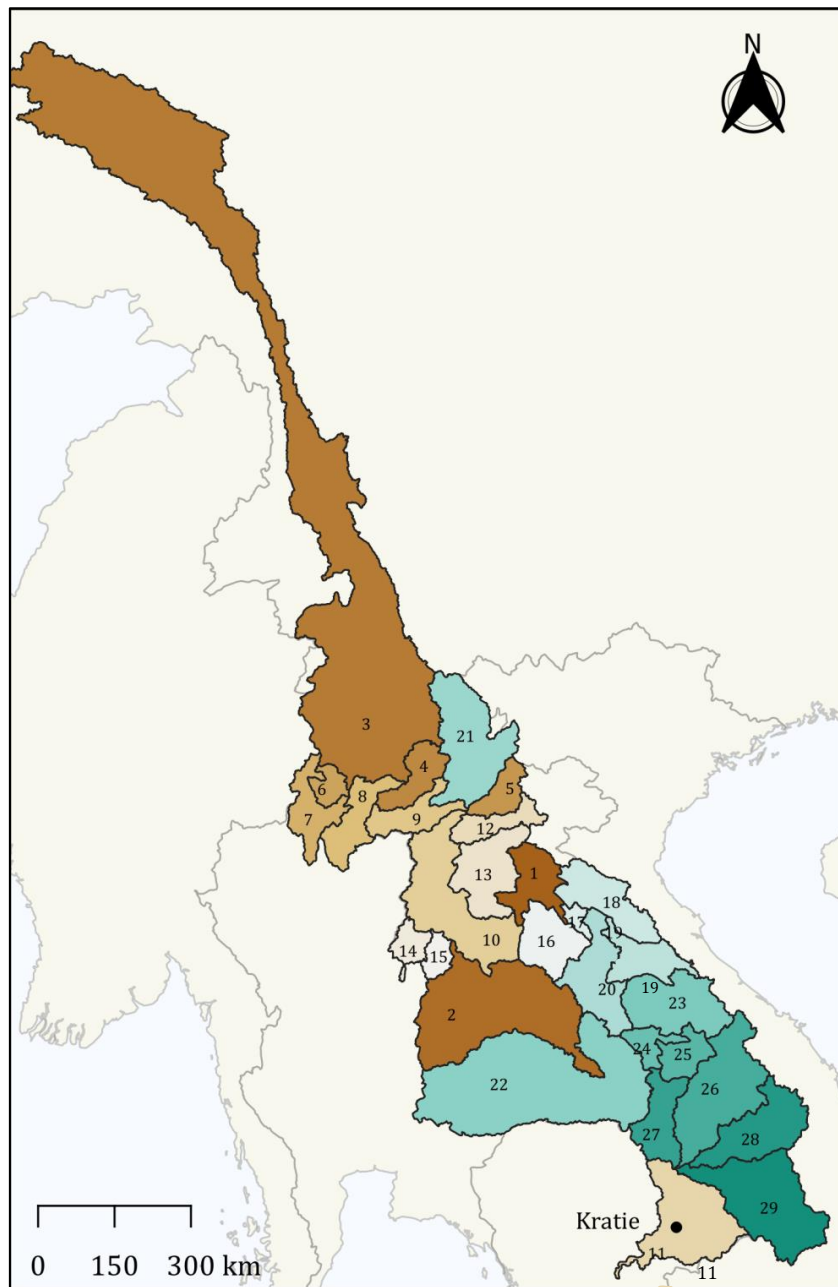


Figure 11: Sub-basins in the Mekong Basin

4.1.2 Division into sub-basins

To be able to calculate the silt and clay concentrations, the Mekong Basin was divided into 29 sub-basins (Figure 11).

4.2 Model input

4.2.1 Expected future dams

In order to research the effect of hydropower development on the silt and clay load in the Mekong Delta, a baseline and 3 different reference years have been chosen.

The baseline is the period before any hydropower dam development in the Mekong Basin, meaning the undisturbed silt and clay concentrations in the Mekong Delta. The 2004 situation is the period when large scale hydropower development emerged. The present situation covers all hydropower dams built until 2020, even though at the moment, the current hydropower development has already passed this. The 2040 situation includes all planned dams that are constructed and operational in the year 2040.

Outlined, the following four periods were examined:

- Baseline – Before hydropower development
- 2004 situation – Hydropower development until 2004
- Present situation – Hydropower development until 2020
- Future situation – Hydropower development in 2040

4.2.2 Sub-basin discharge

A monthly timescale was applied because the response time of silt and clay concentrations on changes in the catchment area is more or less instantaneous (as is water).

Monthly rainfall radar data (GPM) was used from the NASA database for the estimation of monthly discharges. This radar data was added as a raster dataset in QGIS and with the tool *zonal statistics* the mean monthly precipitation [mm] for each sub-basin of the Mekong Basin was calculated.

According to Wang et al. (2017) the GPM data overestimates the amount of rain in the Mekong Basin in the dry season and underestimates it in the wet season in 2014-2016. Except for the UMB, where the rainfall is overestimated in the wet season.

In order to verify the GPM data for this research, the data of 5 rain gauges from Visual Crossing Corporation (2023) was used to interpolate (Appendix D).

Inverse Distance Weighting (IDW) interpolation was applied. The underlying assumption of IDW interpolation is that nearby locations are more similar to one another than the ones farther away. IDW applies weights proportional to the inverse of the distance raised to the power value p to the measured rain gauge data surrounding the prediction location in order to predict values. If $p=0$, there is no decrease with distance, and as p increases, the weight for distant points decreases quickly. This means that the ratio at which the weight decreases depends on p . In general, p values greater than 1 are used with a default value of $p=2$ (ArcGIS, 2023). Therefore, IDW interpolation was applied to the 5 data points for $p=1$ and $p=2$.

It was concluded that the 5 rain gauge data locations were not sufficient to interpolate and that the outcomes of Wang et al. (2017) could not be validated for this data (Appendix D). Therefore, it was assumed that the results of Wang et al. (2017) also hold for the GPM datasets used in this

research. In line with the graphs in this article, a precipitation correction factor (cf_P) of 0.8 was applied for overestimation and 1.2 for underestimation (Table 2).

However, not all precipitation that falls within a drainage basin enters the river directly because water can infiltrate, run-off, evaporate or transpire. All precipitation that falls will eventually flow to the outlet point, unless it is first removed by evaporation and transpiration. Run-off is precipitation that does not infiltrate but instead moves on the Earth's surface toward streams and has the most direct effect on the river's discharge (NWS, 2023). It can be generated through saturation excess (i.e. when soils is saturated) and through infiltration excess (i.e. when rain intensity is higher than infiltration rate into the soil) (Yang et al., 2015). Therefore, there is more run-off in the wet season compared to the dry season resulting in more rainfall reaching the river.

In general, approximately a third of precipitation over land enters a river under mediate weather conditions (USGS, 2019).

In order to account for the share of rainfall that does not reach the river, discharge correction factors (cf_D) were applied according to the season. Since approximately 5% of the Mekong Basin is covered with water and because of the high rainfall in the wet season, the discharge correction factor for the wet season is 0.5 and for the dry season 0.4 (Table 2) (Kityuttachai et al., 2016; Ly et al., 2020).

Table 2: Correction factors for Upper Mekong Basin (UMB), Middle Mekong Basin (MMB) and Lower Mekong Basin (LMB)

UMB		MMB & LMB	
Dry season	Wet season	Dry season	Wet season
cf_P	0.8	0.8	1.2
cf_D	0.4	0.5	0.5

Monthly discharges were calculated with the monthly rainfall [mm], total area of the sub-basins [km^2] and the seconds per month (Equation 3.5)

$$Q_{\text{sub},\text{monthly}} = GPM_{\text{sub},\text{monthly}} \cdot 10^{-6} \cdot cf_P \cdot cf_D \cdot A_{\text{sub}} \quad (3.5)$$

$Q_{\text{sub},\text{monthly}}$	Sub-basin monthly discharge [km^3]
$GPM_{\text{sub},\text{monthly}}$	Rainfall radar data [mm]
cf_P	Precipitation correction factor [-]
cf_D	Discharge correction factor [-]
A_{sub}	Sub-basin area [km^2]

2004 situation

For this situation, the GPM data for the years 2001-2004 was downloaded, with 2001 being the first year available.

Present situation

The GPM data for the years 2017-2020 was used for the present situation.

2040 scenario

The NASA GPM data does not provide future rainfall datasets. Therefore, it was assumed that there is no change in rainfall over the coming years, meaning that the same dataset and $Q_{\text{sub},\text{monthly}}$ was used as in the 2020 scenario (2017-2020). Although climate change studies indicate potential changes, they are too uncertain to implement in the approach (Chang et al., 2021). For now, these impacts have not been included.

4.2.3 Catchment area of dams

The catchment areas of dams ($A_{c,dam}$) in the Mekong Basin were estimated by drawing a sub-area upstream of the hydropower dam in QGIS (example sub-basin 2, Figure 11).

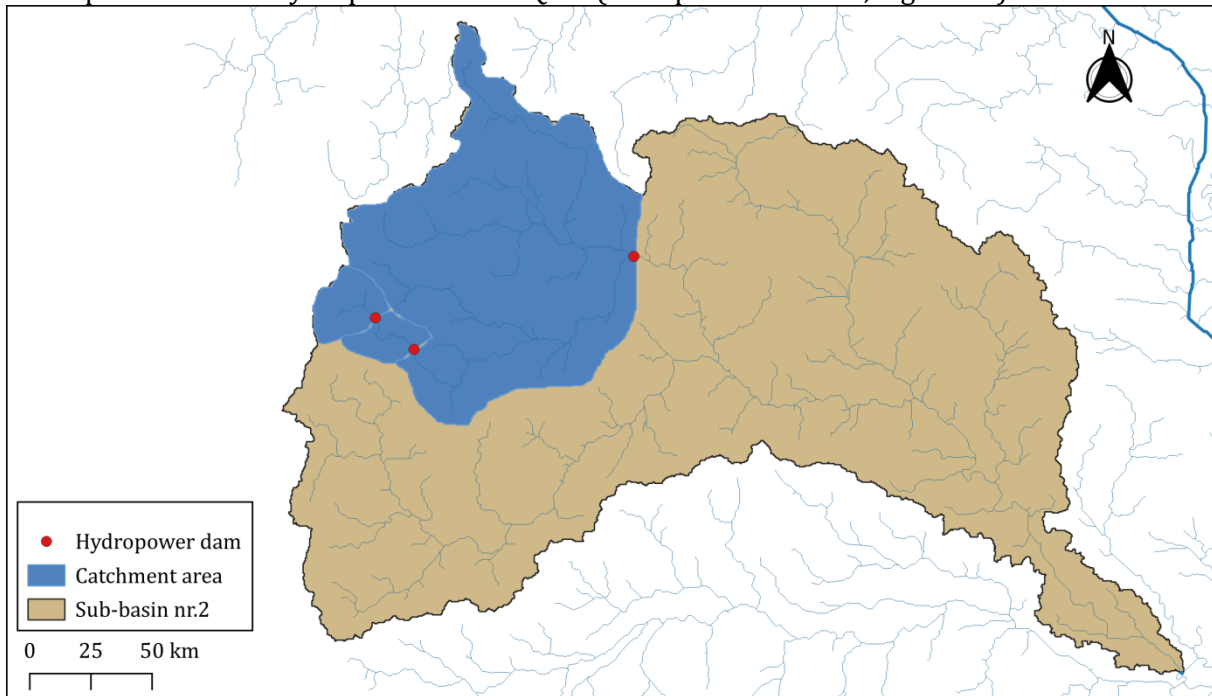


Figure 12: Estimation of catchment area ($A_{c,dam}$)

4.2.4 Active volume of dams

The active volumes of the hydropower dams (C_R) were received from the Mekong River Commission. Dams are considered a *run-of-river* dam if the active volume is smaller or equal to 0.1 km^3 and a *reservoir* dam when the volume is larger (Appendix A).

4.2.5 Sub-basin areas

The sub-basin areas (A_{sub}) were calculated in QGIS (Appendix B).

4.2.6 Specific Sediment Yield

The Specific Sediment Yield (SSY) calculated by Kummu et al. (2010) was used. They calculated the pre-dam mean SSY (1962-2005) for the majority of the sub-basins using a sediment rating curve based on the observed suspended sediment concentration (SSC) and water discharge data. The SSY of the remaining sub-basins was estimated with the help of SWAT model estimations by Sok et al. (2020). Since the SSY is the quantity of sediment exported from a drainage basin, this SSY is the actual yield that enters the river.

It was assumed that the suspended sediment in the Mekong is smaller than $63 \mu\text{m}$, which means that the SSY is representable for silt and clay concentrations in the river (Walling, 2009).

4.3 Determining Trapping Efficiency

4.3.1 Approach 1: TE calculation with Brune Model

The equation for silt and clay (Table 1, Section 3.2.4) was applied for the Mekong Basin and since monthly trapping efficiencies (TE) were preferred, the monthly discharges were used (Section 4.2.2).

4.3.2 Approach 2: Defined Trapping Efficiencies

Predefined TEs were applied based on the type and location of the dam and the season in the Mekong. The choice for the TEs was based on the discharges in the river because there are dry and wet season flows in the Mekong (MRC, 2005). Due to the difference in settling distance, a higher TE was assigned to the dry season than to the wet season (Equation 3.8).

The difference in TE between the *reservoir* and *run-of-river* was assigned to the difference in active volume and consequently the settling velocity (Equation 3.9).

Table 3: Defined Trapping Efficiencies

	Tributary		Mainstream	
	Dry season	Wet season	Dry season	Wet season
Reservoir	0.9	0.6	0.7	0.4
Run-of-river	0.3	0.1	0.2	0

4.4 Sediment Load calculation

4.4.1 Sediment load of sub-basins

Baseline

The baseline annual sediment load (SL) [Mt] of every sub-basin was calculated by multiplying the SSY (Section 4.2.6) and the area of the sub-basin (A_{sub}) (Figure 13) (Section 4.2.5) (Appendix B).

The UMB has the highest sediment load (92 Mt) and the 3S region also has a relatively large combined load (18 Mt).

2004, Present and Future situation

The baseline annual SL [Mt] was also used for the other situations. This means that it was assumed that the SL of each sub-basin has remained constant over the years and remains the same in the future.

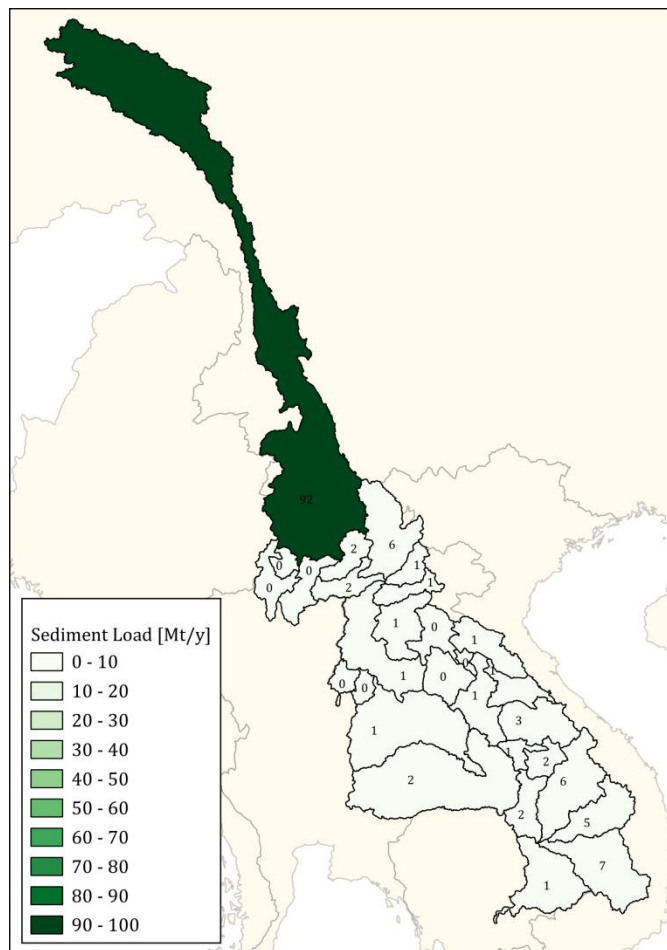


Figure 13: Baseline sediment loads

4.4.2 Downstream Sediment load

Since an empirical relation between the SL and the discharge was established in the Mekong Basin (Sok et al., 2020), the downstream monthly SL at Kratie was calculated by Equation 3.3 and 3.4 (Section 3.2.5). By multiplying this with 4% the average monthly SL to the Mekong Delta was calculated.

4.5 Model verification

4.5.1 Data validation

Sub-basin discharge (Q_{sub})

The Mekong's average annual discharge is 475 km³ (MRC, 2019). Kummu et al. (2010) calculated the annual discharge at Kratie to be much lower (389 km³) with estimations based on observed discharge data (1985-2016) from 9 stations. This annual discharge was reasoned back to the sub-basins, so the used discharges were compared to discharges calculated by Kummu et al. (2010). Nevertheless, it should be mentioned that the accuracy of the discharges estimated by Kummu et al. (2010) cannot be guaranteed. These estimations are namely based on very few observation stations compared to the number of sub-basins.

2004 situation

The calculated total annual discharge at Kratie in 2004 is 512 km³, thus much higher than the total discharge calculated by Kummu et al. (2010).

For the majority of the sub-basins the used annual discharge matched relatively well with the estimated discharges by Kummu et al. (2010). However, there were some outliers. For the sub-basins 9, 10, 14, 15, 16, 20, 22, 24, 27 the calculated discharge was higher and for 17, 19 and 28 lower than the estimated discharge by Kummu et al. (2010) (Figure 14) (Figure 15).

There is no clear explanation for this deviation. However, all sub-basins with a higher discharge are located in one band around the mainstream river in an area of gentle mean slope (Ly et al., 2020). This may suggest that the precipitation was overestimated in this area and that the precipitation correction factor should have been lower. On the other hand this may suggest that less precipitation enters the river due to the flatter topography and less slope and thus that the discharge correction factor must have been lower.

The sub-basins with a lower discharge are located in an area with a strong or steep mean slope (Ly et al., 2020). This may suggest that the precipitation was underestimated in this area and that the precipitation correction factor should have been higher. On the other hand this may suggest that more precipitation enters the river due to a larger slope and thus that the discharge correction factor must have been higher.

Present and future situation

The calculated total annual discharge at Kratie in 2020 is 517 km³. The overall pattern and values of the calculated discharge are similar to the 2004 scenario, thus the same explanation holds. (Figure 14) (Figure 15).

The difference that are visible are a result of different rainfall distribution over the Mekong Basin. In sub-basins 9, 10, 16, 20, 22 and 27 the 2020 discharges are a little lower than the 2004 discharges, whereas in 3, 7, 23 and 29 the 2020 discharge are higher (Figure 15). Also, in sub-basin 7 the percentage difference for 2004 is lower and for 2020 higher (Figure 16), but there is no clear explanation for this.

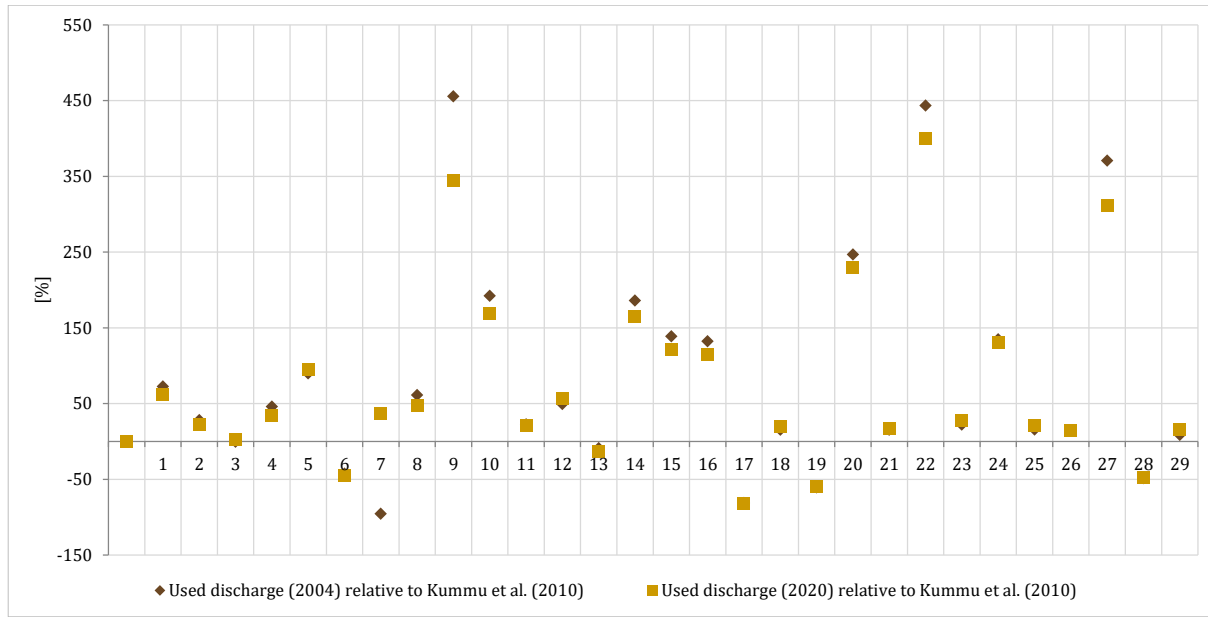


Figure 14: Percentage difference of used discharges of 2004 and 2020 relative to the estimated discharges of Kummu et al. (2010)

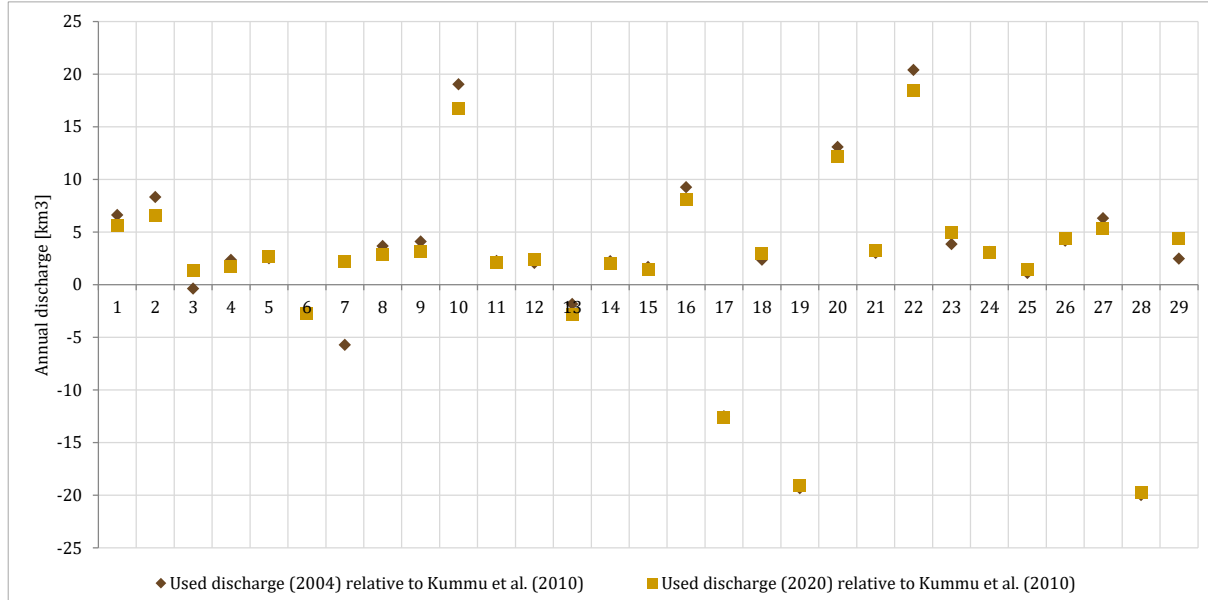


Figure 15: Absolute difference of used discharges of 2004 and 2020 relative to the estimated discharges of Kummu et al. (2010)

SSY

Chuenchum et al. (2020b) used a modified Revised Universal Soil Loss Equation (RUSLE) model and GIS techniques to estimate the SSY of some sub-basins of the Mekong Basin. The RUSLE method illustrates the relationship between soil erosion due to surface runoff and raindrop impact and climate, topography, soil, and land use (Wischmeier & Smith, 1972).

The comparison of the SSY determined by Chuenchum et al. (2020b) and the SSY used in this research shows that used SSY is a little lower than the RUSLE SSY. Nevertheless, the comparison shows that the two are very similar (Figure 16).

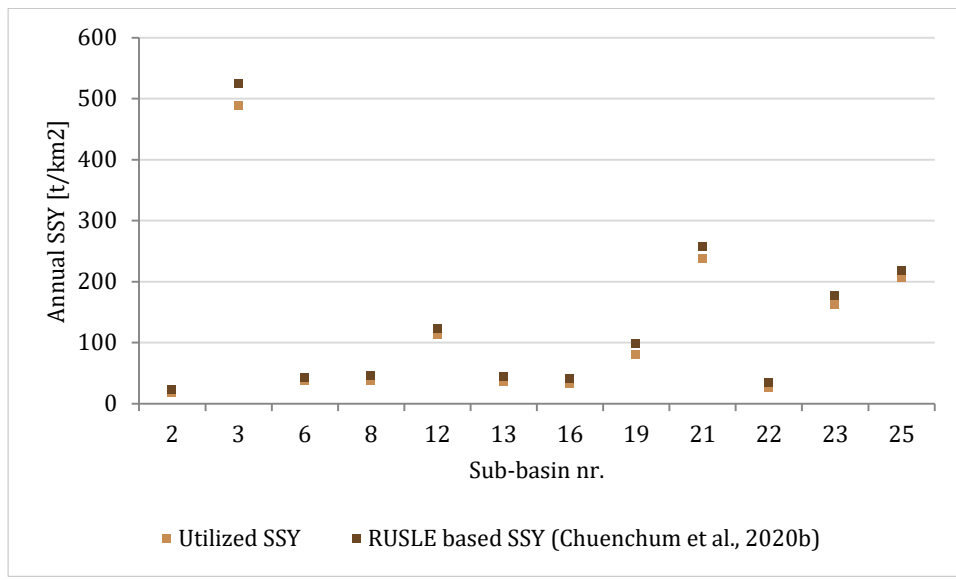


Figure 16: Comparison of utilized SSY based on SSC and discharge measurements and SSY based on RUSLE model (Chuenchum et al., 2020b)

4.5.2 Sensitivity analysis

Precipitation and Discharge correction factors

Approach 1: Brune model

2004

The sensitivity analysis of both the precipitation (cf_P) and discharge correction (cf_D) factor shows that a different correction factor than used has minimal effect on the Sediment Load (SL) in 2004.

Both graphs show that the correction factors of UMB-wet and LMB-wet have the largest effect on the SL (Table 4). However, this change in SL is relatively small, as the largest increase for the precipitation factor is a little over 1% and the lowest is almost 2%. For the discharge correction factor this is 2% and 1% respectively. Therefore, these factors do not impact the SL of 2004 significantly (Appendix E.2.1).

2020

The sensitivity analysis of both cf_P and cf_D shows that a different correction factor than used has more effect on the SL in 2020 compared to the SL in 2004 (Table 4).

Both graphs show that the correction factors of UMB-wet, MMB-wet and LMB-wet have the largest effect on the SL. Even though the decreasing percentages are relatively large, the absolute decrease is considered small (Appendix E.2.1).

2040

The sensitivity analysis of both cf_P and cf_D shows that a different correction factor for LMB-wet has effect on the SL in 2040 (Table 4). However, this effect can be considered minimal (Appendix E.2.1).

Approach 2: Defined TE model

2004

The sensitivity analysis of both cf_P and cf_D shows that a different correction factor than used has more effect on the SL compared to on the Brune model. Both graphs show that the correction factors of UMB-wet and LMB-wet have the largest effect on the SL (Table 4). This change in SL is larger than in the Brune model, as the largest increase for the precipitation factor is almost 3% and largest decrease is over 7%. For the discharge correction factor this is 2% and

5% respectively. Therefore, these factors have a larger impact on the calculation for the SL than in the Brune model (Appendix E.2.2).

2020

The pattern of the sensitivity analysis of the Defined TE model is similar to the Brune model analysis (Table 4). The only difference is that the Defined TE model is more sensitive to change in the correction factors compared to the Brune model (Appendix E.2.2).

2040

The sensitivity analysis shows that the 2040 Defined TE model is much more sensitive than for the Brune model. For both cf_P and cf_D , the LMB-wet has a large effect when the factors decrease (Appendix E.2.2).

Overall, the models are not sensitive to changes in correction factors.

Table 4: Categories for which the models are sensitive to a change in discharge and precipitation correction factors

Year	Brune & Defined TE Model
	cf_P & cf_D
2004	UMB-wet & LMB-wet
2020	UMB-wet, MMB-wet & LMB-wet
2040	LMB-wet

Sub-basin discharge

Approach 1: Brune model

Changing the discharges for the over or underestimated sub-basins does not have significant effect on the SL in 2004 and 2020 (Appendix E.3.1). However, the sensitivity analysis showed that the models are sensitive to a change in the correction factors and thus the discharge. This means that the sensitivity of the correction factors is caused by sub-basin without deviation. In the future situation, the SL is sensitive to changes in the underestimated discharge (Table 5).

Approach 2: Defined TE model

Changing the discharges for the overestimated sub-basins does not have a significant effect on the SL, whereas changing the discharge for the underestimated sub-basins has more effect on the SL in 2004 (Appendix E.3.2) (Table 5).

For the present model, the sensitivity analysis is almost similar to the Brune model, but changing the underestimated discharge has more effect than in the Brune model.

Contrary to the analysis of the Brune model for 2040, changing the underestimated discharge values has no effect and changing the overestimated discharges has effect (Table 5).

Overall, the models are not sensitive to changes in the over- and underestimated discharges.

Table 5 Sub-basin numbers for which the models are sensitive to a change in discharge
(Over and underestimated compared to Kummu et al. (2010))

Year	Brune		Defined TE	
	Overestimated	Underestimated	Overestimated	Underestimated
2004	9	19, 28	9, 10, 20, 22, 27	17, 19, 28
2020	27	28	10, 27	28
2040	n.a.	28	27	n.a.

Specific Sediment Yield

Approach 1: Brune model

The sensitivity analyses show that the SL for the baseline, the 2004 and the 2020 situation is extremely sensitive to a change in SSY in the UMB (sub-basin number 3) (Table 6) (Appendix E.1.1). This is caused by the high SSY of the UMB compared to the SSYs of the other sub-basins (Appendix B) because of the high elevation of the Tibetan Plateau and Three Rivers area (Figure 5) and the glaciers on the Tibetan Plateau.

The sensitivity analysis of 2040 shows that the SL is extremely sensitive to a decrease of SSY in sub-basins 11, 26, 27, 28 and 29 (Table 6) (Appendix E.1.1). These are the most downstream sub-catchments in the Mekong Basin, thus a decrease in SSY here has a more direct effect on the SL than a decrease in SSY further upstream. Furthermore, in these areas relatively many dams will be constructed (Figure 2), meaning that a decrease in SSY leads to less sediment passing the dam and thus a lower SL.

Approach 2: Defined TE model

Similar to the Brune model, the years 2004 and 2020 extremely sensitive to a change in the SSY in the UMB (Table 6)(sub basin number 3).

The 2040 situation is, similar to the Brune model, sensitive to a decrease of SSY in sub-basins 11, 26, 27, 28 and 29. However, now the model is also sensitive to an increase of SSY in sub-basin 26 (Table 6)(Appendix E.1.2).

Overall, the models tend to be sensitive to changes in SSY.

Table 6: Sub-basin numbers for which the models are sensitive to a change in SSY

Year	Brune	Defined TE
Baseline	3	3
2004	3	3
2020	3	3
2040	11, 27, 28, 29	11, 26, 27, 28, 29

Pre-defined TEs

2004 situation

The sensitivity graph shows that the model is sensitive to changes in TE of Mainstream-Reservoir-Dry and Mainstream-Reservoir-Wet. This is caused by the large storage capacity of mainstream reservoir dams and the high flows going through these types of dams. This causes them to trap high loads of sediment and thus have a more direct effect on the SL than (e.g.) tributary dams or dams with a smaller volume (Figure 17).

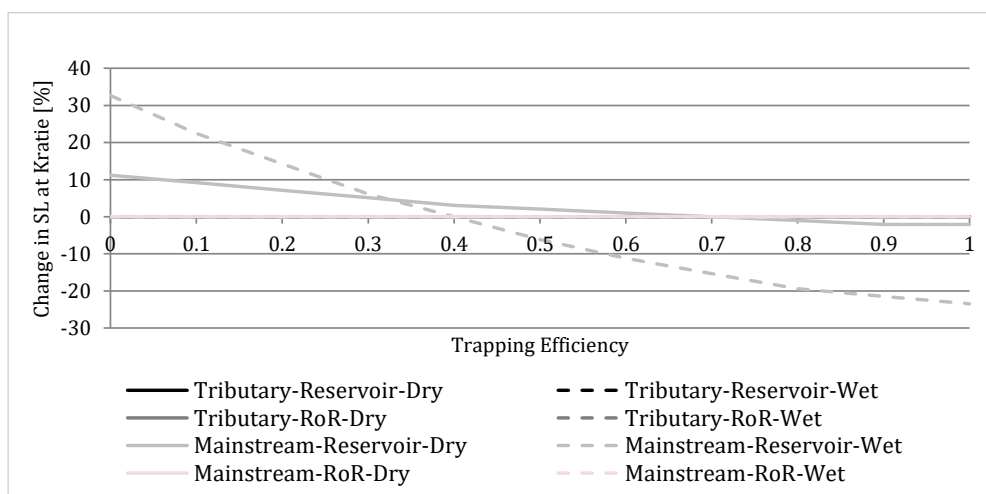


Figure 17: Sensitivity analysis of Defined TE's on the SL in 2004

2020 situation

The sensitivity graph shows that the model is extremely sensitive to changes in TE of Mainstream-Reservoir-Wet for similar reasons stated for the 2004 model. The model is also sensitive to a change in Mainstream-Reservoir-Wet and Mainstream-RoR-Wet (Figure 18).

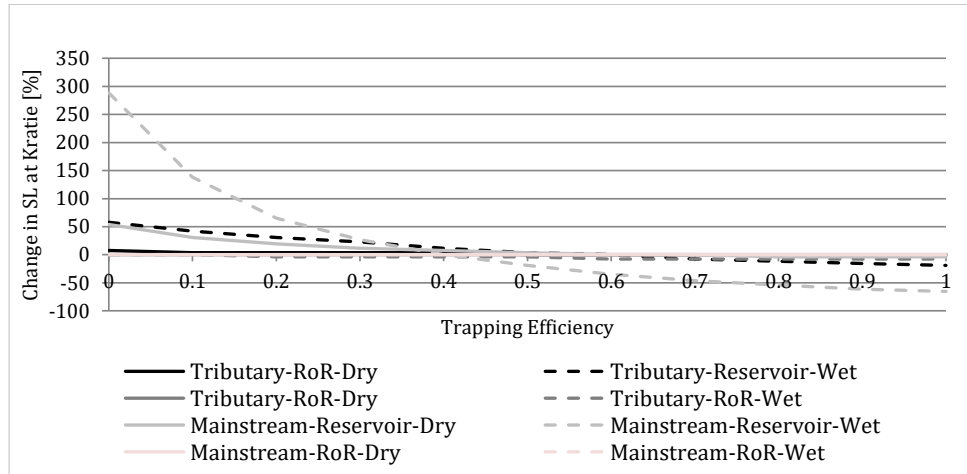


Figure 18: Sensitivity analysis of Defined TE's on the SL in 2020

2040 situation

The sensitivity graph shows that the model is extremely sensitive to changes in TE of Mainstream-Reservoir-Wet for the same reason explained in the 2004 model. Similar to the 2020 model, this model is also sensitive to a change in Mainstream-Reservoir-Dry and Mainstream-RoR-Wet (Figure 19).

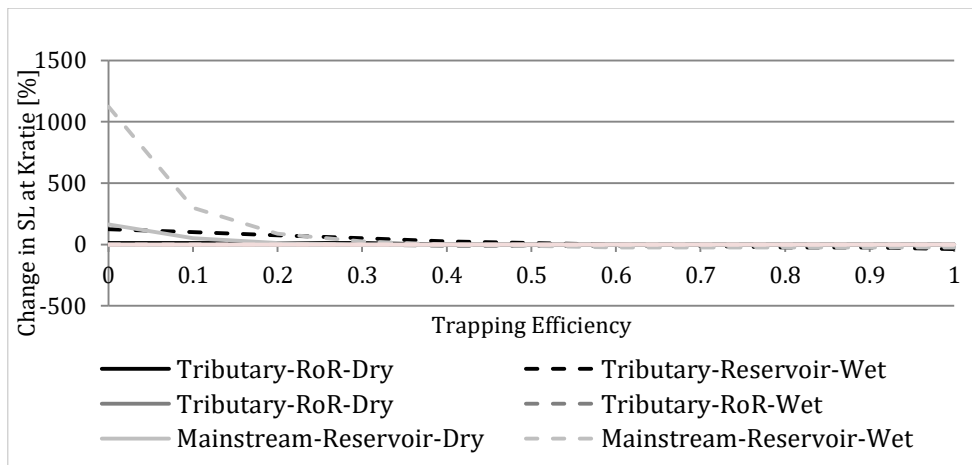


Figure 19: Sensitivity analysis of Defined TE's on the SL in 2040

Overall, the models tend to be sensitive to changes in the pre-defined TEs.

Glacier melting

According to Yao, et al. (2012), the retreat of glaciers on the Tibetan Plateau has become more intense since the 1990s. The retreat of glaciers has led to intensified meltwater and increased sediment availability, which has caused an increase in suspended sediment fluxes in proglacial areas (Lu et al., 2022). The Tibetan plateau contains 36,800 glaciers that cover a total area of 50,000 km², while the total area of the plateau is 2,500,000 km², meaning that 20% is covered in glaciers (Lu et al., 2022). The Tibetan Plateau covers 70,000 km² in the Mekong Basin, assuming this 20% also applies here means that 14000 km² of the Mekong Basin in the UMB consists of glaciers. According to Lu et al. (2022) the mean annual sediment yield of the glaciers in the Mekong Basin is 1739 t/km², which gives an annual SL of 24 Mt. If this doubles, the SL of UMB changes to almost 116 Mt/year and the annual SSY to 617 t/km². This value is in line with Chuenchum et al. (2020a), stating that the annual SSY of UMB is 611 t/km² in 2040 as a result of climate change and land use change.

If glacier melting was taken into account in the present model, it would have had an effect of almost 8% in both models, resulting in a SL at Kratie of 28 Mt instead of 26 Mt. However, the melting of glaciers has no effect on the future SL according to both models (Appendix E.4). Therefore, the models are not sensitive to changes in the pre-defined TEs.

Land Cover Change

In the whole basin, deforestation has been happening for many years. The land cover is often replaced by secondary growth or agricultural systems, which are prone to soil erosion and thus increase SLs (Carling, 2009)

Chuenchum et al. (2020a) has tried to estimate the SSYs of each sub-basin in 2040 as a result of climate change and land use change (Appendix B). Applying these SSY to the future scenario shows that the percentage increase is very significant and that the absolute numbers are relatively large. It changes the SL at Kratie calculated with the Brune model from 4 to 7 Mt and with the Defined TE model from 8 to 13 Mt.

4.6 Model result - Dam impact on silt and clay loads

This section explains the outcomes of the first research question “*What is the effect of hydropower dams in the Mekong Basin on the silt and clay loads in the Mekong Delta?*” The effect of the Mekong Basin, the sub-basins and the countries are discussed.

4.6.1 Impact of Mekong Basin

Hydropower dams have decreased the annual silt and clay load at Kratie dramatically the last decades. The annual sediment load (SL) was 140 ± 40 Mt before hydropower development and this has decreased to 26 ± 9 Mt in 2020. In the future this is expected to reduce another 70-85% resulting in extremely low SLs (Figure 20).

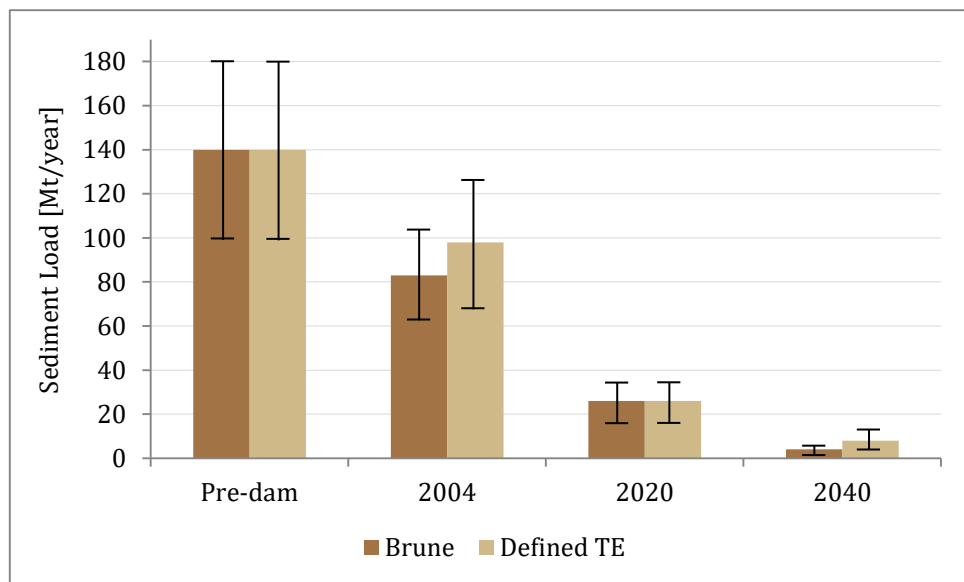


Figure 20: Effect of hydropower dams on the Sediment Load at Kratie over the years

This means that before hydropower development, the annual SL depositing in the delta was approximately 6 ± 2 Mt, which has decreased to 1 ± 0.5 Mt in 2020. With all future dams in operation the sediment delivery to the delta is expected to be close to zero (Figure 21).

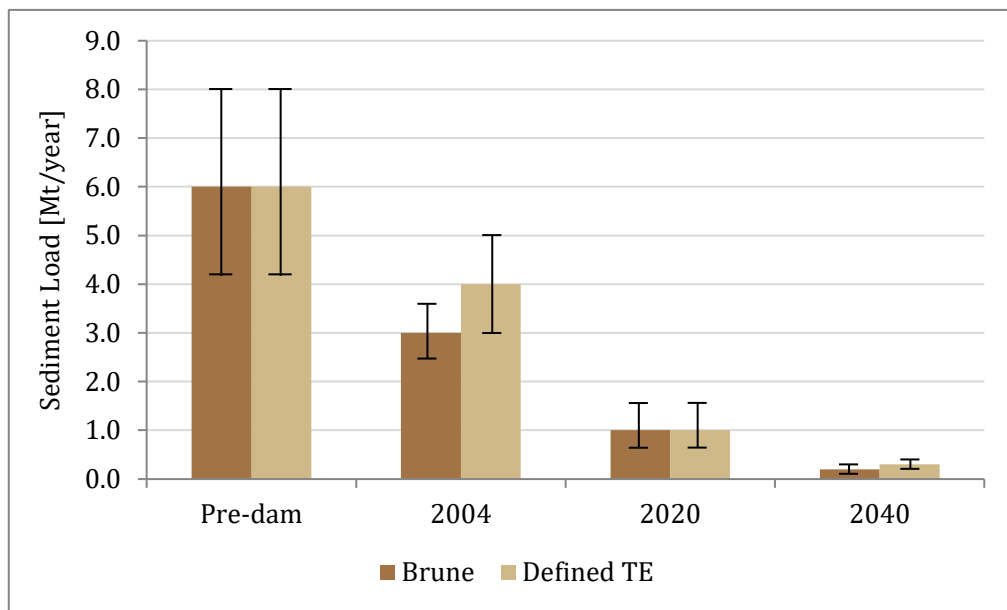


Figure 21: Effect of hydropower dams on the deposited Sediment Load in the Mekong Delta over the years

Both models calculate that the majority of the sediment is trapped in the mainstream dams even though they account for only 10% of the total dams in 2004 and 12% and 16% in 2020 and 2040 respectively (Figure 22). This is predominantly a result of the high sediment loads entering these dams because sediment coming from the tributaries also flow into these dams.

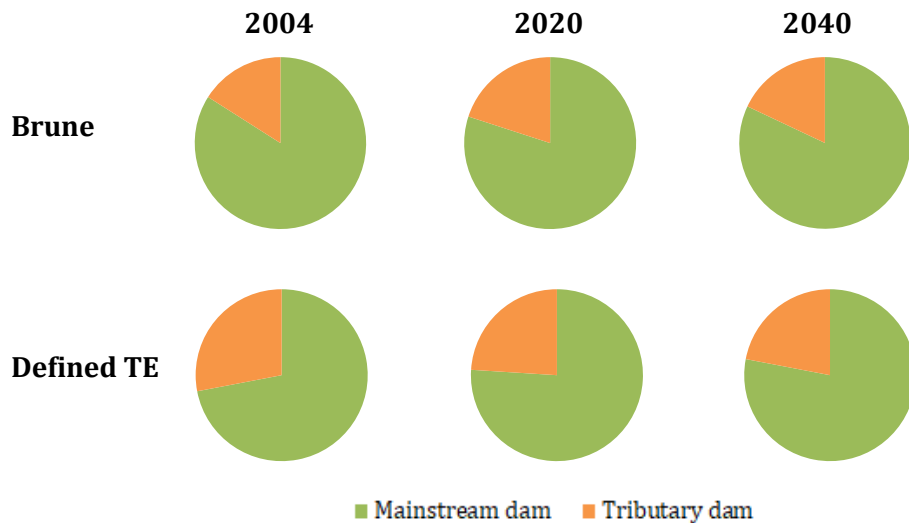


Figure 22: Trapped sediment in mainstream and tributary dams

Difference in models

The results of both models are very similar, the only significant deviation is the SL calculated for 2004, because the Brune model has calculated a significantly lower SL than the Defined TE model (Figure 20) (Figure 21).

The main cause of this deviation is related to the mainstream dams. The mainstream dams trap the majority of the sediment, but in the Brune model more sediment is trapped in the mainstream dams compared to the Defined TE model (Figure 22).

Furthermore, in 2004 only two mainstream dams were present in the Mekong Basin (Figure 2) (Appendix A). Both were situated in the Upper Mekong Basin and thus in the most upstream sub-basin. Since there are no other mainstream dams more downstream, the additional sediment (caused by the lower TE) is not trapped in other dams and reaches Kratie and the Delta.

Concluding, the higher SL calculated by the Defined TE model is a result of lower TEs and the small number of mainstream dams in 2004.

4.6.2 Impact per sub-basin

Impact change over the years

During the past years, most of the silt and clay was trapped in the Upper Mekong Basin (sub-basin 3) and this is expected to continue in the future according to both models (Figure 23). The high amount of mainstream dams in and the high SSY of the UMB cause the trapped SL to be extremely large (Appendix A) (Appendix B).

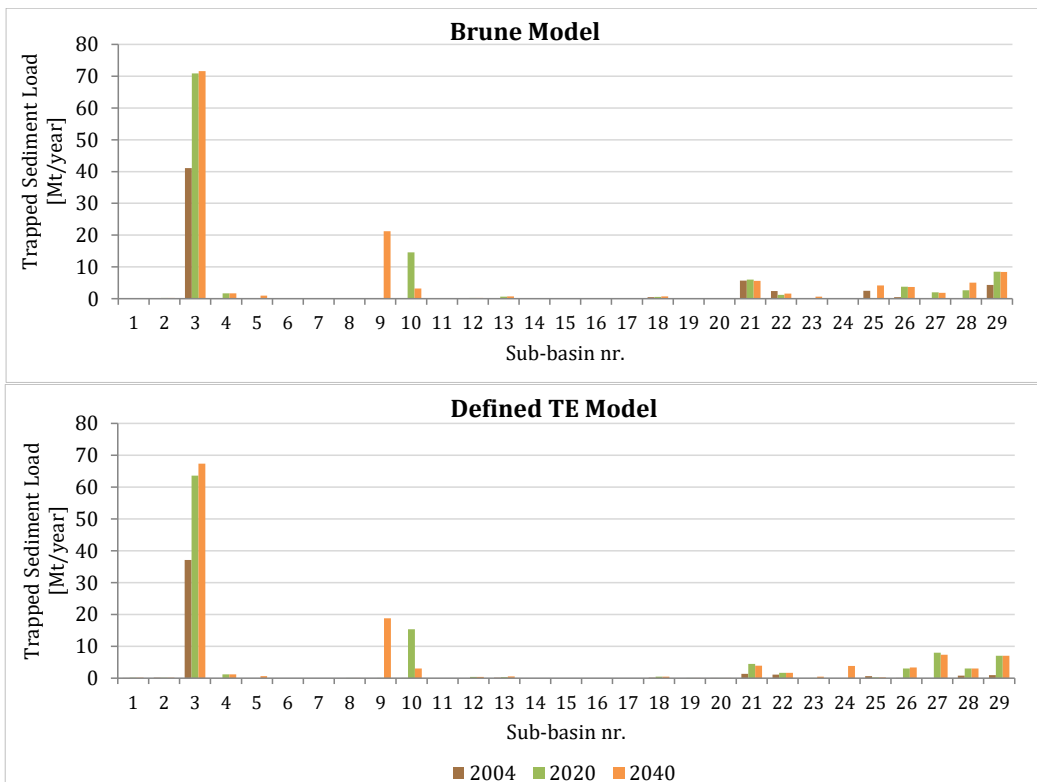


Figure 23: Trapped Sediment Load over the years per sub-basin

According to both models, the trapped SL is expected to increase the coming years in the sub-basins Nam Beng/Nam Ngeun (9) and Se Bang Nouan (24). This is a result of the planned construction of mainstream dams in these sub-basins (Figure 23) (Appendix A.3).

Another development that stands out is that even though three mainstream dams are expected in Huai Luang/Nam Phoung/Nam (10), the trapped SL is decreasing according to both models. This can be caused by the large amounts of trapped SL in sub-basin 9, which result in less sediment availability to be trapped in sub-basin 10 (Figure 23).

Again, it is visible that the sub-basins with mainstream dams trap the most sediment. Mainstream dams occur in the sub-basins 3, 9, 10, 24 and 27 in 2040. The other sub-basins that trap significantly amounts of sediment (21, 22, 26, 28 and 29) have relatively high baseline SLs and relatively many dams are present. For example the 3S basins (26, 28 and 29) have a combined baseline SL of 18 Mt (Figure 13).

Future impact

In 2040, it is expected that most of the total trapped sediment load gets trapped in the Upper Mekong Basin (53% and 51%) because of the high amount of mainstream dams with large active volumes and the high SSY of this sub-basin. Also sub-basin 9 is expected to trap a relatively amount of sediment (16% and 14%) which can be explained by the large amount of sediment leaving the UMB and the mainstream dams within the basin itself (Figure 24).

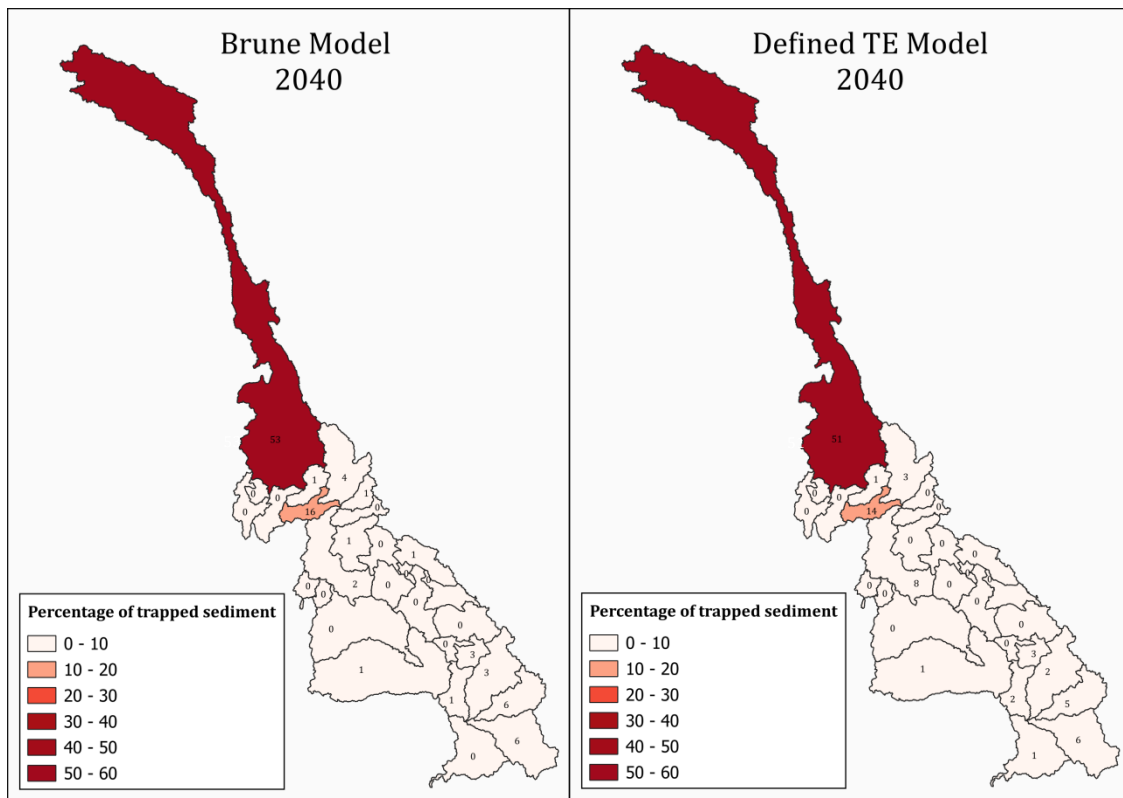


Figure 24: Percent contributions of each sub-basin to the Mekong's total annual SL in 2040

Over the years, the contribution of the UMB to the total downstream sediment load (SL) has decreased. In 2004 and 2020 the UMB contributed the most to the total SL, but both models calculated that in 2040 the UMB does not contribute the most anymore. This means that (almost) all sediment coming from the UMB gets trapped in the dams and does not reach the Delta in 2040. The Brune Model calculated that 0% of the sediment coming from the UMB reaches downstream, whereas the Defined TE Model calculated a contribution of 2%. This model difference is a result of the lower TEs of mainstream dams in the Defined TE model (Figure 25).

The contribution of the 3S Basins (Se Kong, Se San and Sre Pok) is expected to increase significantly the coming years. Both model calculated that this region contributes 80% and 85% in 2040 which is caused by their downstream location, meaning that there are no mainstream dams interfering. Furthermore, the mountain ranges located in this area cause relatively high SLs (Figure 25) (Appendix C).

The maps of 2040 show some differences between the two models. In the Se Kong sub-basin the Brune model calculated a contribution of 52% and the Defined TE model a contribution of 37%. However, the absolute difference is very small as for the Brune Model this means a contribution of 2 Mt and for the Defined TE model 3 Mt. This also holds for the other 2 sub-basins.

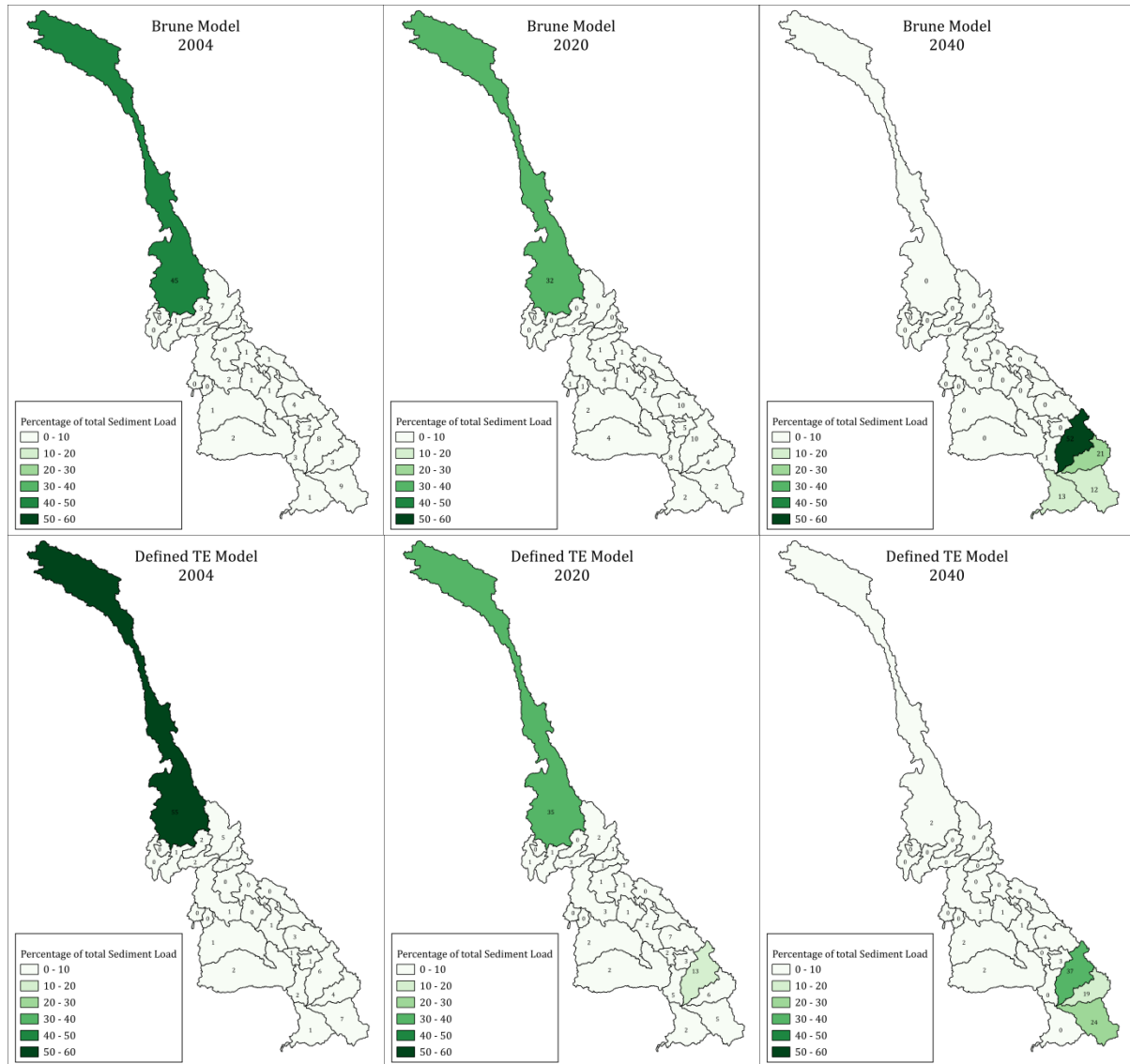


Figure 25: Percentage of total Sediment Load coming from the sub-basins

4.6.3 Impact per country

Both models calculated that most sediment gets trapped in the Chinese dams in the future even though only 15 dams are expected (Figure 26). The majority (13) of these dams are located on the mainstream and have very large active volumes with an average of 1.78 km^3 and two outliers: Nuazhadu (12.3 km^3) and Xiaowan (9.9 km^3).

In Laos less sediment will get trapped even though almost 8 times as many dams as in China will be present here in the future (Figure 26). Seven of these dams are mainstream dams and have smaller active volumes (average of 0.48 km^3) than the ones in China.

In Thailand and Cambodia almost the same amount of dams will be present in the river, but the amount of trapped sediment differs substantially. The absence of mainstream dams in Thailand causes less trapping, whereas the mainstream dam (active volume of 0.74 km^3) in Cambodia causes more trapping (Figure 26).

Three of the dams in Vietnam are mainstream dams with moderate active volumes (average 0.53 km^3).

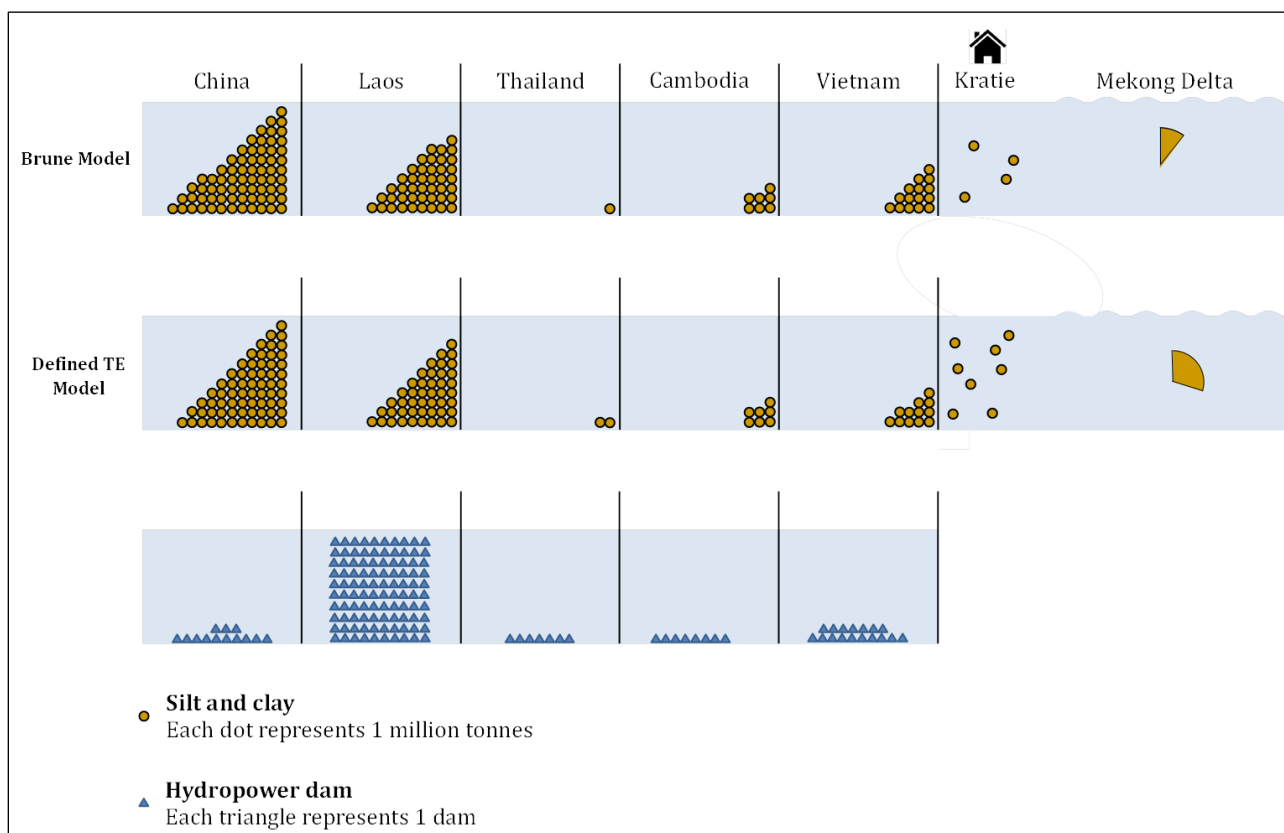


Figure 26: Trapped Sediment Load per country in 2040

The trapped SL per Chinese mainstream dam shows an important difference between the two models. In the Brune Model more variation between the trapped loads is visible because the TE is dependent on the active volume of the dam. In the Defined TE model less variation is recognisable because the TEs are independent on the active volume. The TEs in the Defined TE model are dependent on the season and dam type. This leads to more even distributions of the trapped sediment load (Figure 27).

However, it is clear that the Wu Nong Long, Li Di, Xiaowan and Nuazhadu dam trap the most sediment. This is result of the high loads coming from the Tibetan Plateau that are trapped in the first two dams and the large active volumes of the Xiaowan and Nuazhadu dam (Figure 27).

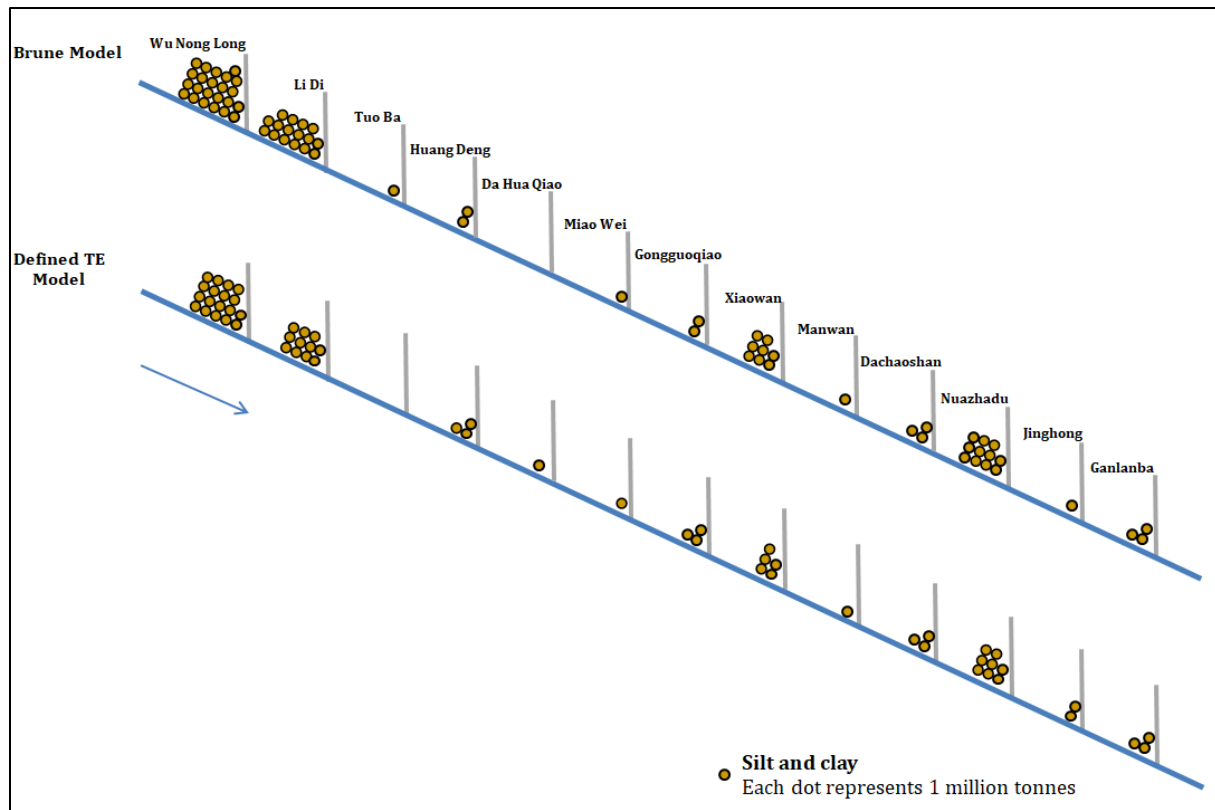


Figure 27: Trapped Sediment Load per Chinese mainstream dam in 2040

5. Strategies for Sediment Load increase

5.1 Overview of different strategies

There are multiple strategies for increasing the sediment load downstream of a reservoir:

1. **Reservoir flushing.** Flushing is removing deposited sediment by opening the lower outlets to decrease water levels and subsequently increase the flow velocities in the reservoir (Lai & Huang, 2021). This allows the incoming flow to wash away the deposited sediment. This technique is the most effective if (Morris & Fan, 2009):
 - The reservoir is located in a narrow valley with steep slopes
 - The reservoir has steep longitudinal slopes
 - The reservoir contains a low-level gate
 - The river discharge is sufficient to mobilize and transport sediment
 - The ratio of the reservoir storage and mean annual flow does not exceed 4%

For this strategy it is important that careful consideration is given to the most effective months for flushing. Also, a reservoir should be flushed in such a way that the sediment is not fully trapped again in the next dam.

It should be mentioned that only the middle part of the reservoir is flushed and that sediment at the sides are most likely to be left.

2. **Diversion channels and tunnels.** Sediment bypassing is converting part of the sediment-laden water around the reservoir during high flows. This means that water does not enter the reservoir when sediment concentrations are high. The sediment-laden waters are diverted into a channel or tunnel upstream of the reservoir that transports the water downstream of reservoirs where it enters the river (Kondolf et al., 2014). This strategy is the most effective if:
 - The reservoir is located in an area of high relief (Hydro, 2017).
 - The reservoir is relatively short because this leads to sufficient gradient for the bypass (Kondolf et al., 2014)
 - The bypass is situated at a location where the river has a sharp bend, such that the length of the channel or tunnel can be minimized and that the gradient can be used for gravity flow (Kondolf et al., 2014)

Consideration must be given where this may have the largest effect. One could consider applying this to dams in sub-basins that have a high sediment yield or in dams that retain a lot of sediment. It is also important to examine where the sediment should be directed to.

3. **Reservoir dredging.** Reservoir dredging is simply removing sediment from the reservoir itself. The dredged sediment can be returned to the river at a more downstream location (Hydro, 2017). It is also possible to direct sediment-laden waters to a reservoir, where all the sediment deposits and the sediment is later dredged. For this option some sort of silt collection system can be designed such that sediment can be removed in a concentrated manner (Kondolf et al., 2014).

For both dredging options, it is important to consider (Kondolf et al., 2014):

- The means of transport
- The frequency of dredging
- The location where the dredged sediment is deposited
- For the silt collection system it is also of high importance to think of a suitable location for the system.

It is important to mention that this strategy can be efficient but that dredging needs to continue for the timespan of the reservoir which can mean significant cost impacts (Hydro, 2017).

4. **Cancelling planned dams.** If dams are planned in a river basin, it may be beneficial to investigate whether the future sediment load increases if these planned dams are cancelled. This cancellation has effect on the energy generation in the area.
5. **Reservoir sluicing:** Sluicing is passing incoming sediment-laden water through the reservoir by discharging high flows to enable sediment to move past the dam without depositing (Lai & Huang, 2021; Morris & Fan, 2009). While some previously deposited sediment can be set in motion again (reservoir flushing), the main goal of sluicing is reducing incoming sediment trapping (Kondolf et al., 2014). An advantage of this strategy is that the sediment that passes the dam will be naturally discharged by the river during flood season (Kondolf et al., 2014). There are no clear conditions for reservoir sluicing, but the flow velocity in the reservoir should be sufficient to transport the sediment (Hydro, 2017).

5.2 Selected Strategies for the Mekong Basin

The strategies *Cancelling planned dams* and *Reservoir sluicing* were chosen for the Mekong Basin for two main reasons. For both strategies the reservoir and river must meet the least conditions and there is no investment required.

5.2.1 Strategy 1: Cancelling planned dams

The goal of this strategy was to find out which planned dams should not be constructed in order to maximize the future sediment load. In this report the future scenario is defined as all years after 2020, but at the time of writing, some of these dams have already been put into use. Furthermore, it takes approximately 5-10 years to finish a dam project in the Mekong Basin, which means that the construction of for example the dam *Mekong at Pakbeng* has already started even though it will be in operation in 2029. Therefore, despite the additional 31 dams in the future scenario, only 16 of these dams can possibly be cancelled (Appendix F.1).

If dams are not constructed, there is no additional active volume and consequently no extra trapping efficiency. This means that the active volumes and thus the TEs of the planned dams were zero in both models.

An analysis was executed in which every unique combination of dam cancellation is compared to the effect it has on the SL. According to MRC (2023c), over \$160 billion in economic benefits are projected if hydropower is fully developed by 2040. Therefore, it is of high importance for the countries in the Mekong Basin to keep investing in these types of dams. This explains why the optimum was established by searching for the highest SL generated by cancelling the least amount of dams.

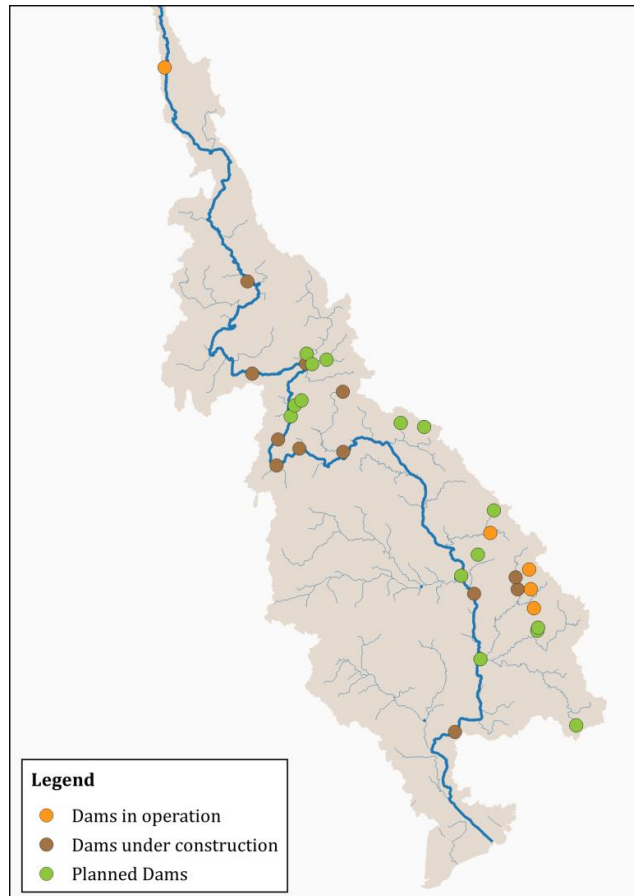


Figure 28: Future dams in the Mekong Basin

5.2.2 Strategy 2: Reservoir sluicing

Unlike strategy 1, it was assumed that all planned dams are constructed in the future. The goal of this strategy was to determine if more sediment reaches the delta if dams that trap relatively large amounts of sediment, are sluiced. The goal of reservoir sluicing is to enable sediment to move past the dam without depositing (Morris & Fan, 2009). This can be described as an optimisation strategy and is based on a research by Schmitt et al. (2018) that tried to improve the SL by strategic dam planning.

The settling distance of a particle was calculated in order to find out if it is useful to sluice a dam. The settling distance or length is defined as the longitudinal distance a sediment particle has travelled given an initial elevation before it settles for the first time. A sediment particle may settle more than once because a settled particle may become re-suspended again. However, the settling distance applies only to the first settling event (McNair, 2006). In the calculation it was assumed that the initial elevation of particles is the same as the average depth of the reservoir ($\bar{d}_{reservoir}$).

To calculate this distance (Equation 3.9), the average depth of the reservoir, the average flow velocity in the reservoir and the settling velocity of the sediment was calculated. For the calculation of the settling velocity of silt, the average particles size of silt (33 μm) was used.

The average depth of the reservoir was calculated by dividing the total volume of the reservoir by the area of the reservoir:

$$\bar{d}_{reservoir} = \frac{V_{total,reservoir}}{A_{reservoir}} \quad (3.6)$$

$\bar{d}_{reservoir}$	Average depth of the dam reservoir [m]
$V_{total,reservoir}$	Total volume of dam reservoir [m^3]
$A_{reservoir}$	Area of dam reservoir [m^2]

The average flow velocity in the reservoir was calculated by applying the simplified flow rate formula:

$$\bar{v}_{reservoir} = \frac{Q_{reservoir}}{A_{cross-sec,reservoir}} \quad (3.7)$$

$\bar{v}_{reservoir}$	Average flow velocity of the dam reservoir [m/s]
$Q_{reservoir}$	Flow rate in dam reservoir [m^3/s]
$A_{cross-sec,reservoir}$	Cross-sectional area of dam reservoir [m^2]

The settling velocity of clay and silt was calculated with the Stokes' formula:

$$w_s = \frac{(\rho_s - \rho_w) g \cdot D^2}{18\mu} \quad (3.8)$$

w_s	Settling velocity of sediment [m/s]	g	Gravitational field strength [m/s ²]
ρ_s	Mass density of the particle [kg/m^3]	D	Diameter of particle [m]
ρ_w	Mass density of water [kg/m^3]	μ	Dynamic viscosity [$kg/(m.s)$]

The settling distance was calculated with a very simple first approach in which turbulence in the water column was not considered:

$$l_{settling} = \frac{\bar{d}_{reservoir} \cdot \bar{v}_{reservoir}}{w_s} \quad (3.9)$$

$l_{settling}$	Settling distance of sediment [m]
$\bar{d}_{reservoir}$	Average depth of the dam reservoir [m]
$\bar{v}_{reservoir}$	Average flow velocity of the dam reservoir [m/s]
w_s	Settling velocity of sediment [m/s]

If the settling distance of the sediment was larger than the length of the reservoir, then it was considered useful to sluice the fine sediment through the reservoir and vice versa.

$$sluicing = \begin{cases} \text{useful}, & \text{if } l_{settling} > l_{reservoir} \\ \text{not useful}, & \text{if } l_{settling} < l_{reservoir} \end{cases} \quad (3.10)$$

For both clay and silt the utility of sluicing dams was calculated. If sluicing was calculated to be potentially useful, an analysis was executed in which every unique combination of sluicing was

compared to the effect on the SL. Similar to strategy 1, the optimum was established by searching for the highest SL at Kratie generated by sluicing the least amount of dams.

Two analyses have been conducted, one with a focus on sluicing in June and the other on sluicing in both May and June. This has multiple reasons.

First of all, hydropower energy generation is highly dependent on head and flow. A higher head results in higher water pressure through the turbine and therefore an increase in power generation. A higher water pressure also causes a faster rotating turbine, which means lower torque and thus less costs. Furthermore, it means that a smaller turbine can be used, which costs less than low-head turbines (Renewables, 2015). Also, in the wet season the demand of energy is less and other dams can run full power when others are sluiced. This explains why it is not preferred to sluice in the wet season.

Additionally, the reservoir level is low in May and June making sluicing more effective. The months July and August can then be used to fill the reservoir again. Also, the first floods at the beginning of the wet season contain the highest sediment loads (hysteresis) (Malutta et al., 2020).

6. Results – Strategy application to the Mekong Basin

This section explains the outcomes of the second sub-question “*What are possible strategies to mitigate the effect on the Mekong Delta?*” The effect of the two sediment management strategies on the SL at Kratie and the Delta is discussed.

The possibility of applying measures depends on the Mekong River Commission (MRC). The MRC is an “intergovernmental organisation that works directly with the governments of Cambodia, Laos, Thailand, and Vietnam to jointly manage the shared water resources and the sustainable development of the Mekong River” (MRC, 2017). Since China is not member of the MRC, fewer measures can be applied to dams in this country. Therefore, dams in China are not considered in the aforementioned strategies.

6.1 Results - Strategy 1: Cancelling planned dams

In the analysis 244 different combinations of cancelling planned dams were tested regarding the effect on both the Sediment Load (SL) at Kratie and the deposited SL in the Delta (Appendix F.1). The annual SLs in 2020 were calculated in the first sub-question and are 26 Mt at Kratie and 1 Mt in the Delta (Section 4.6) and are considered the maximum achievable Sediment Loads (SLs).

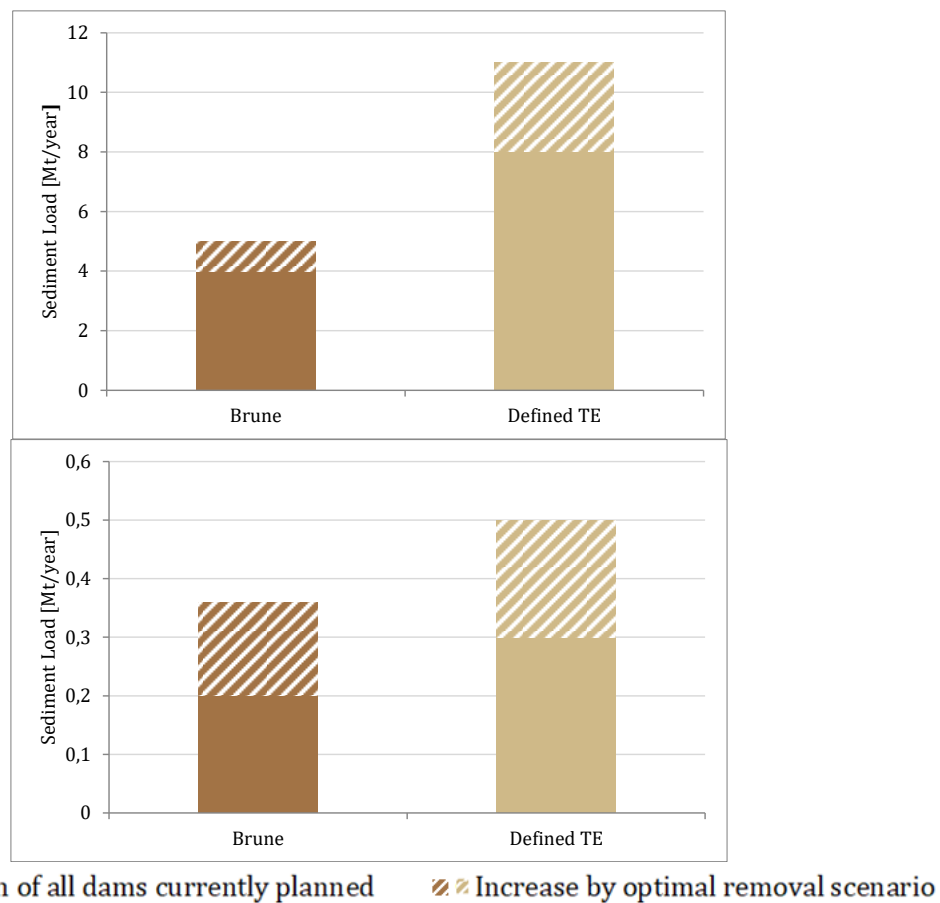


Figure 29: Maximum Sediment Load at Kratie (top) and the Delta (bottom) that can be achieved by cancelling planned

The term 'optimum' here means removing as few dams as possible in exchange for the highest possible SL. The analysis of the Brune model showed that the maximum increase in SL at Kratie is 1 Mt and in the Delta 0.15 Mt, an increase of 25%. The optimum is cancelling the Stung Treng dam, which will reduce the annual energy generation by 9% (Figure 29) (Figure 30) (Appendix F.1.1).

The analysis of the Defined TE model shows that the maximum increase in SL at Kratie is 3 Mt and 0.2 Mt in the Delta, an increase of 38%. There is one optimum: cancelling the Stung Treng dam together with the Mekong at Ban Kum, both mainstream dams. This reduces the annual energy generation by 23% (Figure 29) (Figure 30) (Appendix F.1.2).

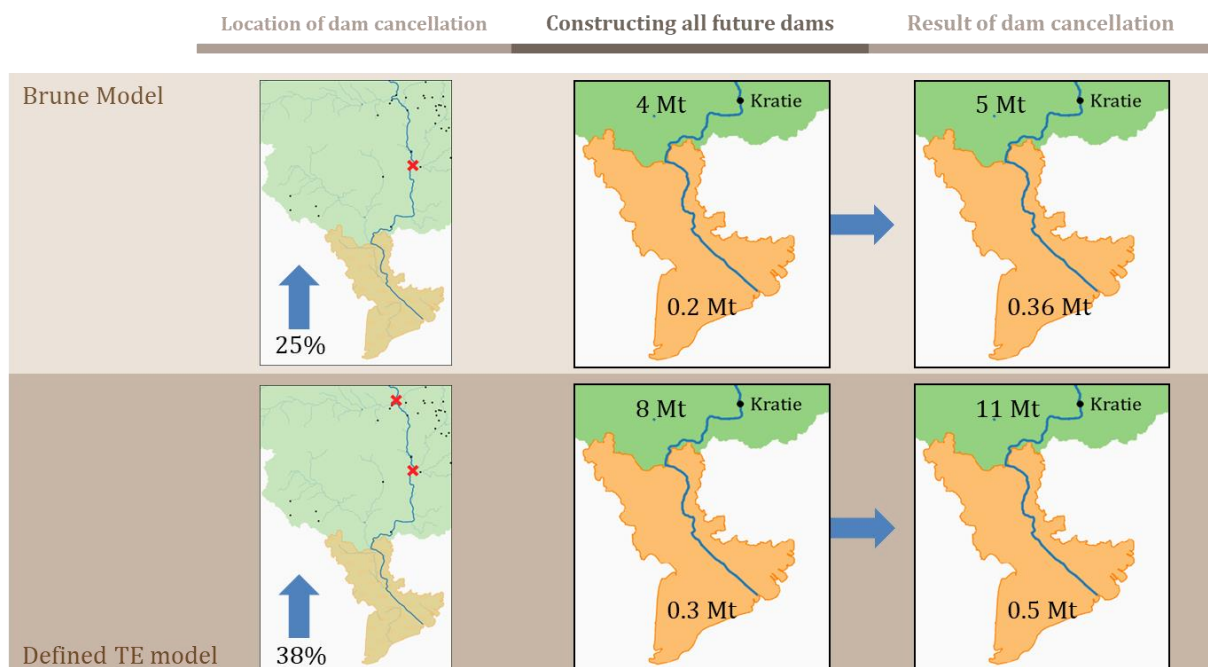


Figure 30: Effect of optimal dam cancellation on the Sediment Load at Kratie and in the Delta

The analysis showed that the maximum SL at Kratie cannot be approached (Figure 29) and that the SL increase in the Delta is minimal. The majority of the sediment is namely trapped in dams that are in operation or currently under construction (Figure 31). Therefore, it remains to be determined whether this increase is worth the decrease in energy generation.

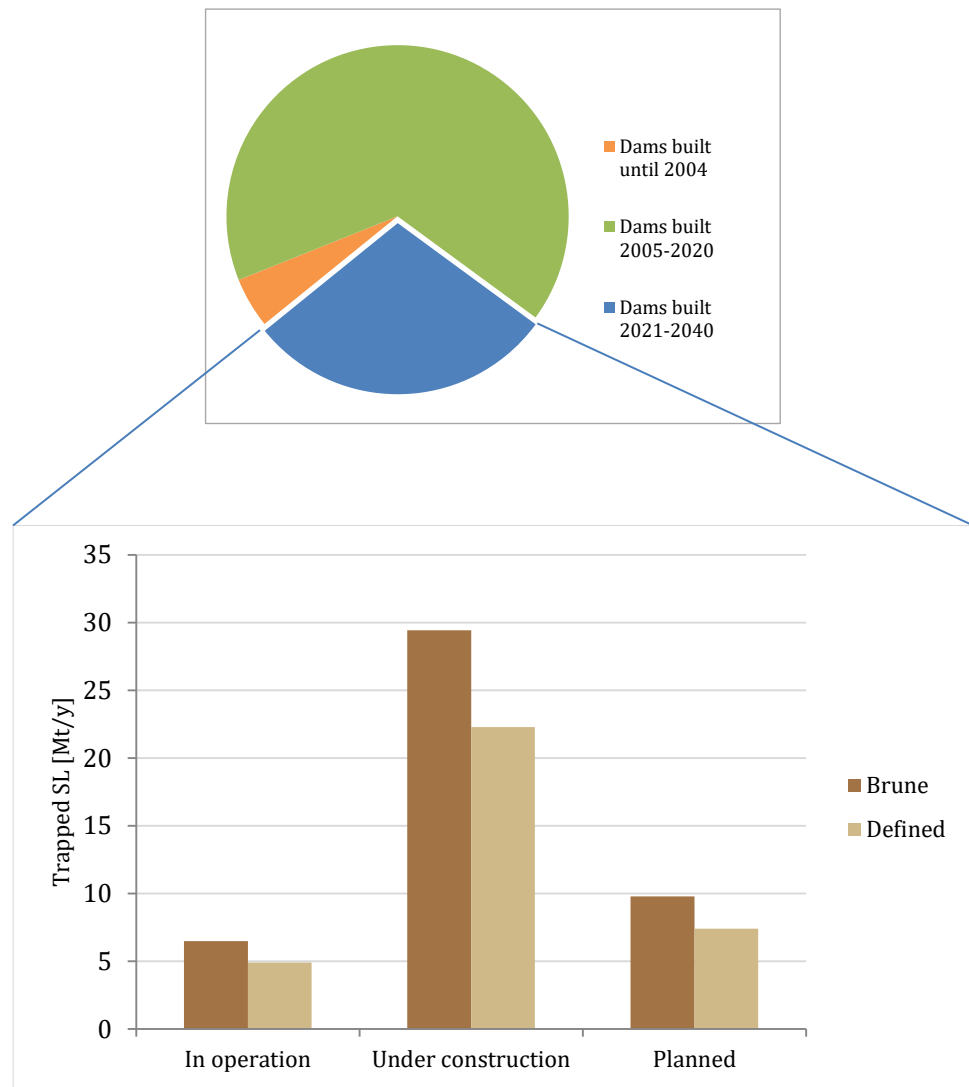


Figure 31: Top figure: Trapped Sediment Load per period of dam construction. Bottom figure: Trapped SL in future dams for dams that are in operation, under construction and planned

6.2 Results - Strategy 2: Reservoir sluicing

First a selection was made based on the contribution of each dam to the low SL at Kratie and the Delta in the future. Dams that trap 1% or more of the total trapped SL are selected. The Chinese dams are not part of the MRC, so they have been left out of the selection even though these dams have the highest contribution. This means that for the Brune model, 9 dams were considered and 12 dams in the Defined TE model (Table 7).

The settling length of silt and clay per month was calculated for all these dams. The higher settling velocity of silt resulted in a smaller settling length compared to clay. Since the reservoir lengths are fixed and the settling length of silt is smaller, the calculation showed that reservoir sluicing is far less effective for silt than for clay (Appendix F.2).

Therefore, the analysis has merely been applied to clay. The suspended sediment consists for approximately 50% of clay, thus the calculated increase of SL at Kratie and the Delta was divided by two (Walling, 2009). This is a crude assumption, but useful to make a comparison.

Table 7: Dams with highest contribution to the low SL at Kratie and the Delta and their accompanying percentage of trapped sediment for both the Brune model and the Defined TE model.

Sub-basin nr.	Dam Name	Trapped sediment (%) Brune	Trapped sediment (%) Fixed	Country
3	Dachaoshan	2	2	China
3	Gongguoqiao	1	2	China
3	Jinghong	2	4	China
3	Li Di	11	7	China
3	Nuazhadu	8	5	China
3	Tuo Ba	1	0	China
3	Wu Nong Long	17	13	China
3	Xiaowan	6	4	China
3	Huang Deng	1	5	China
3	Da Hua Qiao	<1	3	China
3	Manwan	1	2	China
4	Nam Tha 1	1	1	Laos
9	Mekong at Pakbeng	9	9	Laos
9	Mekong at Luangprabang	6	5	Laos
10	Mekong at Xayabuly	1	4	Laos
10	Mekong at Paklay	<1	2	Laos
10	Mekong at Sanakham	<1	2	Laos
21	Nam Ou 3	1	<1	Laos
22	Pak Mun	1	1	Thailand
24	Mekong at Ban Kum	3	3	Vietnam
27	Mekong at Don sahong	1	2	Laos
27	Mekong at Latsua (Phou Ngoy)	4	2	Vietnam
27	Stung Treng	1	1	Vietnam
29	Lower Se San 2	1	2	Cambodia
29	Lower Sre Pok 3 (3A)	2	2	Cambodia

6.2.1 Brune Model

The analyses of reservoir sluicing (Section 5.2.2) showed that it may be effective for 6 dams (Appendix F.2). All reservoir sluicing combinations of these dams were tested regarding their effect on the Sediment Load (SL) at Kratie and the Delta.

Reservoir sluicing in June

The results of reservoir sluicing in June show that the maximum SL increase is 25% by sluicing the Lower Se San 2 dam (Appendix F.2). This results in a SL of 5 Mt at Kratie and a SL of 0.25 Mt in the Delta (Figure 33).

Reservoir sluicing in May and June

The outcomes of May and June show that the maximum SL increase is 50% resulting in a SL of 6 Mt at Kratie and a SL of 0.3 Mt in the Delta (Figure 33). This is achieved by the following sluicing combination: sluicing the Lower Se San 2 and Lower Sre Pok 3 (3A) dams in May and flushing Nam Tha 1, Mekong at Ban Kum, Mekong at Don Sahong, Mekong at Latsua (Phou Ngoy), Lower Se San 2 and Lower Sre Pok 3 (3A) in June (Figure 32) (Appendix F.2).

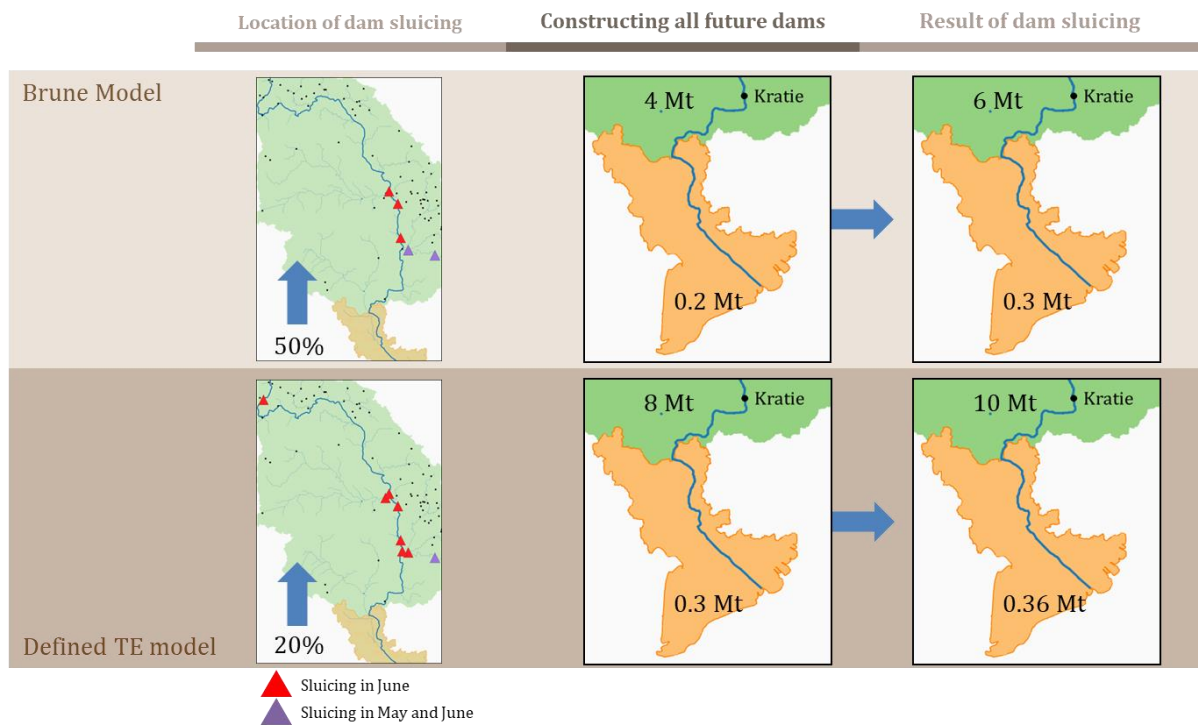


Figure 32: Effect of optimal reservoir sluicing on the Sediment Load at Kratie and in the Delta

6.2.2 Defined TE Model

The analyses of reservoir sluicing showed that it may be effective for 8 dams (Appendix F.2). All reservoir sluicing combinations of these dams were tested regarding their effect on the Sediment Load (SL) at Kratie and the Delta.

Reservoir sluicing in June

The results of reservoir sluicing in June show that the maximum SL increase is 12.5%, which can be achieved by 3 optima (Appendix F.2). This results in a SL of 9 Mt at Kratie and 0.34 Mt in the Delta (Figure 33).

Reservoir sluicing in May and June

The outcomes of May and June show that the maximum SL increase is 20% resulting in a SL of 10 Mt at Kratie and 0.36 in the Delta (Figure 33). This is achieved by the following sluicing combination: sluicing Lower Sre Pok 3 (3A) in May and flushing Mekong at Paklay, Pak Mun, Mekong at Ban Kum, Mekong at Don Sahong, Mekong at Latsua (Phou Ngoy), Stung Treng, Lower Se San 2 and Lower Sre Pok 3 (3A) in June (Appendix F.2) (Figure 32).

The low increase of SL in both models is caused by not including the Chinese dams. The majority of the total trapped sediment load is namely trapped in China (Table 7).

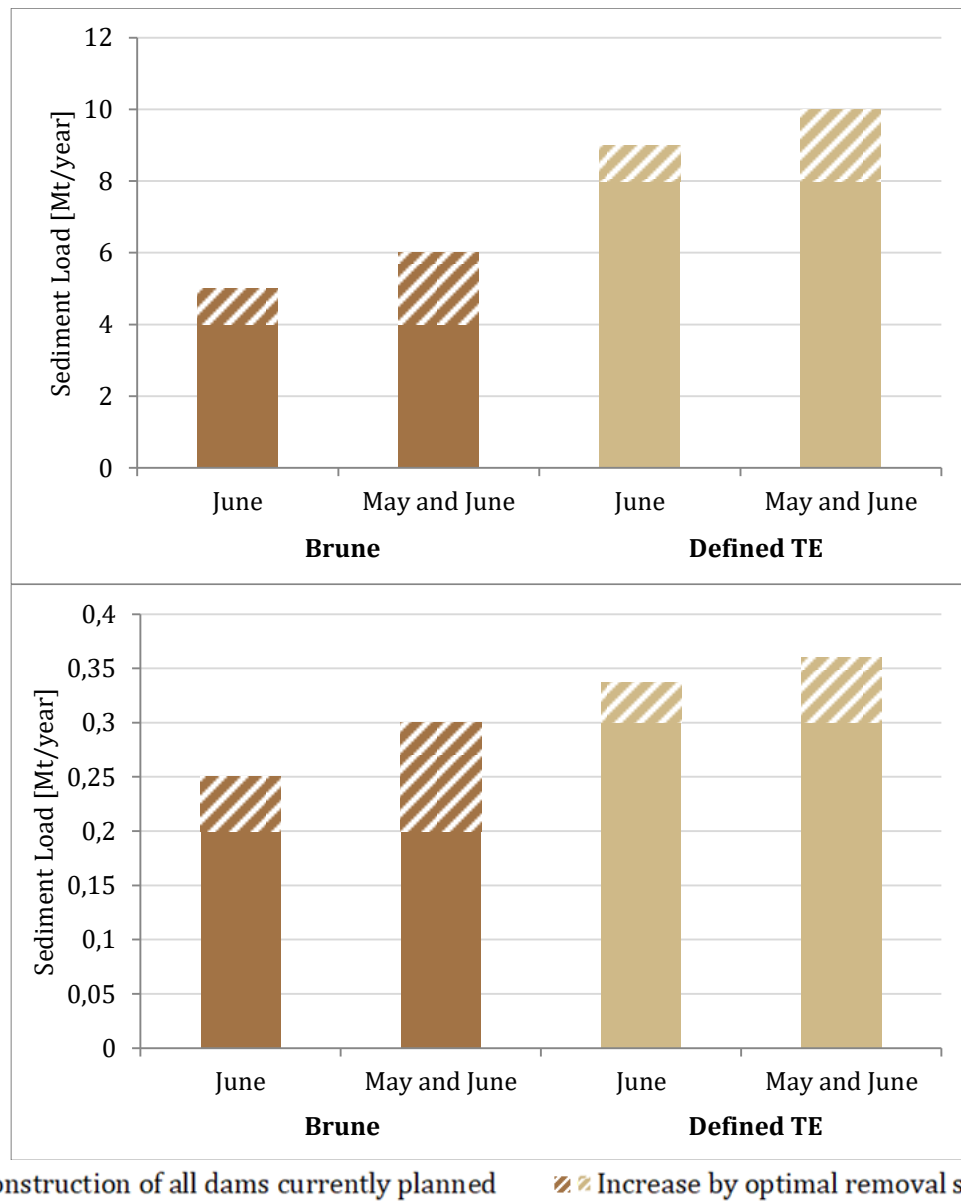


Figure 33: Maximum Sediment Load at Kratie (top) and the Delta (bottom) that can be achieved by reservoir sluicing

7. Discussion

The outcomes have provided insight into the effects of hydropower dams on the silt and clay loads in the Delta and into the effectiveness of two sediment management strategies to increase the sediment load. However, the results should be interpreted with caution due to the limitations of the research. This chapter provides an overview of these restraints and of implications for the interpretation of the results.

7.1 Discussion - Dam impact on silt and clay loads

The research has showed that the sediment load (SL) was 140 ± 40 Mt at Kratie and 6 ± 2 Mt in the Delta before hydropower construction. This outcome was compared to other literature studies that have estimated the baseline SL.

The result is in line with Ha et al. (2018) that estimated an annual sediment load at Kratie before 1980 of 145-160 Mt and with Chua & Xi (2022) that states it was 150-170 Mt before 1992.

The impact of operational dams on the sediment load at Kratie and the Delta over the years was determined with the help of the two approaches.

In the 2004 situation the impact of operational dams on the sediment load at Kratie and the Delta was determined. The first approach calculated a SL at Kratie of 83 ± 20 Mt and a SL in the Delta of 3 ± 0.6 Mt. The second approach determined a SL of 98 ± 31 Mt and 4 ± 1 Mt respectively. These results are in line with Sok et al. (2020) that states that in 2003 the average suspended load at Kratie was approximately 90 Mt.

In the present situation the impact of operational dams on the sediment load at Kratie and the Delta in 2020 was determined. Both approaches calculated an annual SL at Kratie of 26 ± 9 Mt and a SL in the Delta of 1 ± 0.5 Mt. The result tends to be in line with Chua & Xi (2022) and MRC (2018) that estimate an annual SL (including coarse material) at Kratie of 50 Mt in 2017-2020 and with Ha et al. (2018) that approximated a SL of 40 Mt in the period 2009-2016.

In the future situation the impact of operational dams on the sediment load at Kratie and the Delta in 2040 was determined. The first approach calculated a load at Kratie of 4 ± 3 Mt and a load in the Delta of 0.1 ± 0.05 Mt. The second approach determined a load of 8 ± 5 Mt and 0.3 ± 0.1 Mt respectively. These results correspond to MRC (2018) that estimate a future sediment load at Kratie of 5 Mt in 2040 and with Kondolf et al. (2013) that calculated that 4% of the pre-dam sediment load is expected to reach Kratie when all planned dams are constructed. In this study this would resemble almost 6 Mt.

Regardless of the above, some limitations are worth noting.

The study mainly focusses on the sediment load at Kratie in order to make comparison to other literature simple. However, dam development also changes the hydrological regime of the river which determines how much silt and clay remains behind on the floodplains and in the Tonle Sap Lake. This means that the effect on the Vietnamese Delta is not exactly the same as the effect on Kratie, even though this was assumed in the research.

For the calculation of the trapping efficiency (TE) the Brune Model was applied. Yet, the Brune method is developed based on data from 44 reservoirs in the USA, which means that it is based on annual averages and moderate climates (Mulu & Dwarakishb, 2015). This makes the method less suitable for monthly averages and rain season discharges and thus for the type of research conducted. However, this method is suitable as first indication for the TE of dams.

Not only the increasing hydropower development but also other human activities can have an impact on the suspended SL of a river (Walling, 2009). Land use changes such as deforestation are increasing sub-basin SSYs and thus the SLs in the sub-basins (Carling, 2009). On the other

hand, mineral extraction and sand mining activities tend to decrease the sediment transport in the Mekong River (Walling, 2009), which was described by Deltares and CEFID (2023). The sensitivity analysis showed that both approaches are sensitive to changes in the Specific Sediment Yield and land cover change.

Four main assumptions were made in the models: no change in hydrological regime, no storage component, no dam opening and no hysteresis (Section 3.2.1). These assumptions were made because of unknown details.

Nevertheless, if these aspects were considered, they may have had an effect on the calculated SLs.

Hydropower dams change the hydrological regime in a river and consequently the sediment transportation pattern is affected. The Specific Sediment Yield does not change due to hydropower development, thus a changing discharge distribution only impacts the SL if clay and silt are less likely to be washed away at low discharges and partly remain behind in reservoirs or on floodplains and vice versa. Since the models do not contain such a “storage” component, including this discharge change would have little or no effect on the monthly and annual SL (Räsänen et al., 2017).

The annual SL most likely increases when dam opening and hysteresis were included in the models.

When reservoirs are filled and suddenly all water is released, a peak of sediment enters the river. This may decrease the TE of a dam and increase the amount of sediment transported by the river. Hysteresis increases the sediment transport in the months at the beginning of the wet season, also leading to a higher SL downstream. However, the exact effect is unknown.

7.2 Discussion – Two strategies to mitigate the impact on silt and clay loads

7.2.1 Discussion strategy 1: Cancelling planned dams

The impact of cancelling planned dams in the Mekong Basin on the future sediment load at Kratie and the Delta was tested with two approaches. Both models calculated a different optimum of which the absolute sediment load increase was lower than anticipated because the majority of the sediment is trapped in dams built between 2005 and 2020 and not in those built after 2030. This is in line with Chuenchum et al. (2023), confirming that most sediment accumulates in reservoirs built until 2018. Therefore, it should be considered if the increase in SL is worth the decrease in annual energy generation.

7.2.2 Discussion strategy 2: Reservoir sluicing

The impact of reservoir sluicing in the Mekong Basin on the future SL at Kratie and the Delta was tested with two approaches. Both models calculated a different optimum, but both resulted in a lower SL than calculated for cancelling planned dams. The Chinese dams were not included in this strategy even though half of the total trapped sediment load is trapped in these dams. This explains why the SL increase is low.

This is in line with Kondolf et al. (2013), confirming that more than 40% of the SL of the Mekong will get lost in the reservoirs of the Upper Mekong Basin.

However, some limitations are worth noting.

In order to calculate the effectiveness of sluicing, the settling length was compared to the reservoir length to check if the flows were able to transport the sediment past the dam without depositing.

The length of the reservoirs was based on maps because of the absence of this data. A larger actual length would mean less effectiveness of sluicing and vice versa.

For the calculation of the average flow velocity in the dam reservoir, the continuity equation was used. This equation is used for the analysis of uniform flow of fluids and is based on the principle of mass conservation for a steady, one-dimensional flow. In other words, the mean velocities are equal at all cross sections having equal areas. As a first indication, this method is sufficient to calculate the average flow velocity in a water column. However, a larger actual flow velocity would mean a larger settling length and therefore a higher effectiveness of sluicing (and vice versa).

Another simplified formula was used for the calculation of the average depth of the dam reservoir. It was assumed that the reservoir has a rectangular shape and that the depth is equal everywhere in the reservoir. It gives a first indication on the average depth in the reservoir, but a larger actual depth would result in a lower flow velocity and consequently a lower settling length. This would mean a lower effectiveness of sluicing.

For the computation of the settling distance a simplified formula was applied which did not consider turbulence. It is very likely that the calculated settling length is in reality larger due to turbulence, resulting in a higher effectiveness of sluicing.

Most notably, this is the first study to my knowledge to investigate the effectiveness of cancelling planned dams and sluicing on the future SL as previous research has mainly focused on mapping future SL. The results validate that more research is needed into the effects of other strategies on the silt and clay load in the Mekong Delta.

8. Conclusion

The hydropower development in the Mekong Basin affects the silt and clay concentrations in the river which has ecological as well as socio-economic effects on the Mekong Delta and its inhabitants. Therefore, the first objective of this research was to obtain a better understanding of the effects of hydropower dams in the Mekong Basin on silt and clay loads in the Mekong Delta. The second objective was to determine possible sediment management strategies to mitigate negative impacts on silt and clay concentrations in the Mekong Delta caused by the hydropower dams in the Mekong Basin. In order to meet these objectives, the following research questions were answered:

- What is the effect of hydropower dams in the Mekong Basin on the silt and clay loads in the Mekong Delta?
- What are possible strategies to mitigate the effect on the silt and clay loads in the Mekong Delta?

It was estimated by means of a sediment balance model with distributed sediment yield and individual trapping efficiencies of dams that the annual sediment load at Kratie was 140 ± 40 Mt before hydropower development. This has decreased to 26 ± 9 Mt in 2020 and is expected to reduce to $4-8 \pm 3-5$ Mt the coming decades due to dam development.

In the Mekong Delta, the deposited load has decreased from 6 ± 2 Mt/year before dam development to 1 ± 0.5 Mt/year in 2020 and is expected to be close to zero in 2040.

Both models calculated that approximately 80-85% of the sediment load that reaches the Delta in 2040 has its source in the 3S region (Se Kong, Se San and Sre Pok). This is caused by its downstream location and the presence of the mountain ranges Kontum Massif and Volcanic Uplands that provide large loads of sediment transport.

The significant future reduction is largely caused by the Chinese dams that trap approximately 50% of the total trapped sediment load even though they account for 9% of the total amount of dams. This is caused by high loads of sediment transportation due to mountainous areas, large reservoirs having large trapping efficiencies and a long mainstream dam cascade.

All mainstream dams combined trap 75% of the total trapped sediment load even though they account for 16% of the total amount of dams. Two of these mainstream dams are run-or-river dams, which trap far less sediment (1%) compared to the reservoir mainstream dams (77%). The high sediment trapping of the mainstream dams is not a result of large trapping efficiencies, but rather of large sediment fluxes entering these reservoirs. Sediment coming from tributaries also enters these reservoirs leading to higher amounts of trapped sediment.

This indicates that hydropower dams have a significant effect on the silt and clay concentrations in the Mekong Delta and that sediment management strategies are urgently needed in order for the Mekong Delta to sustain ecosystems and to maintain its high productivity.

Two sediment management strategies were reviewed in this research: cancelling planned dams and reservoir sluicing.

The analysis showed that cancelling mainstream dams is the most effective. However, the maximum sediment load increase at Kratie is only 1-3 Mt and in the Delta 0.03-0.1 Mt. Most of the sediment is trapped in operational dams or dams that are currently under construction. The contribution of the planned dams is much smaller, which explains the low sediment load increase.

The analysis also demonstrated that sluicing mainstream and the most downstream tributary dams is the most effective. However, the maximum sediment load increase at Kratie is only 2-3 Mt and in the Delta 0.05-0.1 Mt. Most of the sediment is trapped in Chinese dams, but these were not included in this study. The contribution of the other mainstream dams is much smaller, which explains the low sediment load increase.

The effect of both strategies on the sediment load at Kratie and the Delta is lower than anticipated, suggesting that these strategies are not providing the solution for the Mekong Basin. However, the results indicate that effective sediment management strategies are urgently needed and that more research is needed into the effects of other strategies on the silt and clay load in the Mekong Delta.

9. Recommendations

The current study can be interpreted as a first step in the research on sediment management strategies for the Mekong Basin. However, the results of this study should be treated with caution due to the absence of specific details in the models. Therefore, future research could further improve the model accuracy by modelling more details such as the reservoir flow velocity or the falling velocity of the sediment particles in the reservoir. Also, modelling the higher concentration peaks during dam opening or river turbidity improves the accuracy of the model.

This results in better estimations of the sediment transport and trapping efficiencies of the hydropower dams and thus in more accurate calculations of the annual sediment loads. This will also lead to better assessments on whether and if so, how adequately strategies work to increase the annual sediment load downstream.

The effect of two sediment management strategies on the sediment load has been examined in this research. However, there are many other strategies that could be tested in future research. Examples are sediment bypassing by means of diversion channels and tunnels, reservoir flushing and reservoir dredging. Moreover, an operation strategy with "alternating sluicing" (e.g. sluicing 1 dam every year) of dam cascades could be examined.

Applying a strategy in the Upper Mekong Basin is recommended because approximately half of the total trapped sediment load is trapped in the Chinese dam cascade in 2040. It is most likely the most effective if the mainstream dams outside China are also included in such a strategy since the mainstream dams outside China trap 25% of the total trapped sediment load.

This immense amount of trapping is the reason why it is advised to limit the construction of dams on the mainstream river in the future. This will further increase sediment trapping and decrease the deposited sediment load in the Delta.

Furthermore, it is recommended not to propose new projects for the 3S (Se Kong, Se San and Sre Pok) region because approximately 80-85% of the future annual sediment load has its source in this region. By proposing new dam projects in this area, the trapped sediment load increases and the sediment delivery to the Delta decreases which can have disastrous effects.

The downstream sediment load tends to increase if strategies are applied in China, the mainstream dams and/or the 3S basins. Therefore, construction of additional dams in these areas is not recommended and sediment management strategies are advised.

In summary, these are the recommendations for practitioners:

- Limit the construction of hydropower dams on the mainstream river
- Do not propose new dam projects in the 3S region
- Apply sediment management strategies in the Upper Mekong Basin to decrease the trapping efficiencies of the Chinese dams
- Apply sediment management strategies in the mainstream dams and the 3S region

Bibliography

- Annandale, G. W., Morris, G. L., & Karki, P. (2016). *Extending the Life of Reservoirs - Sustainable Sediment Management for Dams and Run-of-River Hydropower*. Washington: World Bank Group.
- Anthony, E. J., Brunier, G., Basset, M., Goichot, M., Dussouillez, P., & Nguyen, V. (2015). Linking rapid erosion of the Mekong River delta to human activities. *Scientific Reports*, 5:14745.
- ArcGIS. (2023, September 25). *How inverse distance weighted interpolation works*. Retrieved from Esri: <https://pro.arcgis.com/en/pro-app/latest/help/analysis/geostatistical-analyst/how-inverse-distance-weighted-interpolation-works.htm#:~:text=As%20p%20increases%2C%20the%20weights,points%20will%20influence%20the%20prediction.&text=Geostatistical%20Analyst%2>
- Assallay, A. M., Rogers, C. D., Smalley, I. J., & Jefferson, I. F. (1998). Silt: 2–62 µm, 9–4φ. *Earth-Science Reviews*, (45)61–88.
- Baran, E., Guerin, E., & Nasielski, J. (2015). *Fish, Sediment and Dams in the Mekong*. Penang: WorldFish, and CGIAR Research Program on Water, Land and Ecosystems (WLE).
- Bayoudh, M., Touati, H., & N'Ticha, H. B. (2019). Study of the effect of particles on the kinetic parameters of a. *Energy Procedia*, 162: 201–210.
- Behrami, E., Xhaxhiu, K., Reka, A., Andoni, A., Hamiti, X., & Drushku, S. (2021). 11th International Conference on Research in Engineering, Science & Technology. *Adsorption of Benalaxyil and Atrazine in Natural Clays Brari (Tirana) and Dardha (Korça)*, (pp. 136-151). Budapest.
- Beierle, B. D., Lamoureux, S. F., Cockburn, J. M., & Spooner, I. (2002). A new method for visualizing sediment particles size distributions. *Journal of Paleolimnology*, 27: 279-283.
- Binh, D. V., Sumi, T., & Kantoush, S. A. (2019). Changes to long-term discharge and sediment loads in the Vietnamese Mekong Delta caused by upstream dams. *Geomorphology*.
- Blom, A. (2021, September). *Topic 6. Bedforms and bedload transport [Powerpoint-slides]*, TU Delft Faculty of Civil Engineering and Geosciences. Retrieved August 31, 2023, from <https://brightspace.tudelft/login>
- Bogen, J., & Bønsnes, T. E. (2001). The impact of a hydroelectric power plant on the sediment load in downstream water bodies, Svartisen, northern Norway. *Sci Total Environ*, 266(1-3):273-80.
- Britannica. (2023, January 20). *clay*. Retrieved from T. Editors of Encyclopaedia: <https://www.britannica.com/science/clay-geology>
- Brown, C. B. (1944). Discussion of sedimentation in reservoirs. In: Witzig J., editor. *Proceedings of the American Society of Civil Engineers*, 69, 1493–1500.
- Brune, G. M. (1953). Trap efficiency of reservoirs. *Eos, Transactions American Geophysical Union*, (43):3 407-418.

- Bussi, G., Darby, S. E., Whitehead, P. G., Jin, L., Dadson, S. J., Voepel, H. E., . . . Nicholas, A. (2021). Impact of dams and climate change on suspended sediment flux to the Mekong delta. *Science of the Total Environment*, 755: 142468.
- Caballero, B. (2003). *Encyclopedia of Food Sciences and Nutrition*. Elsevier.
- Campbell, I. C., Say, S., & Beardall, J. (2009). Chapter 10 - Tonle Sap Lake, the Heart of the Lower Mekong. In I. C. Campbell, *The Mekong - Biophysical Environment of an International River Basin* (pp. 251-272). New York: Academic Press.
- Carling, P. A. (2009). Geomorphology and Sedimentology of the Lower Mekong River. In I. C. Campbell, *The Mekong* (pp. 77-111). Cambridge: Academic Press.
- Chang, S., Zi-Niu, X., & Nguyen, M. (2021). Projection on precipitation frequency of different intensities and precipitation amount in the Lancang-Mekong River basin in the 21st century. *Advances in Climate Change Research*, 162-171.
- Chua, S. D., & Xi, L. X. (2022). Sediment load crisis in the Mekong River Basin: Severe reductions over the decades. *Geomorphology*, Vol. 419, 108484.
- Chuenchum, P., Xu, M., & Tang, W. (2020a). Predicted trends of soil erosion and sediment yield from future land use and climate change scenarios in the LancangeMekong River by using the modified RUSLE model. *International Soil and Water Conservation Research*, (8): 213-227.
- Chuenchum, P., Xu, M., & Tang, W. (2020b). Estimation of Soil Erosion and Sediment Yield in the Lancang–Mekong River Using the Modified Revised Universal Soil Loss Equation and GIS Techniques. *Water*, (12) 135.
- Chuenchum, P., Xu, M., & Tang, W. (2023). Assessment of reservoir trapping efficiency and hydropower production under future projections of sedimentation in Lancang–Mekong River Basin . *Renewable and Sustainable Energy Reviews* 184 (2023) 113510.
- Churchill, M. A. (1948). Discussion of analysis and use of reservoir sedimentation data. In: Gottschalk L.C., editor. *Proc. Of Federal Interagency Sedimentation Conference, Denver*, 139–140.
- Corral-Pazos-de-Provens, E., Rapp-Arrarás, I., & Domingo-Santos, J. M. (2022). Estimating textural fractions of the USDA using those of the International System: A quantile approach. *Geoderma*, 416:115783.
- Czuba, J. A., Magirl, C. S., Czuba, C. R., Grossman, E. E., Curran, C. A., Gendaszek, A. S., & Dinicola, R. S. (2011, August). Comparability of Suspended-Sediment Concentration and Total Suspended Solids Data Sediment Load from Major Rivers into Puget Sound and its Adjacent Waters. Tacoma, WA, United States.
- Dauphin, L., & Patel, K. (2020, January 25). *Mekong Turns from Brown to Blue-Green*. Retrieved from NASA Earth Observatory:
<https://earthobservatory.nasa.gov/images/146209/mekong-turns-from-brown-to-blue-green>

Deltas and CED. (2023, August). Sand Budget Mekong Delta. *Deltas report 11206927-000. Project by Deltas, Centre for Environmental Fluid Dynamics (CED), with IHE-Delft Institute for Water Education and Southern Regional Hydrometeorological Centre.*

Eastham, J., Mpelasoka, F., Mainuddin, M., Ticehurst, C., Dyce, P., Hodgson, G., . . . Kirby, M. (2008). *Mekong River Basin Water Resources Assessment: Impacts of Climate*. CSIRO: Water for a Healthy Country National Research Flagship.

Efretuei, A. (2016, October 19). *The Soils Cation Exchange Capacity and its Effect on Soil Fertility*. Retrieved July 13, 2023, from Permaculture Research Institute: <https://www.permaculturenews.org/2016/10/19/soils-cation-exchange-capacity-effect-soil-fertility/#:~:text=Clay%20and%20silt%20particles%20have,an%20hold%20on%20to%20cations>.

Eleven, J. (2013, December 10). *Generic Data Model*. Retrieved from Wiki: <https://wiki.c2.com/?GenericDataModel>

ESA. (2007, April 13). *Envisat image of the Mekong Delta in Vietnam*. Retrieved from The European Space Agency: http://www.esa.int/spaceinimages/Images/2007/04/Envisat_image_of_the_Mekong_Delta_in_Vietnam

Flemming, B. W. (2011). Geology, morphology and sedimentology of estuaries and coasts. In E. Wolanski, & D. McLusky, *Treatise on Estuaries and Coasts* (pp. 7-38). Elsevier.

Fondriest Environmental. (2014, December 5). *Sediment Transport and Deposition. Fundamentals of Environmental Measurements*. Retrieved from Fondriest: <https://www.fondriest.com/environmental-measurements/parameters/hydrology/sediment-transport-deposition/>

Groenendyk, D., Ferré, T. P., Thorp, K., & Rice, A. K. (2015). Hydrologic-Process-Based Soil Texture Classifications for Improved Visualization of Landscape Function. *PLoS ONE*, 10(6): e0131299.

Ha, D. T., Ouillon, S., & Vinh, G. V. (2018). Water and Suspended Sediment Budgets in the Lower Mekong from High-Frequency Measurements (2009–2016). *Water*, 10(7), 846.

Harrington, S. T., & Harrington, J. R. (2014). Dissolved and particulate nutrient transport dynamics of a small Irish catchment: the River Owenabue. *Hydrol. Earth Syst. Sci*, 18: 2191–2200.

Hecht, J. S., Lacombe, G., Arias, M. E., Dang, T. D., & Piman, T. (2019). Hydropower dams of the Mekong River basin: A review of their hydrological impacts. *Journal of Hydrology*, 568: 285-300.

Hoque, M., Islam, A., & Ghosh, S. (2022). Environmental flow in the context of dams and development with special reference to the Damodar Valley Project, India: a review. *Sustainable Water Resources Management*, 8:62 .

- Huffman, G. (2023, 05 21). *GPM data*. Retrieved from GPM & TRMM Data: <https://arthurhouhttps.pps.eosdis.nasa.gov/gpmdatas/?C=N;O=A>
- Huffman, M. E., Pizzuto, J. E., Trampush, S. M., Moody, J. A., Schook, M. D., Gray, H. J., & Mahan, S. A. (2022). Floodplain Sediment Storage Timescales of the Laterally Confined Meandering Powder River, USA. *Journal of Geophysical Research: Earth Surface*, 127: 148.
- Hurst, H. E. (1929). The Suspension of Sand in Water. *Proceedings of the Royal Society of London. Series A, Containing Papers of a Mathematical and Physical Character*, 124(793), 196–201.
- Hydro. (2017, February 22). *Dealing with Sediment: Effects on Dams and Hydropower Generation*. Retrieved from Hydro Review: <https://www.hydroreview.com/world-regions/north-america/dealing-with-sediment-effects-on-dams-and-hydropower-generation/#gref>
- IHA. (2022). *Types of hydropower*. Retrieved from International Hydropower Association: <https://www.hydropower.org/oha/discover-types-of-hydropower#:~:text=Run%2Dof%2Driver%20hydropower%3A,little%20or%20no%20storage%20facility>.
- Kityuttachai, K., Heng, S., & Sou, V. (2016, March). Land Cover Map of the Lower Mekong Basin. *MRC Technical Paper No. 59, Information and Knowledge Management Programme*. Phnom Penh, Cambodia: Mekong River Commission.
- Kondolf, G. M., Rubin, Z. K., & Minear, J. T. (2013). Dams on the Mekong: Cumulative sediment starvation. *Water Resources Research*, 50: 5158–5169.
- Kondolf, M. G., Gao, Y., Annandale, G. W., Morris, G. L., Jiang, E., Zhang, J., ... Yang, C. (2014). Sustainable sediment management in reservoirs and regulated rivers: Experiences from five continents. *Earth's Future*, 2, 256–280.
- Kondolf, M. G., Schmitt, R. J., Carling, P., Darby, S., Aria, M., Bazzi, S., ... Wild, T. (2018). Changing sediment budget of the Mekong: Cumulative threats and management strategies for a large river basin. *Science of the Total Environment*, 625: 114-134.
- Koppes, M. N. (2022). 4.09 - Rates and Processes of Glacial Erosion. In J. F. Shroder, *Treatise on Geomorphology (second edition)* (pp. 169-181). Cambridge: Academic Press.
- Kumari, N., & Mohan, C. (2021). Basics of Clay Minerals and Their Characteristic Properties. In G. M. Nascimento, *Clay and Clay Minerals*. Brazil: IntechOpen.
- Kummu, M., Lu, X. X., Wang, J. J., & Varis, O. (2010). Basin-wide sediment trapping efficiency of emerging reservoirs along the Mekong. *Geomorphology*, 119: 181-197.
- Lai, Y., & Huang, J. (2021). *Technical Report No. ENV-2021-121: Best Practices of Numerically Simulating Hydraulic Flushing – Progress Report*. -: U.S. Department of the Interior.
- Lancaster, N., Baas, A. C., & Sherman, D. J. (2013). 11.1 Aeolian Geomorphology: Introduction. In J. F. Shroder, *Treatise on Geomorphology* (pp. 1-6). Cambridge: Academic Press.

- Lee. (2023, July 13). *Sources of Clay*. Retrieved from Lee College Library:
<https://leecollegelibrary.com/ceramics/clay/clay2.html>
- Li, X., Liu, J. P., Saito, Y., & Nguyen, V. L. (2017). Recent evolution of the Mekong Delta and the impacts of dams. *Earth-Science Reviews*, 175: 1-17.
- Liu, L., Bai, P., Liu, C., Tian, W., & Liang, K. (2020). Changes in Extreme Precipitation in the Mekong Basin. *Advances in Meteorology*, 10 pages.
- Liu, Z., Colin, C., Trentesaux, A., Blamart, D., Bassinot, F., Siani, G., & Sicre, M.-A. (2004). Erosional history of the eastern Tibetan Plateau since 190 kyr ago: clay mineralogical and geochemical investigations from the southwestern South China Sea. *Marine Geology*, 209: 1-18.
- Lu, X. X., & Chua, D. S. (2021). River Discharge and Water Level Changes in the Mekong River: Droughts in an Era of Mega-Dams. *Hydrological Processes*, 19.
- Lu, X., Zhang, T., Hsia, B. L., Li, D., Fair, H., Chua, S. D., . . . Li, S. (2022). Proglacial river sediment fluxes in the southeastern Tibetan Plateau: Mingyong Glacier in the Upper Mekong River. *Hydrological Processes*.
- Ly, K., Metternicht, G., & Marshall, L. (2020). Linking Changes in Land Cover and Land Use of the Lower Mekong Basin to Instream Nitrate and Total Suspended Solids Variations. *Sustainability*, (12) 2992.
- Malutta, S., Kobiyama, M., Chaffee , P. L., & Bonumá, N. B. (2020). Hysteresis analysis to quantify and qualify the sediment dynamics: state of the art. *Water Science & Technology*, 81 (12): 2471-2487.
- Manh, N. V., Dung, N. V., Hung, N. N., Merz, B., & Apel, H. (2014). Large-scale suspended sediment transport and sediment deposition in the Mekong Delta. *Hydrology and Earth System Sciences*, 18 , 3033-3053.
- McCully, P. (1996). *Silenced rivers : the ecology and politics of large dams*. London: Zed Books.
- McNair, J. N. (2006). Probabilistic settling in the Local Exchange Model of turbulent particle transport. *Journal of Theoretical Biology*, 241(2):420-37.
- Mezger, G., del Tánago, M. G., & De Stefano, L. (2021). Environmental flows and the mitigation of hydrological alteration downstream from dams: The Spanish case . *Journal of Hydrology*, 598: 125732.
- Morris, L. G., & Fan, J. (2009). *Reservoir Sedimentation Handbook - Design and Management of Dams, Reservoirs and Watersheds for sustainable use*. New York: McGraw-Hill Book Co.
- MRC. (2005). *Overview of the Hydrology of the Mekong Basin*. Vientiane: Red Plough International Co. Ltd.
- MRC. (2017). *About Mekong River Commission*. Retrieved from Mekong River Commission:
<https://www.mrcmekong.org/about/mrc/about/>
- MRC. (2018, Februari 20). Mekong Sediment from the Mekong River Commission Study. MRC.

MRC. (2019, November). 2 MRC Management Information Booklet Series No.2. *The Flow of the Mekong.*

MRC. (2023a). *Climate*. Retrieved from Mekong River Commission:
<https://www.mrcmekong.org/about/mekong-basin/climate/#:~:text=The%20climate%20of%20the%20Lower,in%20most%20of%20the%20basin.>

MRC. (2023b). *Geography*. Retrieved from Mekong River Commission:
<https://www.mrcmekong.org/about/mekong-basin/geography/#:~:text=The%20Upper%20Mekong%20River%20Basin,PDR%2C%20Cambodia%20and%20Viet%20Nam.>

MRC. (2023c). *Hydropower*. Retrieved from Mekong River Commission:
<https://www.mrcmekong.org/our-work/topics/hydropower/>

Mulu, A., & Dwarakishb, G. S. (2015). Different Approach for Using Trap Efficiency for Estimation of Reservoir Sedimentation. An Overview. *Aqua Procedia*, (4): 847 – 852 .

Murray-Smith, D. J. (2012). 9 - Model management. In D. J. Murray-Smith, *Modelling and Simulation of Integrated Systems in Engineering* (pp. 291-311). Sawston, UK: Woodhead Publishing.

Nathan, M. V. (2017, January). *Soils, Plant Nutrition and Nutrient Management*. Retrieved from Extension University of Missouri: <https://extension.missouri.edu/publications/mg4>

NCDA&CS. (1999, February). Soil Fertility Note 13. *Clay Minerals: Their Importance and Function in Soils*. North Carolina, United States of America.

Nederlands Visbureau. (2022, October 27). *Dutch fish consumption on the rise*. Retrieved from Vakblad Voedingsindustrie: <https://vakbladvoedingsindustrie.nl/en/article/dutch-fish-consumption-on-the-rise>

NWS. (2023, June 12). *Hydrology Education: The Water Cycle*. Retrieved from National Weather Service : https://www.weather.gov/lot/hydrology_education_watercycle

OER Commons. (2019). *Determining Soil Texture*. Retrieved from Open Educational Resources: <https://oercommons.org/courseware/lesson/70533/overview>

Orr, S., Pittock, J., Chapagain, A., & Dumaresq, D. (2012). Dams on the Mekong River: Lost fish protein and the implications for land and water resources. *Global Environmental Change*, 22: 925-932.

Pukinskis, I. (2013). *Mekong Sediment Basics*. State of Knowledge Series 2. Vientiane, Lao PDR Challenge Program on Water and Food.

Räsänen, T. A., Someth, P., Lauri, H., Koponen, J., Sarkkula, J., & Kummu, M. (2017). Observed river discharge changes due to hydropower operations in the Upper Mekong Basin. *Journal of Hydrology*, 28-41.

- Renewables. (2015). *Head and flow detailed review*. Retrieved from Renewables first:
<https://www.renewablesfirst.co.uk/renewable-energy-technologies/hydropower/hydropower-learning-centre/head-and-flow-detailed-review/>
- Schmitt, R. J., Bizzi, S., Castelletti, A., & G., K. M. (2018). Improved trade-offs of hydropower and sand connectivity by strategic dam planning in the Mekong. *Nature Sustainability*, 96-104.
- Schubert, C. (1964). Size-frequency distribution of sand-sized grains in an abrasion mill. *Sedimentology*, 3 (4): 288-295.
- Shrestha, B., Cochrane, T. A., Caruso, B. S., Arias, M. E., & Piman, T. (2016). Uncertainty in flow and sediment projections due to future climate scenarios for the 3S Rivers in the Mekong Basin. *Journal of Hydrology*, 1088-1104.
- Sok, T., Oeurng, C., Ich, I., Sauvage, S., & Sánchez-Pérez, J. M. (2020). Assessment of Hydrology and Sediment Yield in the Mekong River Basin Using SWAT Model. *Water*, 12(12), 3503.
- Southard, J. (2006, Fall). *Introduction To Fluid Motions, Sediment Transport, And Current-Generated Sedimentary Structures*. Retrieved from MIT Open Courseware:
<https://ocw.mit.edu/courses/12-090-introduction-to-fluid-motions-sediment-transport-and-current-generated-sedimentary-structures-fall-2006/>
- Stimson. (2023, Februari 7). *Mekong Dam Monitor*. Retrieved from Stimson eyes on water:
<https://monitor.mekongwater.org/basin-wide-dams-and-connectivity/?v=1642195188734>
- Sun, Z., Sun, L., Zheng, H., & Li, Z. (2022). Estimation of sedimentation in the Manwan and Jinghong reservoirs on the Lancang river. *Water Supply*, Vol. 22 No 4., 4308.
- Tan Yen, B., Quyen, N. H., Duong, T. H., Van Kham, D., Amjath-Babu, T. S., Amjath-Babu, T. S., & Sebastian, L. (2019). Modeling ENSO impact on rice production in. *PLoS ONE*, 14(10).
- Tan, G., Chen, P., Deng, J., Xu, Q., Tang, R., Feng, Z., & Yi, R. (2019). Review and improvement of conventional models for reservoir sediment trapping efficiency. *Heliyon*, 5(9).
- Tang, X., Li, R., Wang, D., Jing, Z., & Zhang, W. (2023). Reservoir flood regulation affects nutrient transport through altering water and sediment conditions. *Water Research*, 233:119728.
- The Brisbane Declaration. (2007). Environmental Flows are Essential for Freshwater Ecosystem Health and Human Well-Being. *The Brisbane Declaration*. Brisbane: International River Foundation.
- Thi Ha, D., Ouillon, S., & Van Vinh, G. (2018). Water and Suspended Sediment Budgets in the Lower Mekong from High-Frequency Measurements (2009–2016). *Water*, 10, 846.
- USGS. (2019, Juni 8). *Surface Runoff and the Water Cycle*. Retrieved from USGS:
<https://www.usgs.gov/special-topics/water-science-school/science/surface-runoff-and-water->

cycle#:~:text=Only%20about%20a%20third%20of,humans%20for%20their%20own%20uses.

Van Campenhout, J., Petit, F., Peeters, A., & Houbrechts, G. (2022). Estimation of the area-specific suspended sediment yield from discrete samples in different regions of Belgium. *Journal of Soils and Sediments*, 22: 704–729.

Van Zalinge, N., Degen, P., Pongsri, C., Nuov, S., Jensen, J. G., Hao, N. V., & Choulamany, X. (2003, February 11-14). Contribution to the Second International Symposium on the Management of Large Rivers for Fisheries. *The Mekong River System*, 11-14. Phnom Penh, Cambodia.

Visual Crossing Corporation. (2023, September 21). *Visual Crossing Weather (2001-2004)*. Retrieved from <https://www.visualcrossing.com/>

Vörösmarty, C. J., Meybeck, M., Fekete, B., Sharma, K., Green, P., & Syvitski, J. P. (2003). Anthropogenic sediment retention: major global impact from registered river impoundments. *Global and Planetary Change*, 169-190.

VRMP. (2005). *River Dynamics 101 - Fact Sheet*. Vermont: Vermont Agency of Natural Resources.

VT Agency of Natural Resources. (2004, April). Appendix O: Particle Entrainment and Transport. Vermont.

Wagner, K., Kuhns, M., & Cardon, G. (2015, June). Utah Forest Facts. *Gardening in Sandy Soils*. United States of America: Utah State University.

Walling, D. E. (2009). The Sediment Load of the Mekong River. In I. C. Campbell, *The Mekong a Biophysical Environment of an International River Basin* (pp. 113-142). Cambridge: Academic Press.

Wang, J. S., Chen, L., Fan, B. L., & Chai, X. L. (2009). Relationship between ion transport and sediment discharge in river. *Advances in Water Science*, 20(5):658-662.

Wang, W., Lu, H., Zhao, T., Jiang, L., & Shi, J. (2017). Evaluation and Comparison of Daily Rainfall From Latest GPM and TRMM Products Over the Mekong River Basin. *IEEE Journal of Selected Topics in Applied Earth Observations and Remote Sensing*, Vol. 10, No. 6, 2540-2549.

Wang, X., Chen, Y., Yuan, Q., Xing, X., Hu, B., Gan, J., . . . Liu, Y. (2022). Effect of river damming on nutrient transport and transformation and its countermeasures. *Marine Sciences*, 9:1078216.

Wentworth, C. K. (1922). A scale of grade and class terms for clastic sediments. *The Journal of Geology*, Vol 30(5):377-392.

Whitehead, P. G., Jin, L., Bussi, G., Voepel, H. E., Darby, S. E., Vasilopoulos, G., . . . Hung, N. N. (2019). Water quality modelling of the Mekong River basin: Climate change and socioeconomics drive flow and nutrient flux changes to the Mekong Delta. *Science of the Total Environment*, 673: 218-229.

- Wischmeier, W. H., & Smith, D. D. (1972, September 26). 4. Erosion Prediction - Revised Universal Soil Loss Equation (RUSLE). In W. H. Wischmeier, & D. D. Smith, *Predicting rainfall-erosion losses from cropland east of the Rocky Mountains* (pp. 2-3). Washington D.C.: USDA. Retrieved from Section 1 – General Reserouce References :
[https://efotg.sc.egov.usda.gov/references/public/WA/Revised_Universal_Soil_Loss_Equation_\(RUSLE\).htm#:~:text=RUSLE%20is%20an%20index%20method,raindrop%20impact%20and%20surface%20runoff](https://efotg.sc.egov.usda.gov/references/public/WA/Revised_Universal_Soil_Loss_Equation_(RUSLE).htm#:~:text=RUSLE%20is%20an%20index%20method,raindrop%20impact%20and%20surface%20runoff)
- World of Earth Science. (2023, July 13). *Clay*. Retrieved from Encyclopedia:
<https://www.encyclopedia.com/science/encyclopedias-almanacs-transcripts-and-maps/clay>
- Wright, J., Smith, B., & Whalley, B. (1998). Mechanisms of loess-sized quartz silt production and their relative effectiveness: laboratory simulations. *Geomorphology*, 23 (1): 15-34.
- Wright, L. D. (1985). River Deltas. In A. R. Davis, *Coastal Sedimentary Environments* (pp. 5-68). New York: Springer.
- Xue, Z. (2014). A source-to-sink study of the Mekong River Delta: Hydrology, delta evolution, and sediment transport modeling.
- Yang, L. (2015). 1 - Fundamentals of nanotechnology and orthopedic materials. In L. Yang, *Nanotechnology-Enhanced Orthopedic Materials* (pp. 1-25). Sawston: Woodhead Publishing.
- Yang, W.-Y., Li, D., Sun, T., & Ni, G.-H. (2015). Saturation-excess and infiltration-excess runoff on green roofs. *Ecological Engineering*, (74): 327-336.
- Yao, T., Thompson, L., Yang, W., Yu, W., Gao, Y., Guo, X., . . . Joswiak, D. (2012). Different glacier status with atmospheric circulations in Tibetan Plateau and surroundings . *Nature Climate Change*, (2)663–667.

Appendix A. Dam information

Appendix A.1 Dam information 2004



Figure 34: Location of operational run-of-river and reservoir dams in 2004

Table 8: General information of dams in operation in 2004

Sub-basin nr.	Sub-catchment name	Project Name	Location	Year of Operation	Active volume [km3]	Regulated area Areg [km2]	Reservoir/run-of-river	Country
1	Nam Nhiep / Nam Sane	Nam Leuk	Tributary	2000	0,23	214	reservoir	Laos
2	Nam Chi	Ubol Ratana	Tributary	1966	1,70	11131	reservoir	Thailand
2	Nam Chi	Chulabhorn	Tributary	1972	0,14	655	reservoir	Thailand
2	Nam Chi	Huai Kum	Tributary	1982	0,02	455	run-of-river	Thailand
3	UMB	Manwan	Mainstream	1996	0,25	107946	reservoir	China
3	UMB	Dachaoshan	Mainstream	2003	0,28	5790	reservoir	China
10	Huai Luang / Nam Phoung / Nam	Nam Dong	Tributary	1970	0,00	75	run-of-river	Laos
13	Nam Ngum	Nam Ngum 1	Tributary	1971	1,00	8189	reservoir	Laos
18	Nam Cadinh	Theun-Hinboun	Tributary	1998	0,02	8513	run-of-river	Laos
20	Nam Kam / Nam Hinboun / Huai	Nam Pung	Tributary	1965	0,16	315	reservoir	Thailand
21	Nam Ou	Nam Ko	Tributary	1996	0,00	11790	run-of-river	Laos
21	Nam Ou	Nam Ngay	Tributary	2002	0,00	887	run-of-river	Laos
22	Nam Mun	Sirindhorn	Tributary	1971	1,14	2255	reservoir	Thailand
22	Nam Mun	Pak Mun	Tributary	1994	0,15	63200	reservoir	Thailand
22	Nam Mun	Lam Ta Khong P.S.	Tributary	2001	0,30	1391	reservoir	Thailand
25	Se Done	Xelabam	Tributary	1970	0,00	5030	run-of-river	Laos
25	Se Done	Xeset 1	Tributary	1991	0,00	1209	run-of-river	Laos
26	Se Kong	Houayho	Tributary	1999	0,53	298	reservoir	Laos
28	Se San	O Chum 2	Tributary	1992	0,00	144	run-of-river	Cambodia
28	Se San	Yali	Tributary	2002	0,78	7464	reservoir	Vietnam
29	Sre Pok	Dray Hlinh 1	Tributary	1990	0,00	8867	run-of-river	Vietnam

Appendix A.2 Dam information 2020



Figure 35: Location of operational run-of-river and reservoir dams in 2020

Table 9: General information of dams in operation in 2020

Sub-basin nr.	Sub-catchment	Project Name	Location	Year of Operation	Active volume [km3]	Regulated area Areg [km2]	Reservoir/run-of-river	Country
1	Nam Nhiep / Nam Sane	Nam Chian	Tributary	2015	0,01	87	run-of-river	Laos
1	Nam Nhiep / Nam Sane	Nam Leuk	Tributary	2000	0,23	214	reservoir	Laos
1	Nam Nhiep / Nam Sane	Nam Mang 1	Tributary	2015	0,01	659	run-of-river	Laos
1	Nam Nhiep / Nam Sane	Nam Mang 3	Tributary	2005	0,05	199	run-of-river	Laos
1	Nam Nhiep / Nam Sane	Nam Ngiep 1	Tributary	2019	1,19	1759	reservoir	Laos
1	Nam Nhiep / Nam Sane	Nam Ngiep 2	Tributary	2017	0,24	312	reservoir	Laos
1	Nam Nhiep / Nam Sane	Nam Ngiep - regulating dam	Tributary	2019	0,00	182	run-of-river	Laos
1	Nam Nhiep / Nam Sane	Nam Ngieu	Tributary	2013	0,02	210	run-of-river	Laos
1	Nam Nhiep / Nam Sane	Nam Phouan	Tributary	2020	0,20	652	reservoir	Laos
1	Nam Nhiep / Nam Sane	Nam Pot	Tributary	2015	0,05	600	run-of-river	Laos
1	Nam Nhiep / Nam Sane	Nam San 3	Tributary	2016	0,00	166	run-of-river	Laos
1	Nam Nhiep / Nam Sane	Nam San 3B	Tributary	2017	0,01	126	run-of-river	Laos
2	Nam Chi	Chulabhorn	Tributary	1972	0,14	655	reservoir	Thailand
2	Nam Chi	Huai Kum	Tributary	1982	0,02	455	run-of-river	Thailand
2	Nam Chi	Ubol Ratana	Tributary	1966	1,70	11131	reservoir	Thailand
3	UMB	Da Hua Qiao	Mainstream	2020	0,41	3811	reservoir	China
3	UMB	Dachaoshan	Mainstream	2003	0,28	5790	reservoir	China
3	UMB	Gongguoqiao	Mainstream	2008	0,12	3404	reservoir	China
3	UMB	Jinghong	Mainstream	2010	0,31	4829	reservoir	China
3	UMB	Li Di	Mainstream	2020	0,15	1306	reservoir	China
3	UMB	Manwan	Mainstream	1996	0,25	1033	reservoir	China
3	UMB	Miao Wei	Mainstream	2020	0,04	1229	run-of-river	China
3	UMB	Nam Long	Tributary	2013	0,00	363	run-of-river	Laos
3	UMB	Nam Pha	Tributary	2016	2,33	2722	reservoir	Laos
3	UMB	Nuazhadu	Mainstream	2016	12,30	24174	reservoir	China
3	UMB	Tuo Ba	Mainstream	2020	0,02	1433	run-of-river	China
3	UMB	Wu Nong Long	Mainstream	2020	0,15	79543	reservoir	China
3	UMB	Xiaowan	Mainstream	2010	9,90	16187	reservoir	China
4	Nam Tha	Nam Tha 1	Tributary	2019	0,68	7591	reservoir	Laos
8	Nam Mae Ing	Nam Nhone	Tributary	2012	0,00	163	run-of-river	Laos
9	Nam Beng / Nam Ngeun	Nam Beng	Tributary	2018	0,00	2016	run-of-river	Laos
10	Huai Luang / Nam Phoung / Nam	Mekong at Xayabuly	Mainstream	2019	0,21	2617	reservoir	Laos
10	Huai Luang / Nam Phoung / Nam	Nam Dong	Tributary	1970	0,00	75	run-of-river	Laos
10	Huai Luang / Nam Phoung / Nam	Nam Phoun	Tributary	2017	0,25	1067	reservoir	Laos
10	Huai Luang / Nam Phoung / Nam	Nam Pouy 1	Tributary	2020	0,50	1893	reservoir	Laos
12	Nam Khan	Nam Khan 2	Tributary	2015	0,53	1732	reservoir	Laos
12	Nam Khan	Nam Khan 3	Tributary	2016	0,05	3368	run-of-river	Laos

Sub-basin nr.	Sub-catchment	Project Name	Location	Year of Operation	Active volume [km3]	Regulated area Areg [km2]	Reservoir/run-of-river	Country
13	Nam Ngum	Nam Lik 1	Tributary	2018	0,01	2700	run-of-river	Laos
13	Nam Ngum	Nam Lik 2	Tributary	2010	0,83	2023	reservoir	Laos
13	Nam Ngum	Nam Ngum 1	Tributary	1971	1,00	2328	reservoir	Laos
13	Nam Ngum	Nam Ngum 2	Tributary	2012	2,97	1924	reservoir	Laos
13	Nam Ngum	Nam Ngum 3	Tributary	2019	1,41	3208	reservoir	Laos
13	Nam Ngum	Nam Ngum 5	Tributary	2012	0,25	488	reservoir	Laos
13	Nam Ngum	Nam Pay	Tributary	2015	0,13	241	reservoir	Laos
13	Nam Ngum	Nam Sana	Tributary	2015	0,00	193	run-of-river	Laos
18	Nam Cadinh	Nam Theun 2	Tributary	2010	3,38	3936	reservoir	Laos
18	Nam Cadinh	Nam Theun1	Tributary	2020	2,92	5275	reservoir	Laos
18	Nam Cadinh	Theun-Hinboun	Tributary	1998	0,02	1656	run-of-river	Laos
18	Nam Cadinh	Theun-Hinboun exp. (NG8)	Tributary	2013	2,26	2921	reservoir	Laos
19	Se Bang Fai	Xe Neua	Tributary	2020	0,49	351	reservoir	Laos
20	Nam Kam / Nam Hinboun / Huai	Nam Hinboun	Tributary	2016	0,56	920	reservoir	Laos
20	Nam Kam / Nam Hinboun / Huai	Nam Hinboun 1	Tributary	2017	1,22	343	reservoir	Laos
20	Nam Kam / Nam Hinboun / Huai	Nam Hinboun 2	Tributary	2017	0,00	79	run-of-river	Laos
20	Nam Kam / Nam Hinboun / Huai	Nam Pung	Tributary	1965	0,16	315	reservoir	Thailand
21	Nam Ou	Nam Bak	Tributary	2020	0,37	902	reservoir	Laos
21	Nam Ou	Nam Ko	Tributary	1996	0,00	947	run-of-river	Laos
21	Nam Ou	Nam Ngao	Tributary	2019	0,43	177	reservoir	Laos
21	Nam Ou	Nam Ngay	Tributary	2002	0,00	887	run-of-river	Laos
21	Nam Ou	Nam Ou 1	Tributary	2019	0,09	3116	run-of-river	Laos
21	Nam Ou	Nam Ou 2	Tributary	2016	0,03	1737	run-of-river	Laos
21	Nam Ou	Nam Ou 3	Tributary	2019	0,02	6364	run-of-river	Laos
21	Nam Ou	Nam Ou 4	Tributary	2019	1,15	1936	reservoir	Laos
21	Nam Ou	Nam Ou 5	Tributary	2017	0,14	4146	reservoir	Laos
21	Nam Ou	Nam Ou 6	Tributary	2017	0,25	1172	reservoir	Laos
21	Nam Ou	Nam Ou 7	Tributary	2018	1,06	3589	reservoir	Laos
21	Nam Ou	Nam Phak	Tributary	2017	0,00	856	run-of-river	Laos
22	Nam Mun	Lam Ta Khong P.S.	Tributary	2001	0,30	1391	reservoir	Thailand
22	Nam Mun	Pak Mun	Tributary	1994	0,15	63200	reservoir	Thailand
22	Nam Mun	Sirindhorn	Tributary	1971	1,14	2255	reservoir	Thailand
22	Nam Mun	Xekaman-Sanxay (2A)	Tributary	2017	0,00	3110	run-of-river	Laos
23	Se Bang Hieng	Tad Salen	Tributary	2013	0,00	124	run-of-river	Laos
23	Se Bang Hieng	Xe Lanong 2	Tributary	2018	0,03	245	run-of-river	Laos
23	Se Bang Hieng	Xe Pon 3	Tributary	2020	0,36	447	reservoir	Laos
25	Se Done	Xe Set 3	Tributary	2016	0,02	333	run-of-river	Laos
25	Se Done	Xelabam	Tributary	1970	0,00	4467	run-of-river	Laos

Sub-basin nr.	Sub-catchment	Project Name	Location	Year of Operation	Active volume [km3]	Regulated area Areg [km2]	Reservoir/run-of-river	Country
25	Se Done	Xeset 1	Tributary	1991	0,00	1209	run-of-river	Laos
25	Se Done	Xeset 2	Tributary	2009	0,01	230	run-of-river	Laos
26	Se Kong	Houay Lamphan Gnai	Tributary	2017	0,12	190	reservoir	Laos
26	Se Kong	Houayho	Tributary	1999	0,53	298	reservoir	Laos
26	Se Kong	Nam Kong 1	Tributary	2019	0,51	492	reservoir	Laos
26	Se Kong	Nam Kong 2	Tributary	2018	0,03	327	run-of-river	Laos
26	Se Kong	Nam Kong 3	Tributary	2017	0,05	765	run-of-river	Laos
26	Se Kong	Xe Kaman 2A	Tributary	2018	0,02	188	run-of-river	Laos
26	Se Kong	Xe Kaman 2B	Tributary	2018	0,33	705	reservoir	Laos
26	Se Kong	Xe Kaman 4A	Tributary	2020	0,33	326	reservoir	Laos
26	Se Kong	Xe Kong 5	Tributary	2019	1,70	2832	reservoir	Laos
26	Se Kong	Xe Nam Noy 5	Tributary	2013	0,01	88	run-of-river	Laos
26	Se Kong	Xekaman 1	Tributary	2017	1,68	1780	reservoir	Laos
26	Se Kong	Xekaman 3	Tributary	2015	0,11	542	reservoir	Laos
26	Se Kong	Xekatam	Tributary	2020	0,12	335	reservoir	Laos
26	Se Kong	Xenamnoy 1	Tributary	2014	0,00	412	run-of-river	Laos
26	Se Kong	Xepian-Houaysoy	Tributary	2020	0,28	8697	reservoir	Laos
26	Se Kong	Xepian-Xenamnoy	Tributary	2019	0,98	343	reservoir	Laos
27	Huai Tomo / Tonle Repon	Mekong at Don sahong	Mainstream	2019	0,12	9283	reservoir	Laos
27	Huai Tomo / Tonle Repon	Nam Phak (Houykatam)	Tributary	2019	0,01	160	run-of-river	Laos
28	Se San	Lower Se San 3	Tributary	2020	3,12	5973	reservoir	Cambodia
28	Se San	O Chum 2	Tributary	1992	0,00	144	run-of-river	Cambodia
28	Se San	Plei Krong	Tributary	2009	0,95	3073	reservoir	Vietnam
28	Se San	Se San 3	Tributary	2006	0,00	280	run-of-river	Vietnam
28	Se San	Se San 3A	Tributary	2007	0,00	300	run-of-river	Vietnam
28	Se San	Se San 4	Tributary	2010	0,26	1097	reservoir	Vietnam
28	Se San	Se San 4A	Tributary	2011	0,01	77	run-of-river	Vietnam
28	Se San	Upper Kontum	Tributary	2014	0,12	363	reservoir	Vietnam
28	Se San	Yali	Tributary	2002	0,78	4028	reservoir	Vietnam
29	Sre Pok	Buon Kuop	Tributary	2009	0,03	4683	run-of-river	Vietnam
29	Sre Pok	Buon Tua Srah	Tributary	2009	0,52	2921	reservoir	Vietnam
29	Sre Pok	Dray Hlinh 1	Tributary	1990	0,00	1263	run-of-river	Vietnam
29	Sre Pok	Dray Hlinh 2	Tributary	2007	0,00	61	run-of-river	Vietnam
29	Sre Pok	Lower Se San 2	Tributary	2017	0,33	3809	reservoir	Cambodia
29	Sre Pok	Lower Sre Pok 3 (3A)	Tributary	2020	3,93	12148	reservoir	Cambodia
29	Sre Pok	Lower Sre Pok 4	Tributary	2020	0,04	3043	run-of-river	Cambodia
29	Sre Pok	Sre Pok 3	Tributary	2010	0,06	362	run-of-river	Vietnam
29	Sre Pok	Sre Pok 4	Tributary	2010	0,01	1232	run-of-river	Vietnam

Appendix A.3 Dam information 2040



Figure 36: Location of operational run-of-river and reservoir dams in 2040

Table 10: General information of dams in operation in 2040

Sub-basin nr.	Sub-catchment	Project Name	Location	Year of Operation	Active volume [km3]	Regulated area Areg [km2]	Reservoir/run-of-river	Country
1	Nam Nhiep / Nam Sane	Nam Chian	Tributary	2015	0,01	87	run-of-river	Laos
1	Nam Nhiep / Nam Sane	Nam Leuk	Tributary	2000	0,23	214	reservoir	Laos
1	Nam Nhiep / Nam Sane	Nam Mang 1	Tributary	2015	0,01	659	run-of-river	Laos
1	Nam Nhiep / Nam Sane	Nam Mang 3	Tributary	2005	0,05	199	run-of-river	Laos
1	Nam Nhiep / Nam Sane	Nam Ngiep 1	Tributary	2019	1,19	1759	reservoir	Laos
1	Nam Nhiep / Nam Sane	Nam Ngiep 2	Tributary	2017	0,24	312	reservoir	Laos
1	Nam Nhiep / Nam Sane	Nam Ngiep - regulating dam	Tributary	2019	0,00	182	run-of-river	Laos
1	Nam Nhiep / Nam Sane	Nam Ngieu	Tributary	2013	0,02	210	run-of-river	Laos
1	Nam Nhiep / Nam Sane	Nam Phouan	Tributary	2020	0,20	652	reservoir	Laos
1	Nam Nhiep / Nam Sane	Nam Pot	Tributary	2015	0,05	600	run-of-river	Laos
1	Nam Nhiep / Nam Sane	Nam San 3	Tributary	2016	0,00	166	run-of-river	Laos
1	Nam Nhiep / Nam Sane	Nam San 3B	Tributary	2017	0,01	126	run-of-river	Laos
2	Nam Chi	Chulabhorn	Tributary	1972	0,14	655	reservoir	Thailand
2	Nam Chi	Huai Kum	Tributary	1982	0,02	455	run-of-river	Thailand
2	Nam Chi	Ubol Ratana	Tributary	1966	1,70	11131	reservoir	Thailand
3	UMB	Da Hua Qiao	Mainstream	2020	0,41	617	reservoir	China
3	UMB	Dachaoshan	Mainstream	2003	0,28	5790	reservoir	China
3	UMB	Gongguoqiao	Mainstream	2008	0,12	3404	reservoir	China
3	UMB	Jinghong	Mainstream	2010	0,31	4829	reservoir	China
3	UMB	Li Di	Mainstream	2020	0,15	1306	reservoir	China
3	UMB	Manwan	Mainstream	1996	0,25	1033	reservoir	China
3	UMB	Miao Wei	Mainstream	2020	0,04	1229	run-of-river	China
3	UMB	Nam Long	Tributary	2013	0,00	363	run-of-river	Laos
3	UMB	Nam Pha	Tributary	2016	2,33	2722	reservoir	Laos
3	UMB	Nuazhadu	Mainstream	2016	12,30	24174	reservoir	China
3	UMB	Tuo Ba	Mainstream	2020	0,02	1433	run-of-river	China
3	UMB	Wu Nong Long	Mainstream	2020	0,15	79543	reservoir	China
3	UMB	Xiaowan	Mainstream	2010	9,90	16187	reservoir	China
3	UMB	Ganlanba	Mainstream	Planned	0,31	2537	reservoir	China
3	UMB	Huang Deng	Mainstream	2022	0,17	3194	reservoir	China
4	Nam Tha	Nam Tha 1	Tributary	2019	0,68	7591	reservoir	Laos
5	Nam Suong	Nam Seuang 1	Tributary	Planned	0,06	614	run-of-river	Laos
5	Nam Suong	Nam Seuang 2	Tributary	Planned	2,01	5116	reservoir	Laos
8	Nam Mae Ing	Nam Nhone	Tributary	2012	0,00	163	run-of-river	Laos
9	Nam Beng / Nam Ngeun	Nam Beng	Tributary	2018	0,00	2016	run-of-river	Laos
9	Nam Beng / Nam Ngeun	Mekong at Pakbeng	Mainstream	2029	0,20	2524	reservoir	Laos
9	Nam Beng / Nam Ngeun	Mekong at Luangprabang	Mainstream	2025	0,12	4324	reservoir	Laos

Sub-basin nr.	Sub-catchment	Project Name	Location	Year of Operation	Active volume [km3]	Regulated area Areg [km2]	Reservoir/run-of-river	Country
10	Huai Luang / Nam Phoung / Nam	Mekong at Xayabuly	Mainstream	2019	0,21	2617	reservoir	Laos
10	Huai Luang / Nam Phoung / Nam	Nam Dong	Tributary	1970	0,00	75	run-of-river	Laos
10	Huai Luang / Nam Phoung / Nam	Nam Phoun	Tributary	2017	0,25	1067	reservoir	Laos
10	Huai Luang / Nam Phoung / Nam	Nam Pouy 1	Tributary	2020	0,50	1893	reservoir	Laos
10	Huai Luang / Nam Phoung / Nam	Nam Feuang 1	Tributary	Planned	0,03	434	run-of-river	Laos
10	Huai Luang / Nam Phoung / Nam	Nam Feuang 2	Tributary	Planned	0,01	188	run-of-river	Laos
10	Huai Luang / Nam Phoung / Nam	Nam Feuang 3	Tributary	Planned	0,00	123	run-of-river	Laos
10	Huai Luang / Nam Phoung / Nam	Mekong at Paklay	Mainstream	2025	0,32	5142	reservoir	Laos
10	Huai Luang / Nam Phoung / Nam	Mekong at Sanakham	Mainstream	2025	0,13	3154	reservoir	Laos
10	Huai Luang / Nam Phoung / Nam	Mekong at Sangthong-Pakchom	Mainstream	2025	0,81	2911	reservoir	Laos
11	Siem Bok	Sambor	Mainstream	Planned	0,74		reservoir	Cambodia
12	Nam Khan	Nam Khan 2	Tributary	2015	0,53	1732	reservoir	Laos
12	Nam Khan	Nam Khan 3	Tributary	2016	0,05	3368	run-of-river	Laos
13	Nam Ngum	Nam Lik 1	Tributary	2018	0,01	2700	run-of-river	Laos
13	Nam Ngum	Nam Lik 2	Tributary	2010	0,83	2023	reservoir	Laos
13	Nam Ngum	Nam Ngum 1	Tributary	1971	1,00	2328	reservoir	Laos
13	Nam Ngum	Nam Ngum 2	Tributary	2012	2,97	1924	reservoir	Laos
13	Nam Ngum	Nam Ngum 3	Tributary	2019	1,41	1705	reservoir	Laos
13	Nam Ngum	Nam Ngum 5	Tributary	2012	0,25	488	reservoir	Laos
13	Nam Ngum	Nam Pay	Tributary	2015	0,13	241	reservoir	Laos
13	Nam Ngum	Nam Sana	Tributary	2015	0,00	193	run-of-river	Laos
13	Nam Ngum	Nam Ngum 4	Tributary	2025	0,33	1503	reservoir	Laos
13	Nam Ngum	Nam Ngum, (down) Lower dam	Tributary	2023	0,24	3529	reservoir	Laos
18	Nam Cadinh	Nam Theun 2	Tributary	2010	3,38	3936	reservoir	Laos
18	Nam Cadinh	Nam Theun1	Tributary	2020	2,92	3448	reservoir	Laos
18	Nam Cadinh	Theun-Hinboun	Tributary	1998	0,02	1656	run-of-river	Laos
18	Nam Cadinh	Theun-Hinboun exp. (NG8)	Tributary	2013	2,26	2406	reservoir	Laos
18	Nam Cadinh	Nam Theun 4	Tributary	Planned	0,68	515	reservoir	Laos
18	Nam Cadinh	Nam Mouan	Tributary	Planned	1,17	1827	reservoir	Laos
19	Se Bang Fai	Xe Neua	Tributary	2020	0,49	351	reservoir	Laos
20	Nam Kam / Nam Hinboun / Huai	Nam Hinboun	Tributary	2016	0,56	920	reservoir	Laos
20	Nam Kam / Nam Hinboun / Huai	Nam Hinboun 1	Tributary	2017	1,22	343	reservoir	Laos
20	Nam Kam / Nam Hinboun / Huai	Nam Hinboun 2	Tributary	2017	0,00	79	run-of-river	Laos
20	Nam Kam / Nam Hinboun / Huai	Nam Pung	Tributary	1965	0,16	315	reservoir	Thailand
21	Nam Ou	Nam Bak	Tributary	2020	0,37	902	reservoir	Laos
21	Nam Ou	Nam Ko	Tributary	1996	0,00	947	run-of-river	Laos
21	Nam Ou	Nam Ngao	Tributary	2019	0,43	177	reservoir	Laos

Sub-basin nr.	Sub-catchment	Project Name	Location	Year of Operation	Active volume [km3]	Regulated area Areg [km2]	Reservoir/run-of-river	Country
21	Nam Ou	Nam Ngay	Tributary	2002	0,00	887	run-of-river	Laos
21	Nam Ou	Nam Ou 1	Tributary	2019	0,09	1141	run-of-river	Laos
21	Nam Ou	Nam Ou 2	Tributary	2016	0,03	1737	run-of-river	Laos
21	Nam Ou	Nam Ou 3	Tributary	2019	0,02	6364	run-of-river	Laos
21	Nam Ou	Nam Ou 4	Tributary	2019	1,15	1936	reservoir	Laos
21	Nam Ou	Nam Ou 5	Tributary	2017	0,14	4146	reservoir	Laos
21	Nam Ou	Nam Ou 6	Tributary	2017	0,25	1172	reservoir	Laos
21	Nam Ou	Nam Ou 7	Tributary	2018	1,06	3589	reservoir	Laos
21	Nam Ou	Nam Phak	Tributary	2017	0,00	856	run-of-river	Laos
21	Nam Ou	Nam Nga 1	Tributary	Planned	1,57	1975	reservoir	Laos
22	Nam Mun	Lam Ta Khong P.S.	Tributary	2001	0,30	1391	reservoir	Thailand
22	Nam Mun	Pak Mun	Tributary	1994	0,15	63200	reservoir	Thailand
22	Nam Mun	Sirindhorn	Tributary	1971	1,14	2255	reservoir	Thailand
22	Nam Mun	Xekaman-Sanxay (2A)	Tributary	2017	0,00	3110	run-of-river	Laos
23	Se Bang Hieng	Tad Salen	Tributary	2013	0,00	124	run-of-river	Laos
23	Se Bang Hieng	Xe Lanong 2	Tributary	2018	0,03	245	run-of-river	Laos
23	Se Bang Hieng	Xe Pon 3	Tributary	2020	0,36	447	reservoir	Laos
23	Se Bang Hieng	Xe Lanong 1	Tributary	2021	0,95	2525	reservoir	Laos
23	Se Bang Hieng	Xe Bang Hieng 2	Tributary	Planned	0,29	707	reservoir	Laos
24	Se Bang Nouan	Xe Bang Nouan	Tributary	Planned	1,48	434	reservoir	Laos
24	Se Bang Nouan	Mekong at Ban Kum	Mainstream	Planned	0,56	3907	reservoir	Vietnam
25	Se Done	Xe Set 3	Tributary	2016	0,02	333	run-of-river	Laos
25	Se Done	Xelabam	Tributary	1970	0,00	4467	run-of-river	Laos
25	Se Done	Xeset 1	Tributary	1991	0,00	1209	run-of-river	Laos
25	Se Done	Xeset 2	Tributary	2009	0,01	230	run-of-river	Laos
26	Se Kong	Houay Lamphan Gnai	Tributary	2017	0,12	190	reservoir	Laos
26	Se Kong	Houayho	Tributary	1999	0,53	298	reservoir	Laos
26	Se Kong	Nam Kong 1	Tributary	2019	0,51	492	reservoir	Laos
26	Se Kong	Nam Kong 2	Tributary	2018	0,03	327	run-of-river	Laos
26	Se Kong	Nam Kong 3	Tributary	2017	0,05	765	run-of-river	Laos
26	Se Kong	Xe Kaman 2A	Tributary	2018	0,02	188	run-of-river	Laos
26	Se Kong	Xe Kaman 2B	Tributary	2018	0,33	705	reservoir	Laos
26	Se Kong	Xe Kaman 4A	Tributary	2020	0,33	326	reservoir	Laos
26	Se Kong	Xe Kong 5	Tributary	2019	1,70	2832	reservoir	Laos
26	Se Kong	Xe Nam Noy 5	Tributary	2013	0,01	88	run-of-river	Laos
26	Se Kong	Xekaman 1	Tributary	2017	1,68	1620	reservoir	Laos
26	Se Kong	Xekaman 3	Tributary	2015	0,11	542	reservoir	Laos

Sub-basin nr.	Sub-catchment	Project Name	Location	Year of Operation	Active volume [km3]	Regulated area Areg [km2]	Reservoir/run-of-river	Country
26	Se Kong	Xekatam	Tributary	2020	0,12	335	reservoir	Laos
26	Se Kong	Xenamnoy 1	Tributary	2014	0,00	412	run-of-river	Laos
26	Se Kong	Xepian-Houaysoy	Tributary	2020	0,28	2367	reservoir	Laos
26	Se Kong	Xepian-Xenamnoy	Tributary	2019	0,98	343	reservoir	Laos
26	Se Kong	Xe Kong 3up	Tributary	2025	0,10	3033	run-of-river	Laos
26	Se Kong	Xe Kong 3d	Tributary	2025	0,17	1356	reservoir	Laos
26	Se Kong	Dak E Mule	Tributary	2022	0,15	301	reservoir	Laos
26	Se Kong	Xesu	Tributary	2022	0,03	1640	run-of-river	Laos
26	Se Kong	Nam Ang Tha Beng	Tributary	2022	0,00	160	run-of-river	Laos
27	Huai Tomo / Tonle Repon	Mekong at Don sahong	Mainstream	2019	0,12	8451	reservoir	Laos
27	Huai Tomo / Tonle Repon	Nam Phak (Houykatam)	Tributary	2019	0,01	160	run-of-river	Laos
27	Huai Tomo / Tonle Repon	Mekong at Latsua (Phou Ngoy)	Mainstream	2025	0,53	992	reservoir	Vietnam
27	Huai Tomo / Tonle Repon	Stung Treng	Mainstream	Planned	0,52	2362	reservoir	Vietnam
28	Se San	Lower Se San 3	Tributary	2020	3,12	4614	reservoir	Cambodia
28	Se San	O Chum 2	Tributary	1992	0,00	144	run-of-river	Cambodia
28	Se San	Plei Krong	Tributary	2009	0,95	3073	reservoir	Vietnam
28	Se San	Se San 3	Tributary	2006	0,00	280	run-of-river	Vietnam
28	Se San	Se San 3A	Tributary	2007	0,00	300	run-of-river	Vietnam
28	Se San	Se San 4	Tributary	2010	0,26	1097	reservoir	Vietnam
28	Se San	Se San 4A	Tributary	2011	0,01	77	run-of-river	Vietnam
28	Se San	Upper Kontum	Tributary	2014	0,12	363	reservoir	Vietnam
28	Se San	Yali	Tributary	2002	0,78	4028	reservoir	Vietnam
28	Se San	Prek Liang 1	Tributary	Planned	0,02	329	run-of-river	Cambodia
28	Se San	Prek Liang 2	Tributary	Planned	0,02	1030	run-of-river	Cambodia
29	Sre Pok	Buon Kuop	Tributary	2009	0,03	4683	run-of-river	Vietnam
29	Sre Pok	Buon Tua Srah	Tributary	2009	0,52	1632	reservoir	Vietnam
29	Sre Pok	Dray Hlinh 1	Tributary	1990	0,00	1263	run-of-river	Vietnam
29	Sre Pok	Dray Hlinh 2	Tributary	2007	0,00	61	run-of-river	Vietnam
29	Sre Pok	Lower Se San 2	Tributary	2017	0,33	3809	reservoir	Cambodia
29	Sre Pok	Lower Sre Pok 3 (3A)	Tributary	2020	3,93	12148	reservoir	Cambodia
29	Sre Pok	Lower Sre Pok 4	Tributary	2020	0,04	3043	run-of-river	Cambodia
29	Sre Pok	Sre Pok 3	Tributary	2010	0,06	362	run-of-river	Vietnam
29	Sre Pok	Sre Pok 4	Tributary	2010	0,01	1232	run-of-river	Vietnam
29	Sre Pok	Duc Xuyen	Tributary	Planned	0,41	1355	reservoir	Vietnam

Appendix B. Sub-basin information

Table 11: The total area, mean SSY and mean SL of each sub-catchment and the SSY including land use change

Sub-basin nr.	Sub-catchment name	Total area [km2]	Mean SSY [t/km2/y] (Kummu, Lu, Wang, & Varis, 2010)	Mean SL (Mt/y)	Mean SSY Land Use Change [t/km2/y] (Sok, Oeurng, Ich, Sauvage, & Sánchez-Pérez, 2020)
1	Nam Nhiep / Nam Sane	11455	40	0	85
2	Nam Chi	49235	18	1	55
3	UMB	187431	489	92	611
4	Nam Tha	8902	240	2	322
5	Nam Suong	6587	170	1	250
6	Nam Mae Kham	4091	38	0	110
7	Nam Mae Kok	10602	38	0	110
8	Nam Mae Ing	11099	38	0	110
9	Nam Beng / Nam Ngeun	9229	230	2	312
10	Huai Luang / Nam Phoung / Nam	30886	47	1	100
11	Siem Bok	11733	50	1	80
12	Nam Khan	7450	113	1	208
13	Nam Ngum	16756	36	1	113
14	Nam Heung	4799	40	0	80
15	Nam Loei	3941	40	0	80
16	Songkhram	12944	33	0	11
17	Nam Thon / Hoaag Hua	2051	40	0	80
18	Nam Cadinh	14760	41	1	80
19	Se Bang Fai	10676	80	1	168
20	Nam Kam / Nam Hinboun / Huai	16555	47,5	1	80
21	Nam Ou	25987	237	6	325
22	Nam Mun	70212	26	2	81
23	Se Bang Hieng	19910	163	3	242
24	Se Bang Nouan	4902	175	1	260
25	Se Done	7322	206	2	322
26	Se Kong	28689	220	6	343
27	Huai Tomo / Tonle Repon	12023	200	2	312
28	Se San	18897	240	5	375
29	Sre Pok	31138	240	7	375
				140	

Appendix C. Extension of Results – Dam impact on silt and clay loads

Appendix C.1 Baseline scenario

The mean SSY of each sub-catchment and its corresponding mean SL is depicted in Appendix B (Table 10). The total pre-dam annual SL at Kratie is calculated to be 140 Mt. More than 65% of this SL comes from the UMB and 20% from the 3S Basins (Se Kong, Se San and Sre Pok).

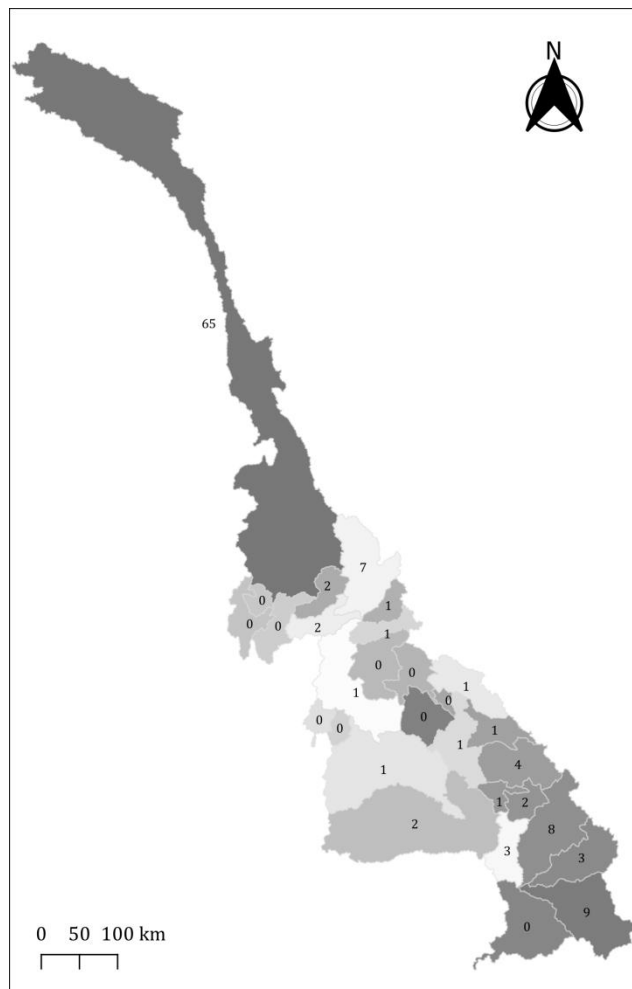


Figure 37: Percent contributions of each sub-basin to the Mekong's total annual SL in the baseline scenario

Appendix C.2 2004 scenario

There were 21 hydropower dams in operation in 2004 in the Mekong Basin (Appendix A.1). The total annual SL at Kratie in 2004 is calculated to be 83 Mt for the Brune Model and 98 Mt for the Defined TE Model. This means a decrease of 40% and 30% respectively compared to the baseline scenario. Even though the SL calculated by the two models differs, the distribution in Figure 38 and Figure 39 are comparable.

The UMB contributes the most to the total SL at Kratie in 2004 according to both models; 55% in the Brune Model and 45% in the Defined TE Model. The 3S Basins also contribute significantly to the annual SL in 2004 with a total contribution of 17% and 20% respectively (Figure 38).

The contribution to the trapped sediment shows that most of the sediment trapped in the UMB, which can be assigned to the fact that two mainstream dams were in operation, which were the only mainstream dams in the Mekong Basin at the time and the fact that the UMB has the highest baseline mean SL (Table 10). The total calculated contribution to the trapped sediment in the Brune Model is 88% and in the Defined TE model 72% (Figure 38).

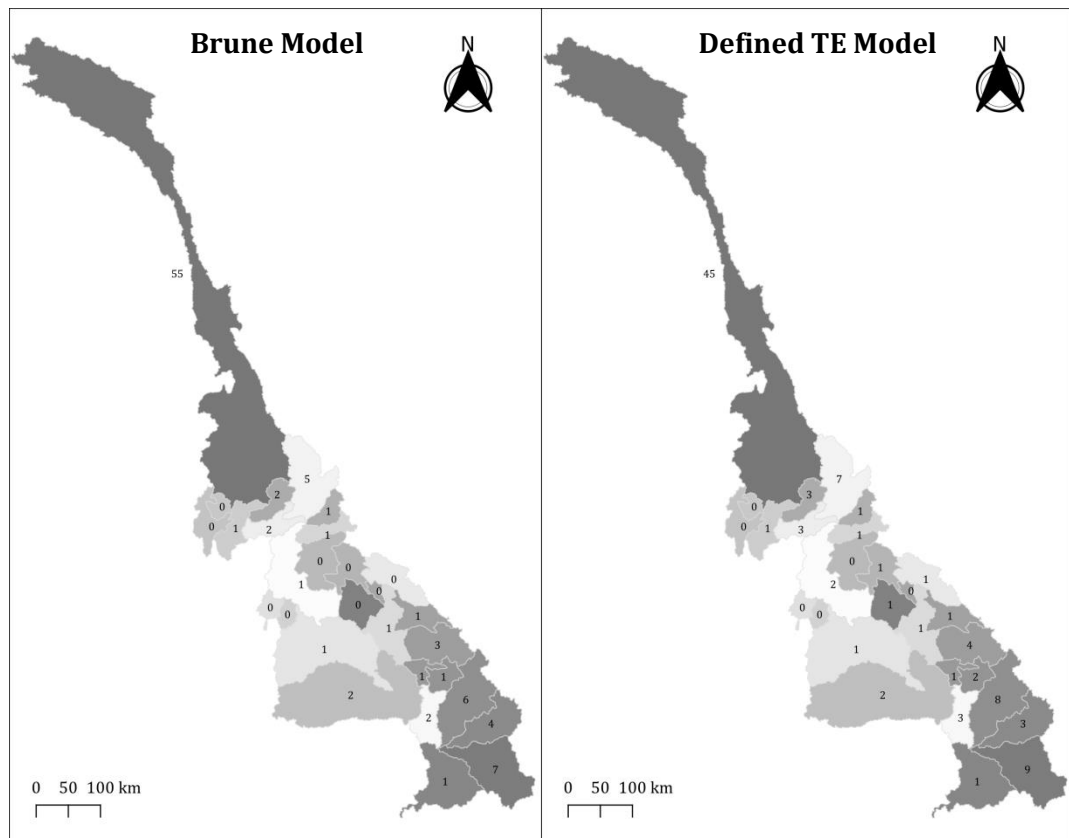


Figure 38: Percent contributions of each sub-basin to the Mekong's total annual SL in 2004.

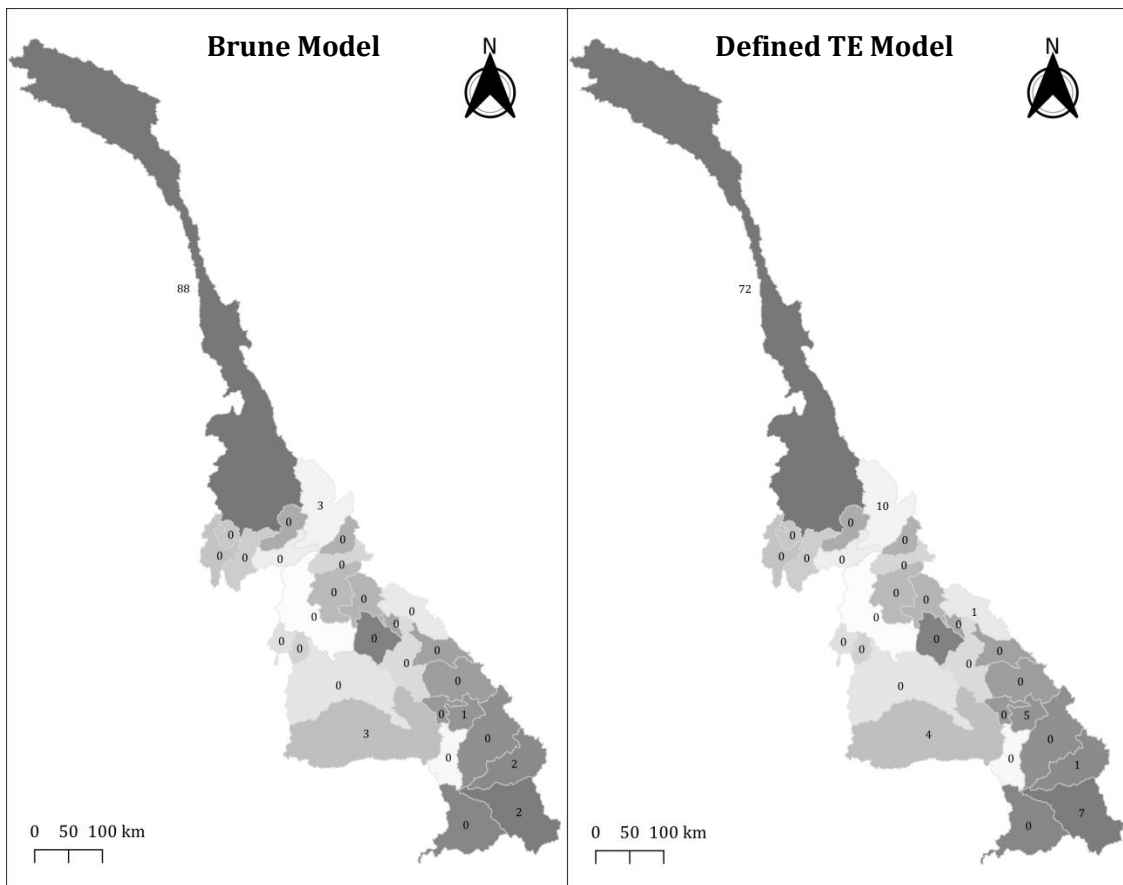


Figure 39: Percent contribution of trapped sediment in each sub-basin in 2004.

Appendix C.3 2020 scenario

There were 113 hydropower dams in operation in 2020 in the Mekong Basin (Appendix A.2). The total annual SL at Kratie in 2020 is calculated to be 26 Mt according to both models. This means a decrease of more than 80% compared to the baseline scenario.

Similar to the 2004 scenario, the UMB contributes the most to the total SL at Kratie in 2020 according to both models; 35% in the Brune Model and 32% in the Defined TE Model. The 3S Basins (Se Kong, Se San and Sre Pok) also contribute significantly to the annual SL in 2020 with a total contribution of 24% and 16% respectively (Figure 40).

The contribution to the trapped sediment shows that most of the sediment trapped in the UMB, which can be assigned to the fact that 11 of the 13 mainstream dams in operation are located in the UMB and again the fact that the UMB has the highest baseline mean SL (Table 10). The total calculated contribution to the trapped sediment in the Brune Model is 56% and in the Defined TE model 62% (Figure 41).

The amount of trapped sediment has changed from 0% in 2004 to 13% in 2020 according to both models in sub basin 10. This is caused by the construction of a mainstream dam in this basin. This is also the case in sub-basin 27 where the contribution has changed from 0 to 12% in the Brune model and to 2% in the Defined TE model.

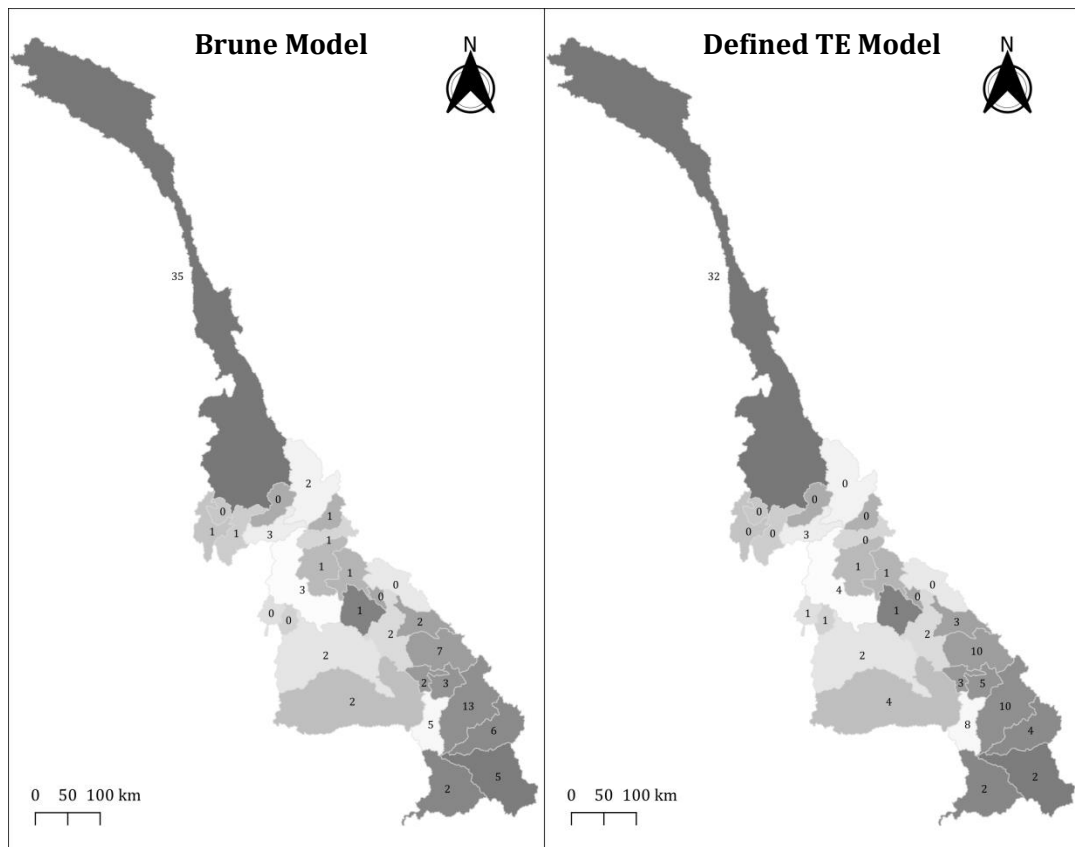


Figure 40: Percent contributions of each sub-basin to the Mekong's total annual SL in 2020

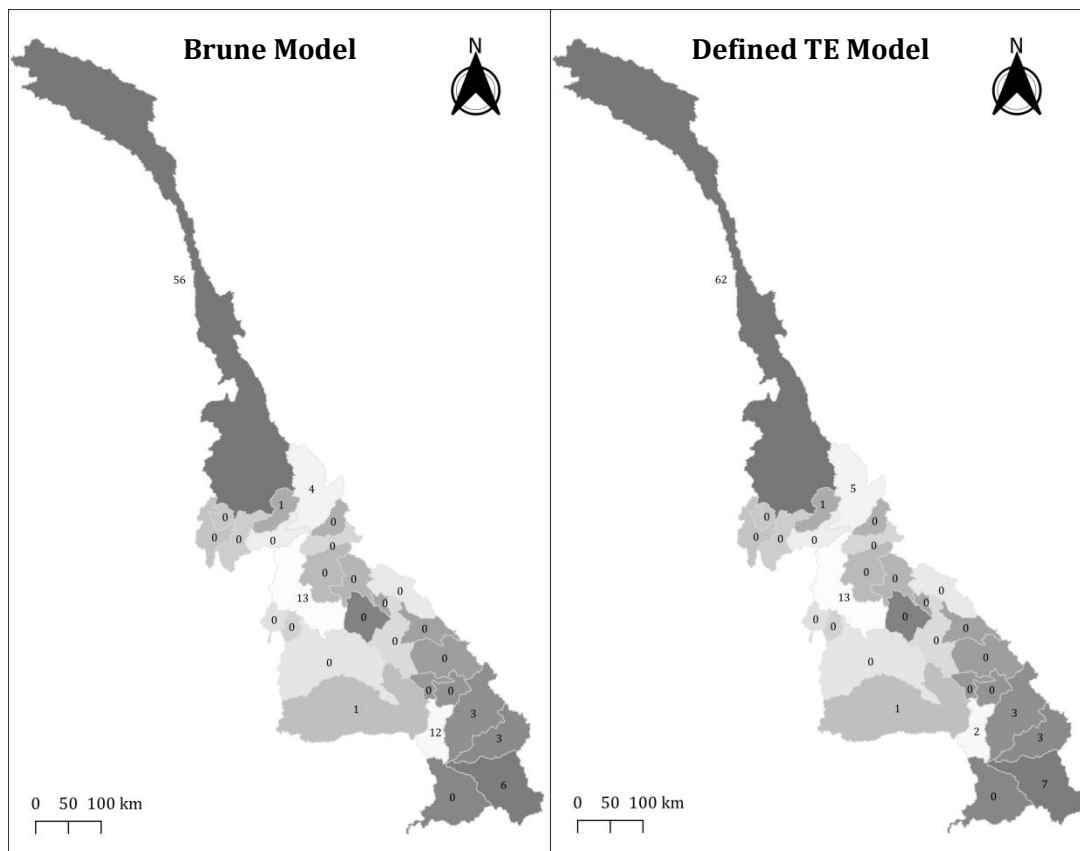


Figure 41: Percent contribution of trapped sediment in each sub-basin in 2020

Appendix C.4 2040 scenario

There will be 145 hydropower dams in operation in 2040 in the Mekong Basin (Appendix A.3). The total annual SL at Kratie in 2040 is calculated to be 4 Mt in the Brune model and 8 Mt in the Defined TE Model. This means a decrease of 97% and 94% respectively compared to the baseline scenario.

Contrary to the 2004 and 2020 scenario, the UMB does not contribute the most to the total SL at Kratie in 2040 according to both models, as it is only 2% in the Brune Model and 0% in the Defined TE Model. This means that almost all the sediment coming from the UMB is trapped in the dams. In the future, the 3S Basins (Se Kong, Se San and Sre Pok) will contribute the most to the annual SL in 2040 with a total contribution, with 80% and 85% respectively (Figure 42).

The contribution to the trapped sediment shows that most of the sediment trapped in the UMB, which can be assigned to the fact that 13 of the 24 mainstream dams in operation are located in the UMB and again the fact that the UMB has the highest baseline mean SL (Table 10). The total calculated contribution to the trapped sediment in the Brune Model is 51% and in the Defined TE model 53% (Figure 43).

The amount of trapped sediment has changed from 0% in 2020 to 14% and 16% in 2040 according to both models in sub basin 9. This is caused by the construction of two mainstream dams in this basin. This is also the case in sub-basin 27 where the contribution has changed from 0 to 12% in the Brune model and 2% in the Defined TE model.

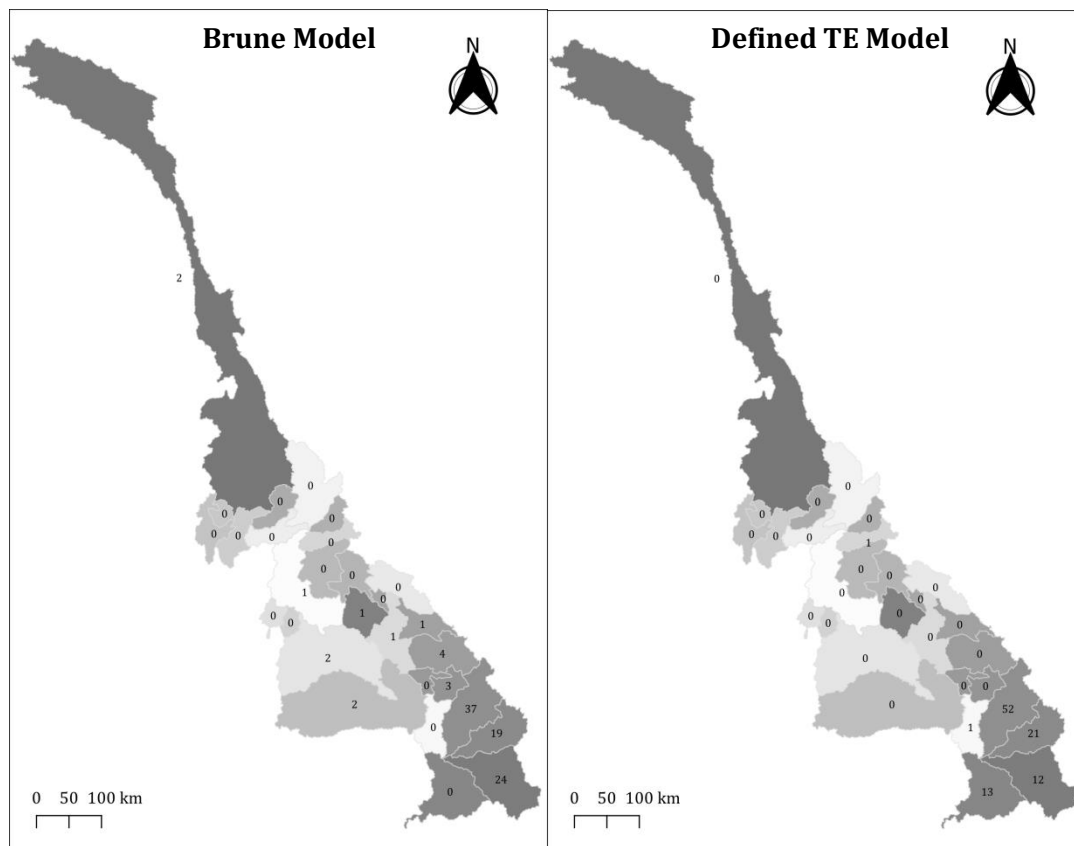


Figure 42: Percent contributions of each sub-basin to the Mekong's total annual SL in 2040

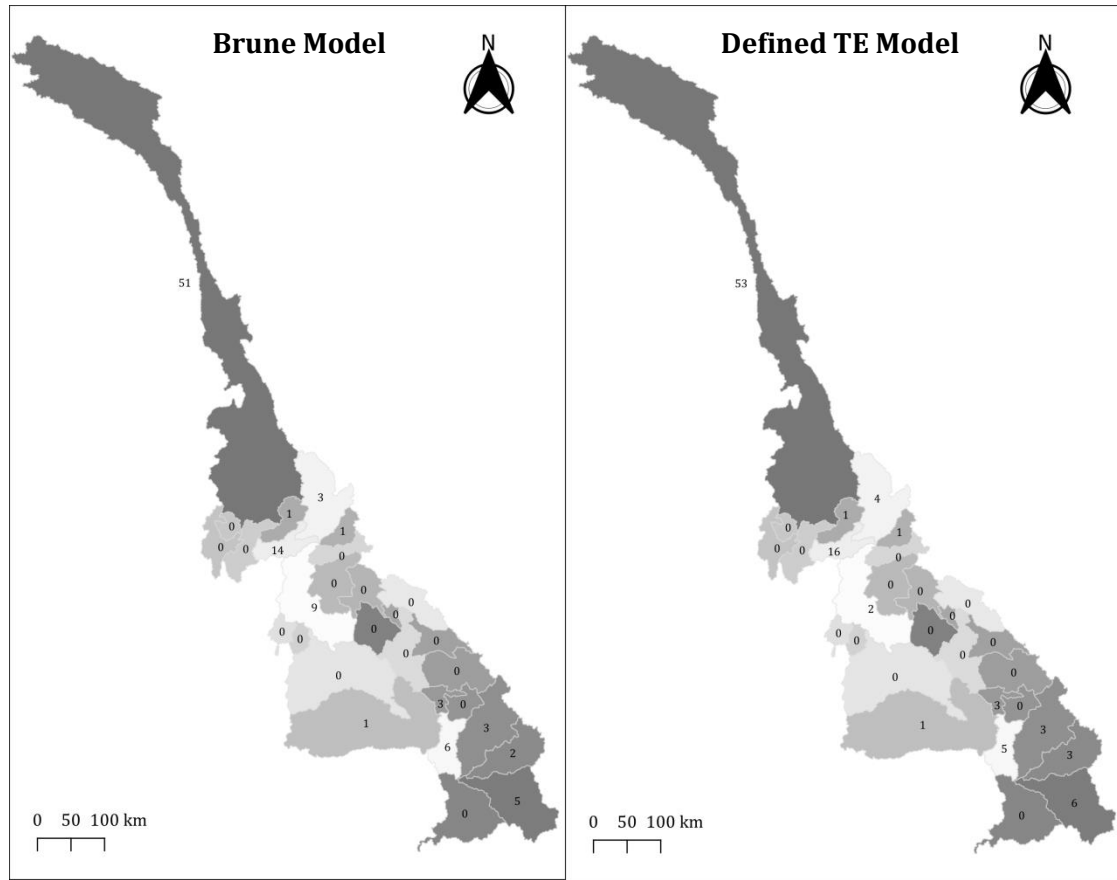


Figure 43: Percent contribution of trapped sediment in each sub-basin in 2040

Appendix D. Rainfall interpolation

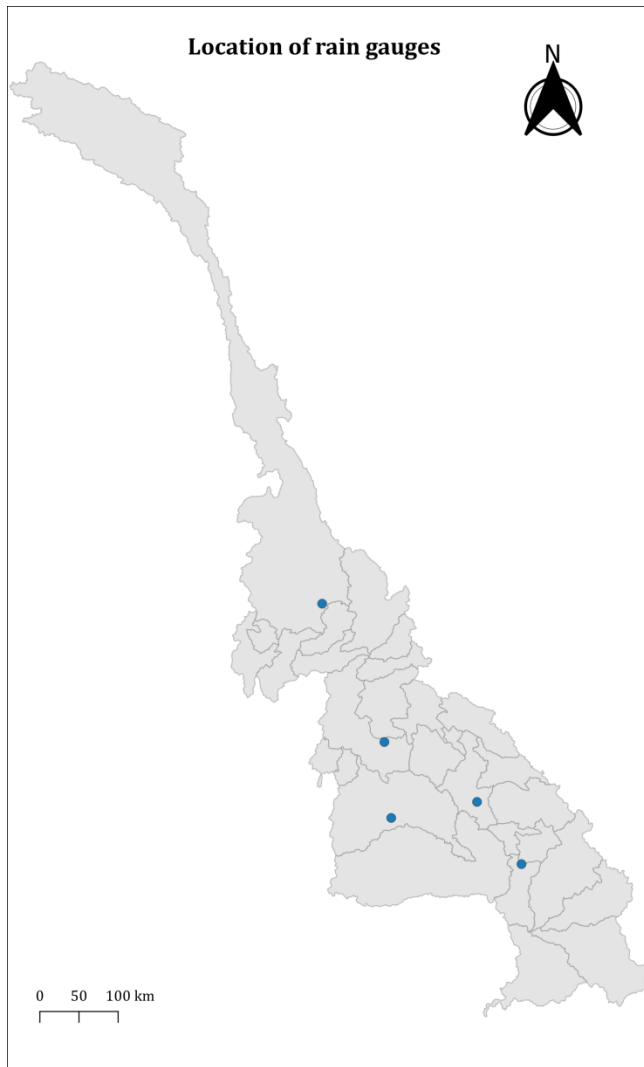


Figure 44: Location of rain gauges used for interpolation

2001-2004

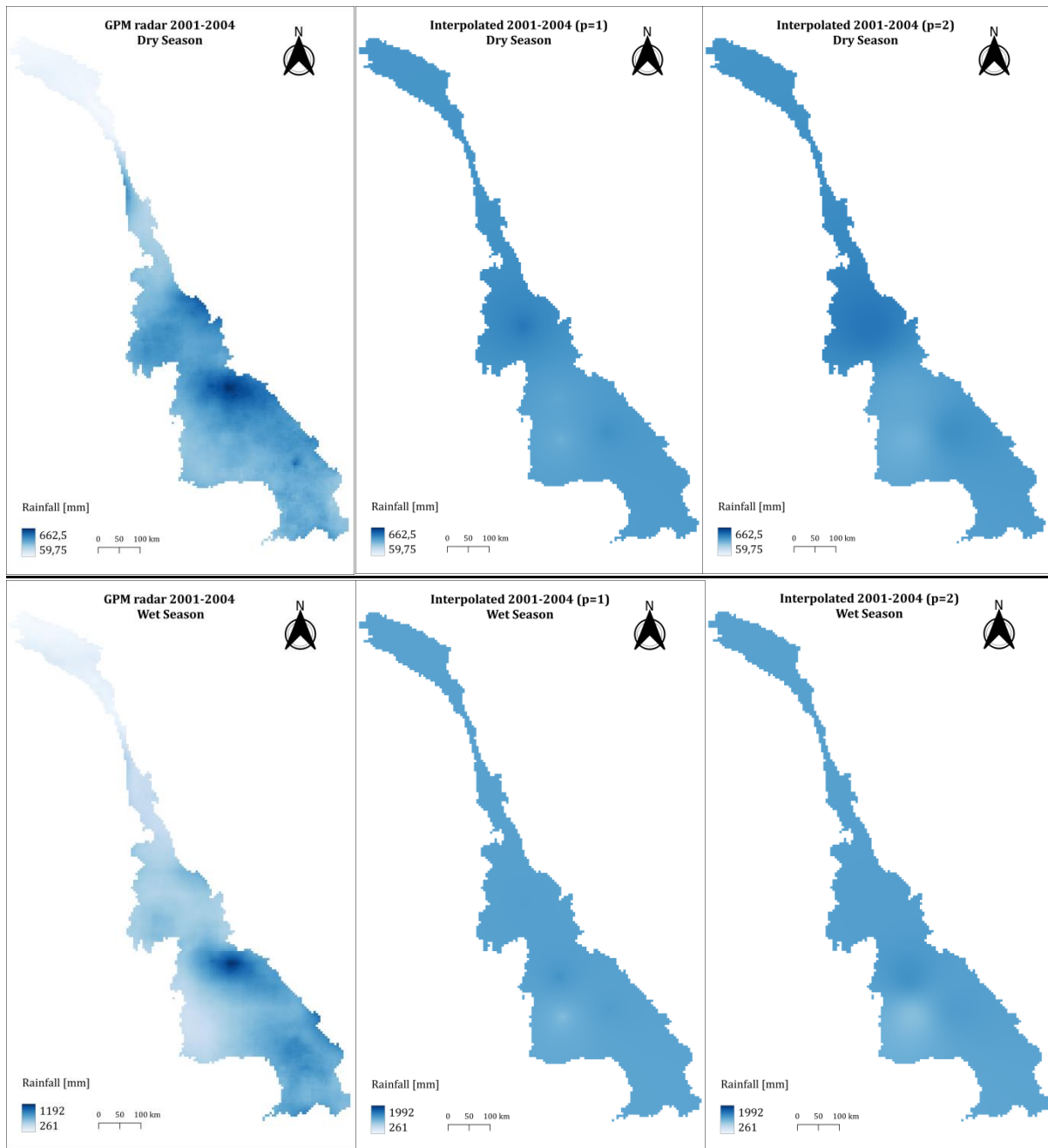


Figure 45: Comparison of radar data and interpolated 2001-2004 rainfall data

Present

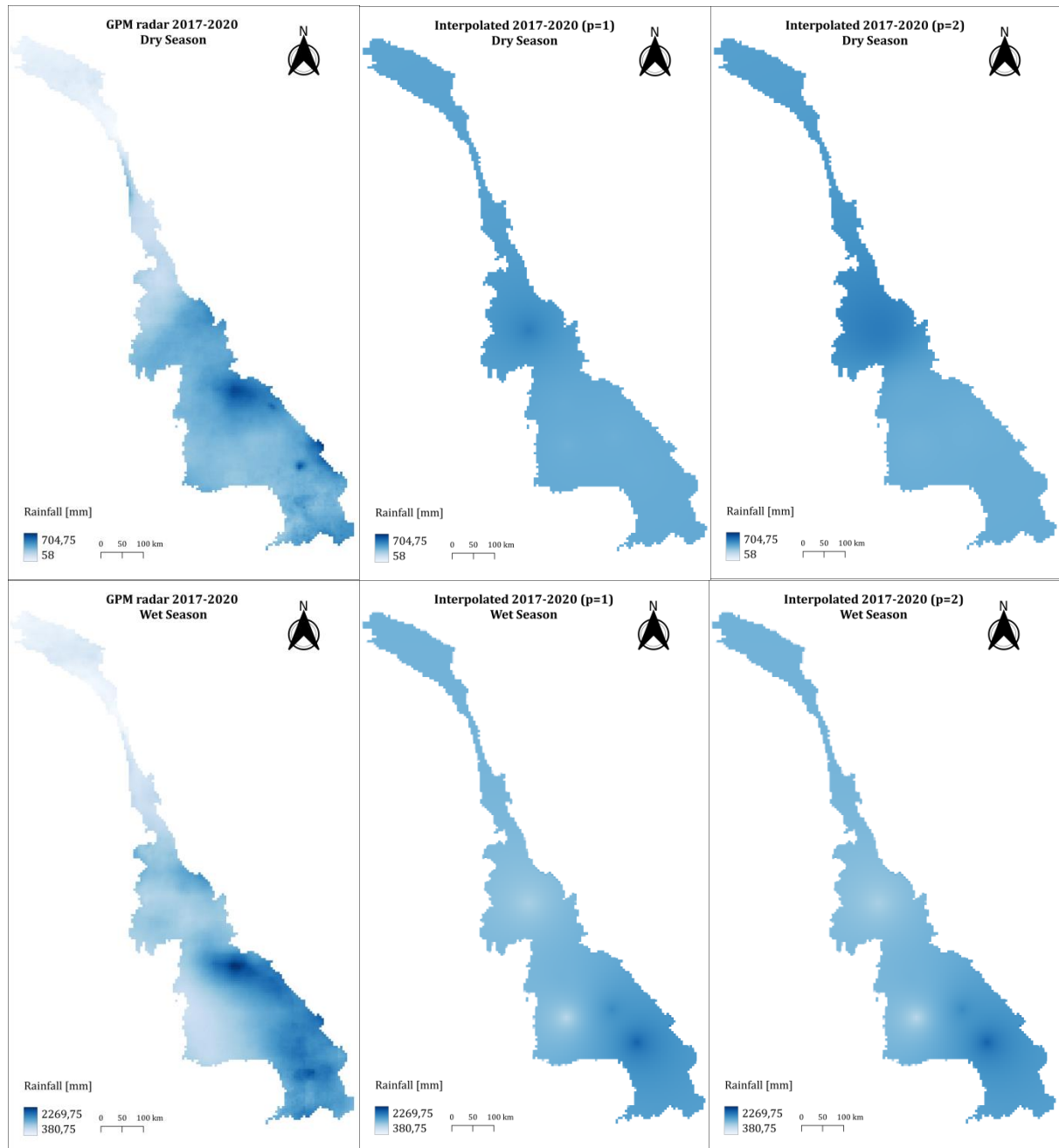


Figure 46: Comparison of radar data and interpolated 2017-2020 rainfall data

Appendix E. Sensitivity analysis of models

Appendix E.1 Sensitivity analysis SSY

Appendix E.1.1 Brune Model

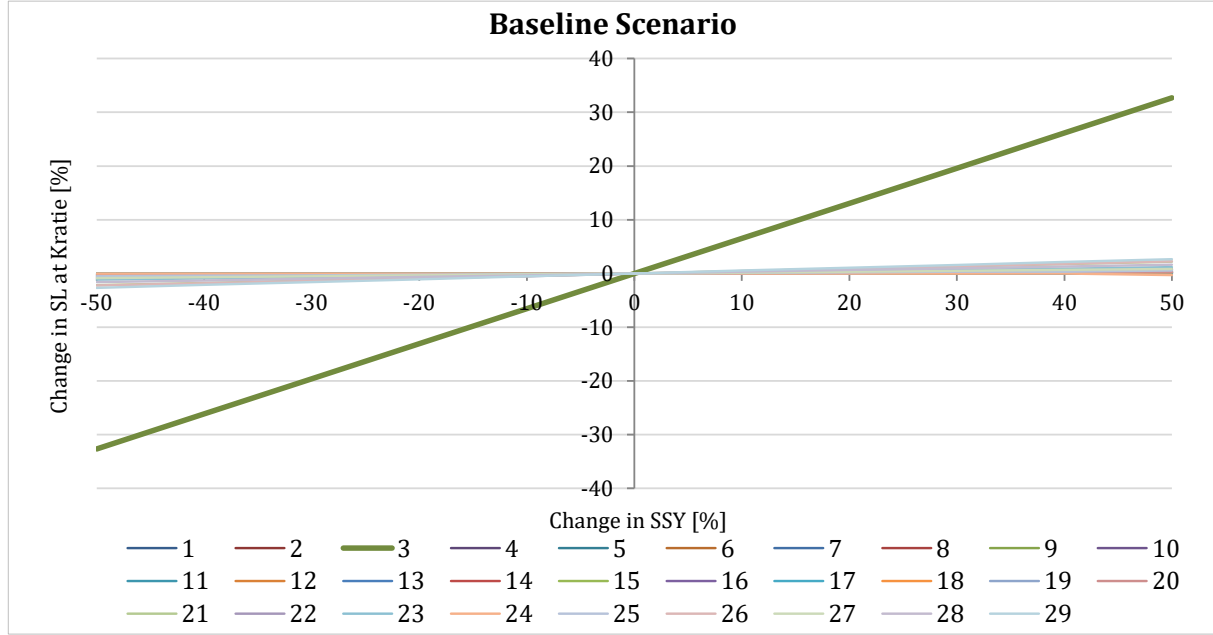


Figure 47: Sensitivity analysis of SSY Baseline scenario for the Brune model

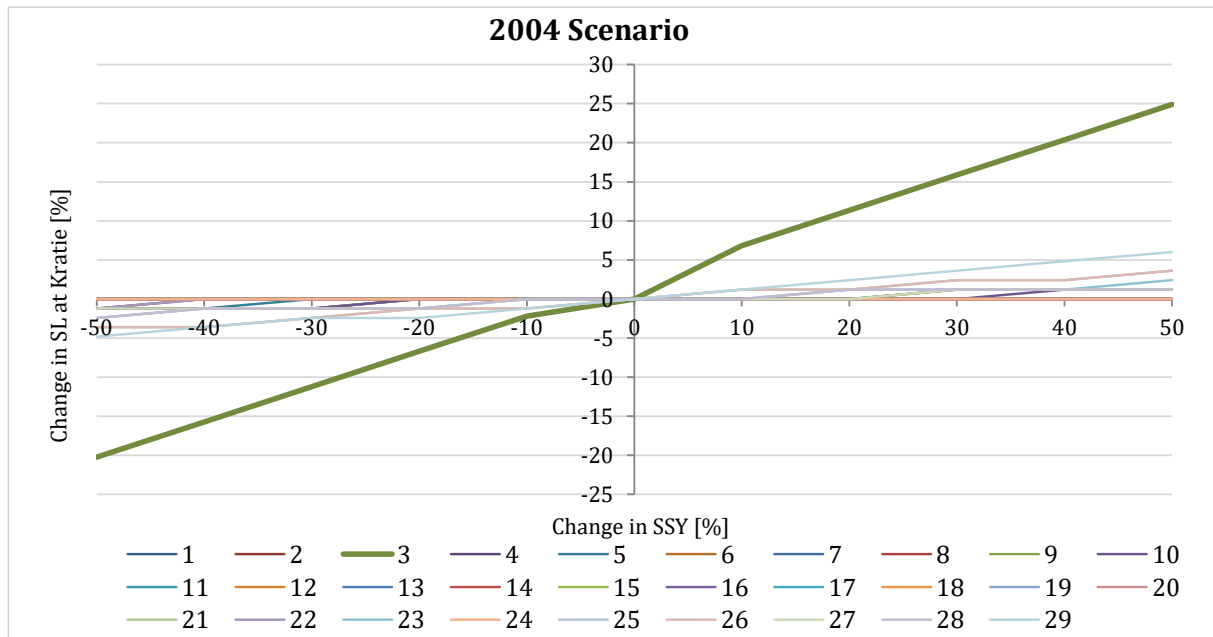


Figure 48: Sensitivity analysis of SSY on SL at Kratie in 2004 for the Brune model

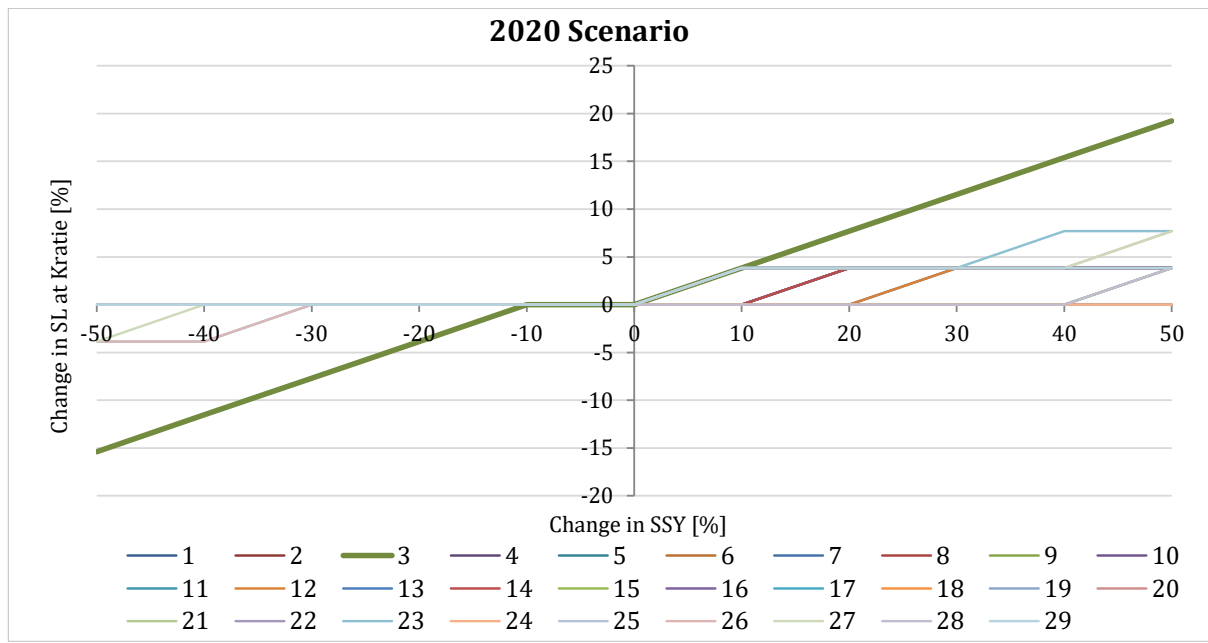


Figure 49: Sensitivity analysis of SSY on SL at Kratie in 2020 for the Brune model

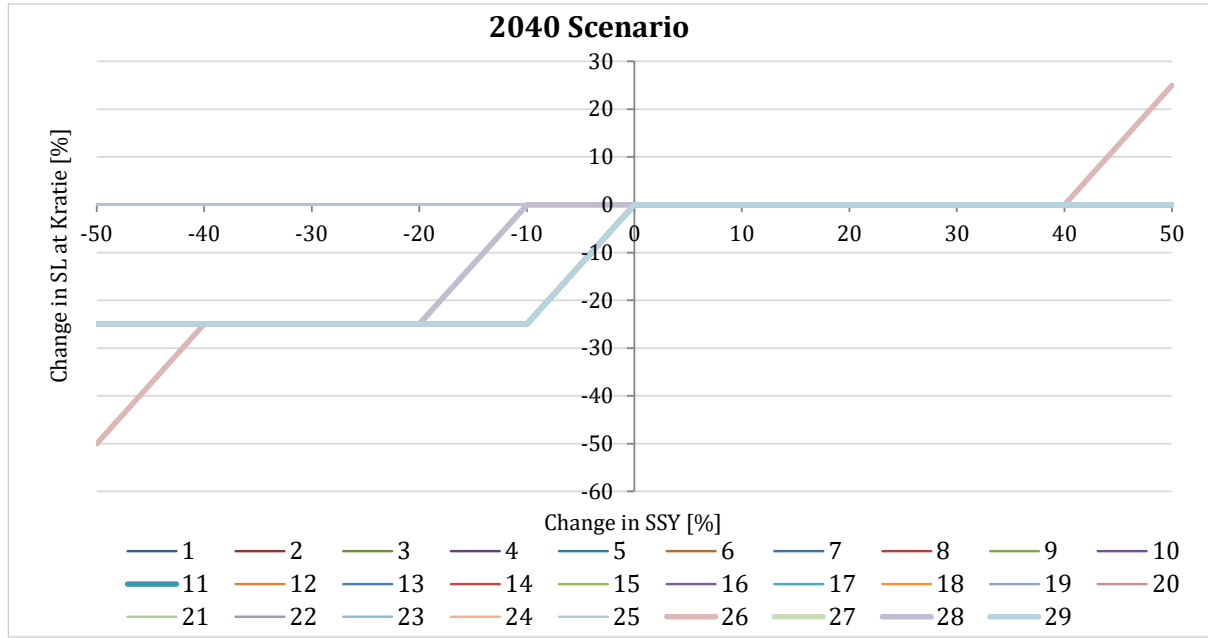


Figure 50: Sensitivity analysis of SSY on SL at Kratie in 2040 for the Brune model

Appendix E.1.2 Defined TE Model

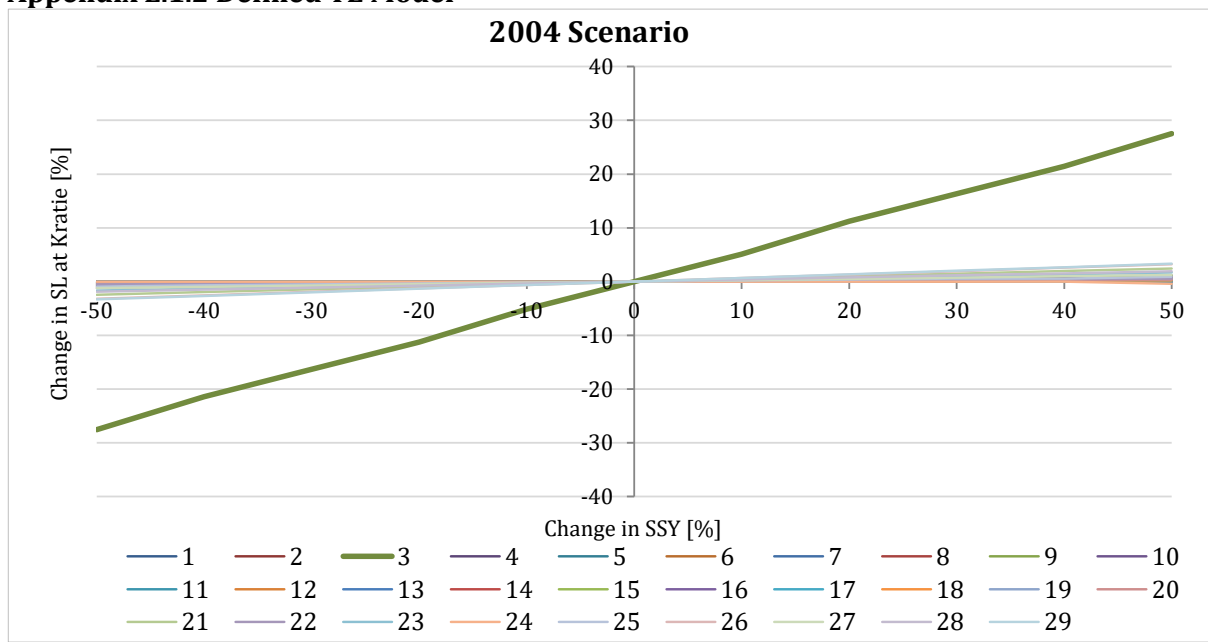


Figure 51: Sensitivity analysis of SSY on SL at Kratie in 2004 for the Defined TE model

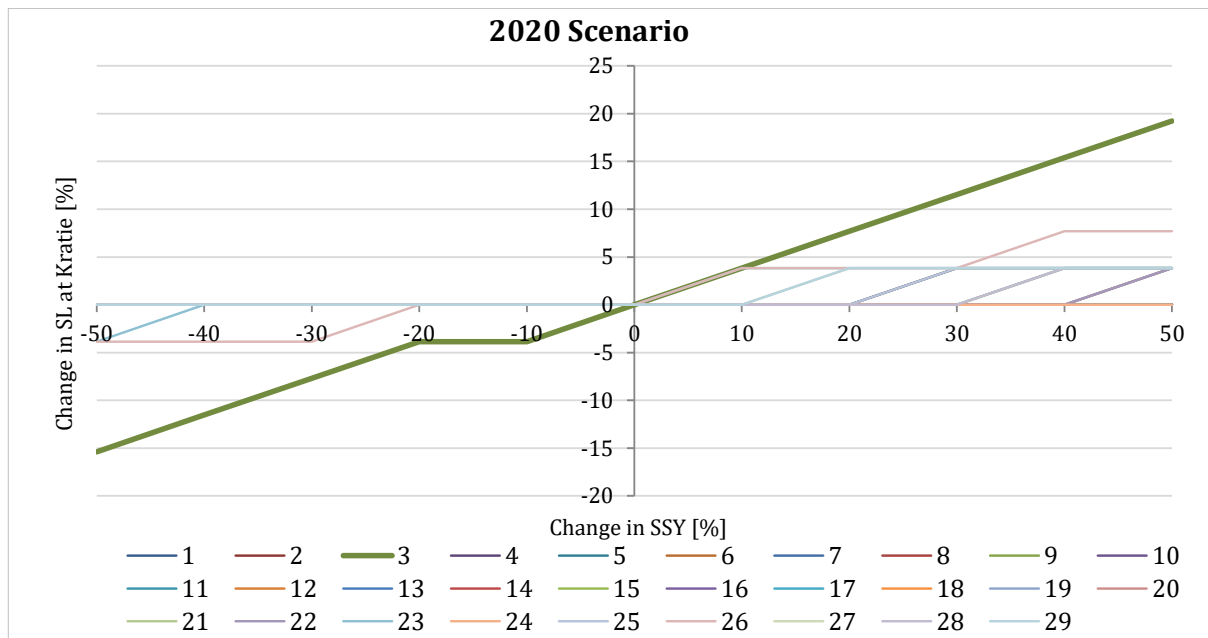


Figure 52: Sensitivity analysis of SSY on SL at Kratie in 2020 for the Defined TE model

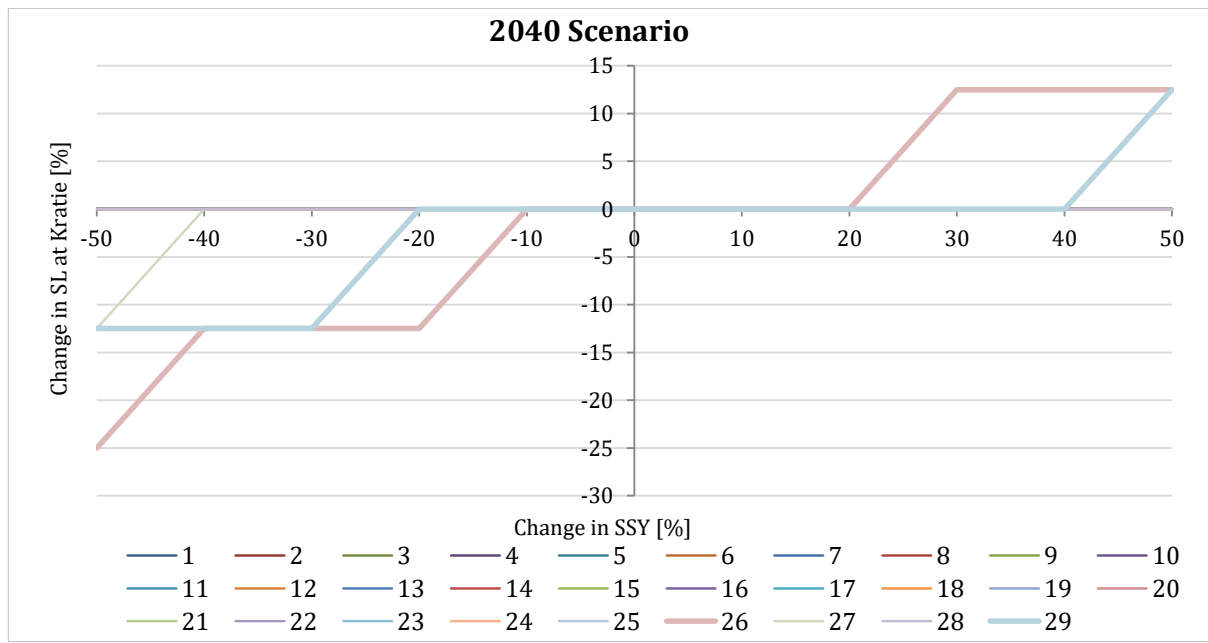


Figure 53: Sensitivity analysis of SSY on SL at Kratie in 2040 for the Defined TE model

Appendix E.2 Sensitivity analysis of Correction Factors

Appendix E.2.1: Brune Model

2004

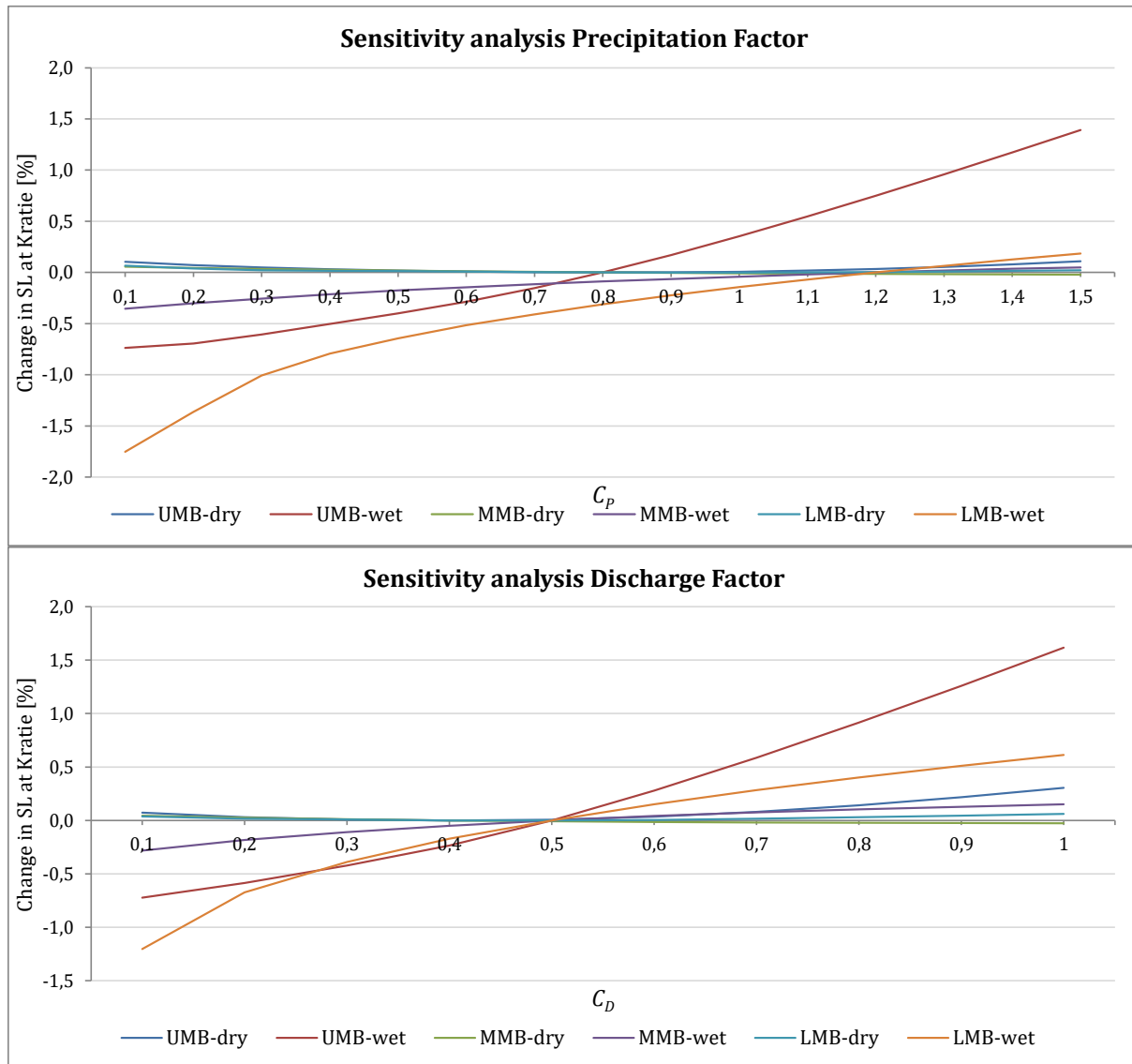


Figure 54: Sensitivity analyses of correction factors for the Brune model in the 2004 scenario

2020

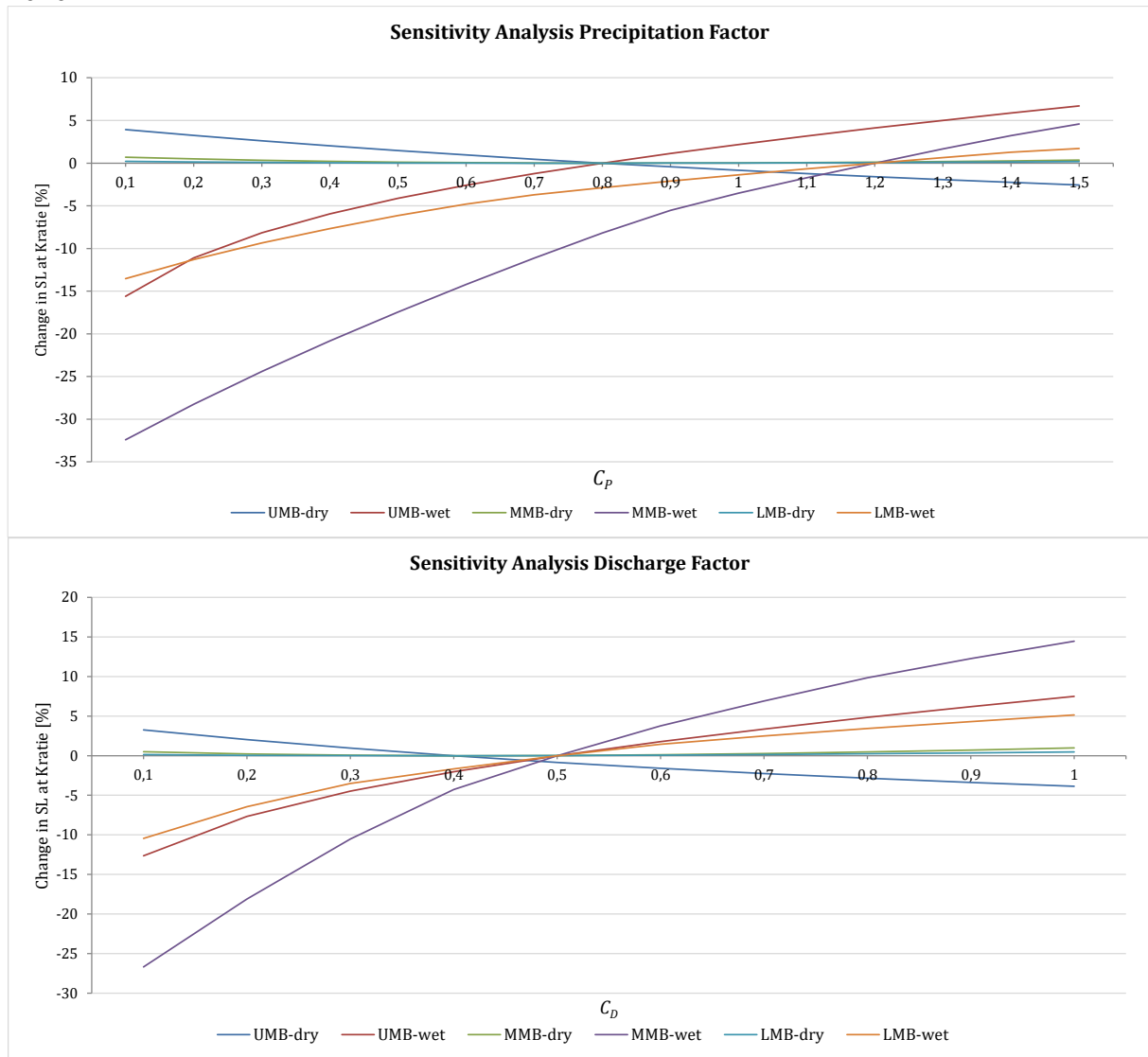


Figure 55: Sensitivity analyses of correction factors for the Brune model in the 2020 scenario

2040

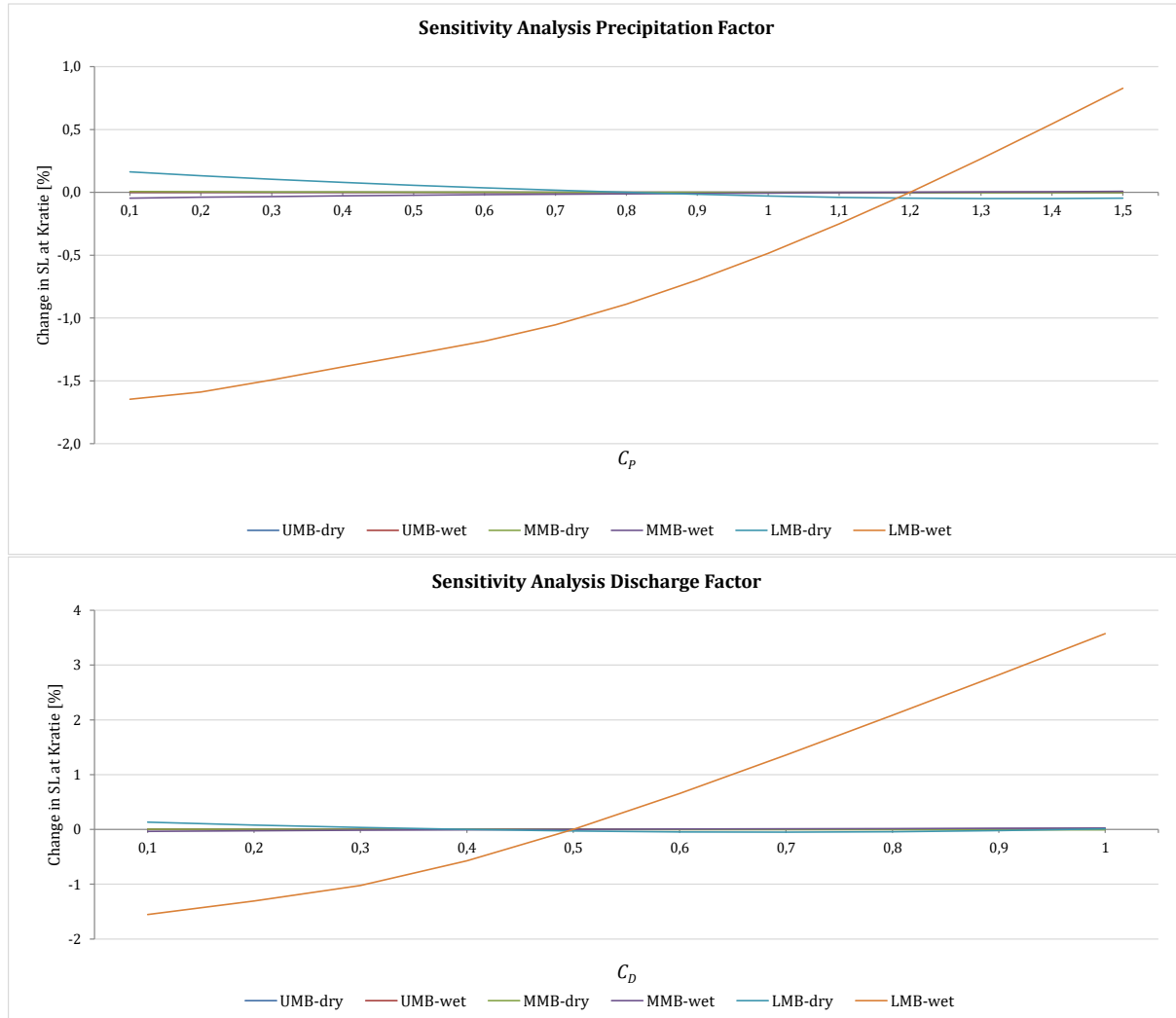


Figure 56: Sensitivity analyses of correction factors for the Brune model in the 2040 scenario

Appendix E.2.2: Defined TE Model

2004

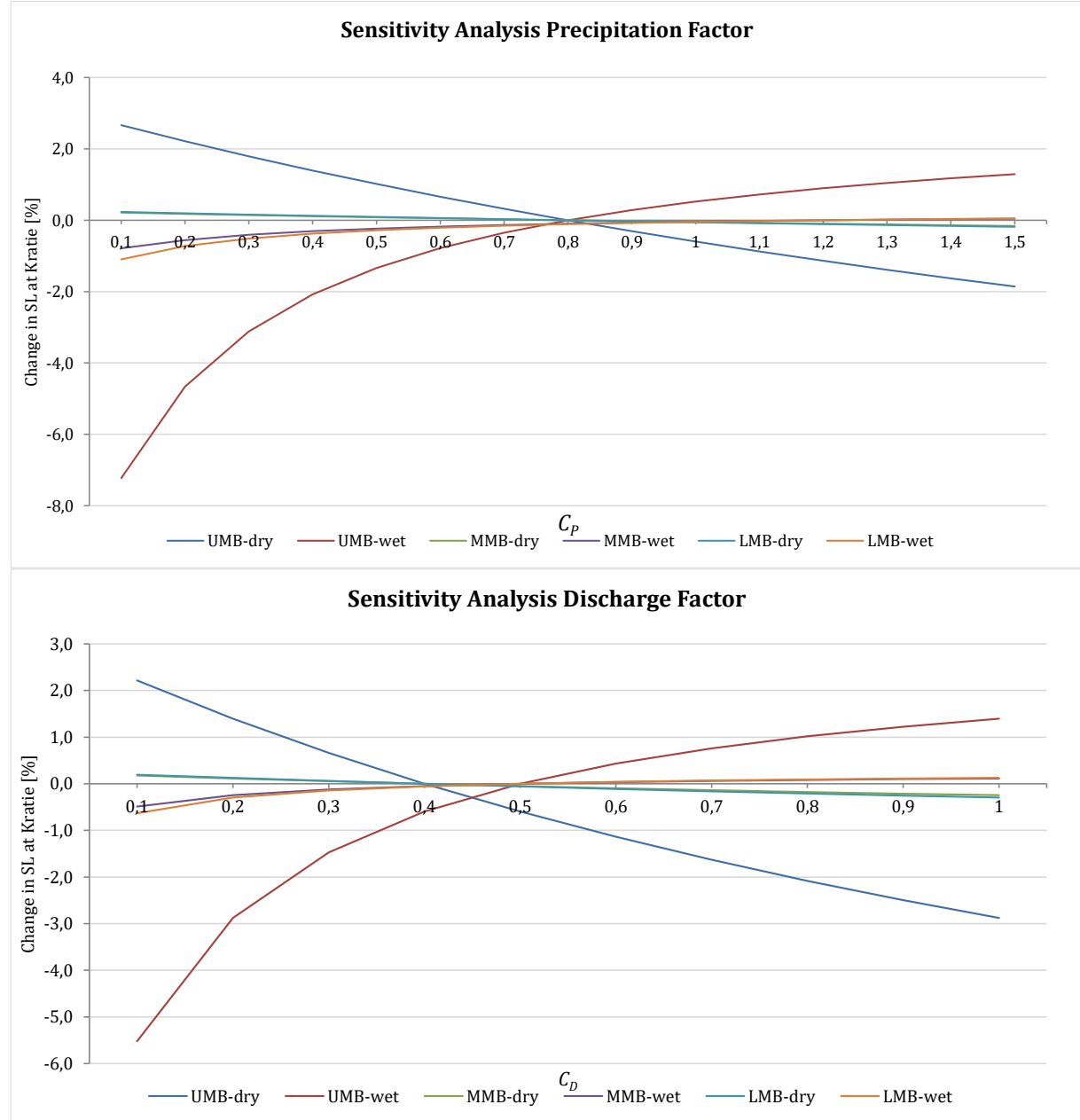


Figure 57: Sensitivity analyses of correction factors for the Defined TE model in the 2004 scenario

2020

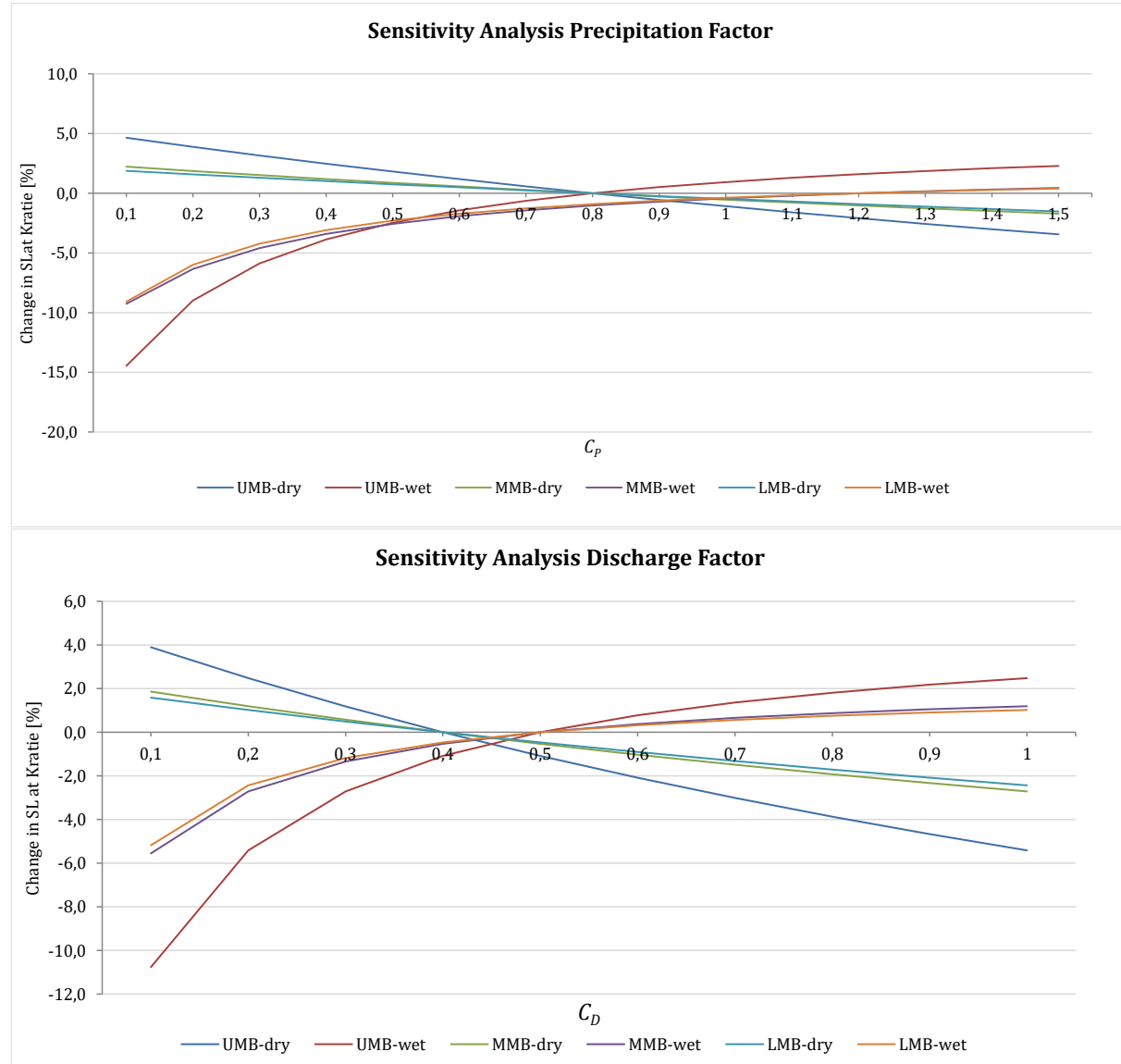


Figure 58: Sensitivity analyses of correction factors for the Defined TE model in the 2020 scenario

2040

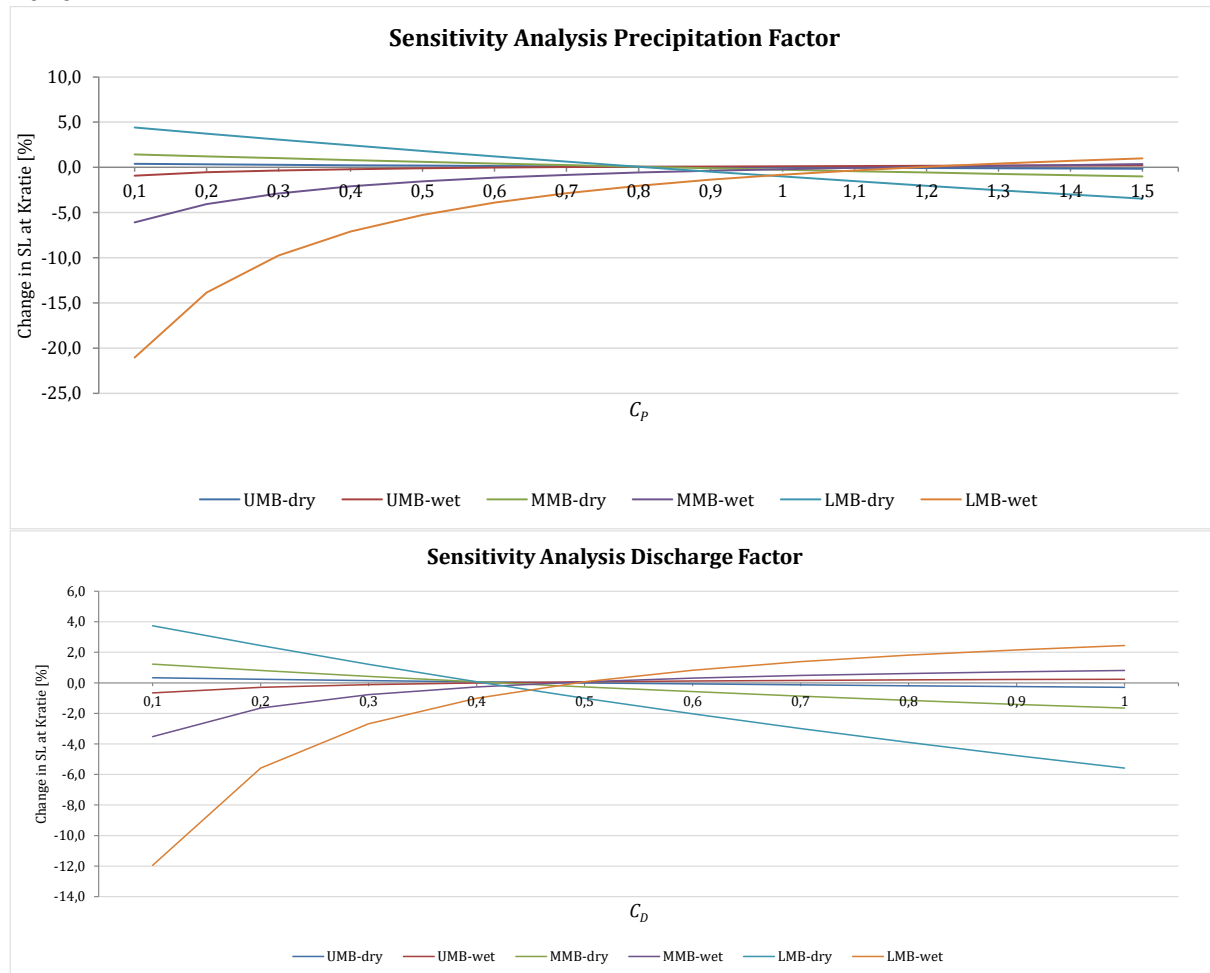


Figure 59: Sensitivity analyses of correction factors for the Defined TE model in the 2040 scenario

Appendix E.3 Sensitivity analysis of Discharge

Appendix E.3.1 Brune Model

2004

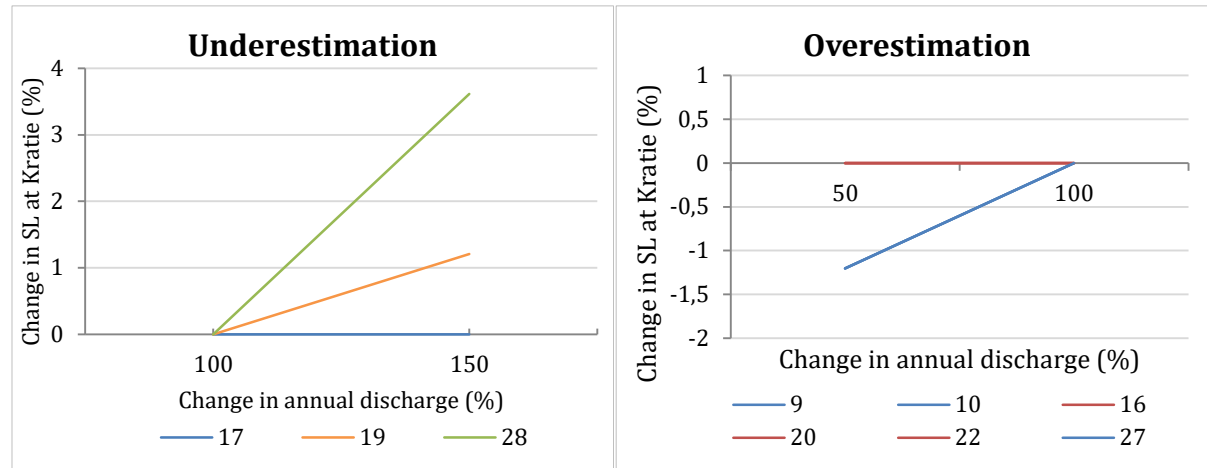


Figure 60: Sensitivity analysis of under- and overestimated discharges for the Brune model in 2004. This is done for the sub-basins for which the discharge was under- or overestimated.

2020

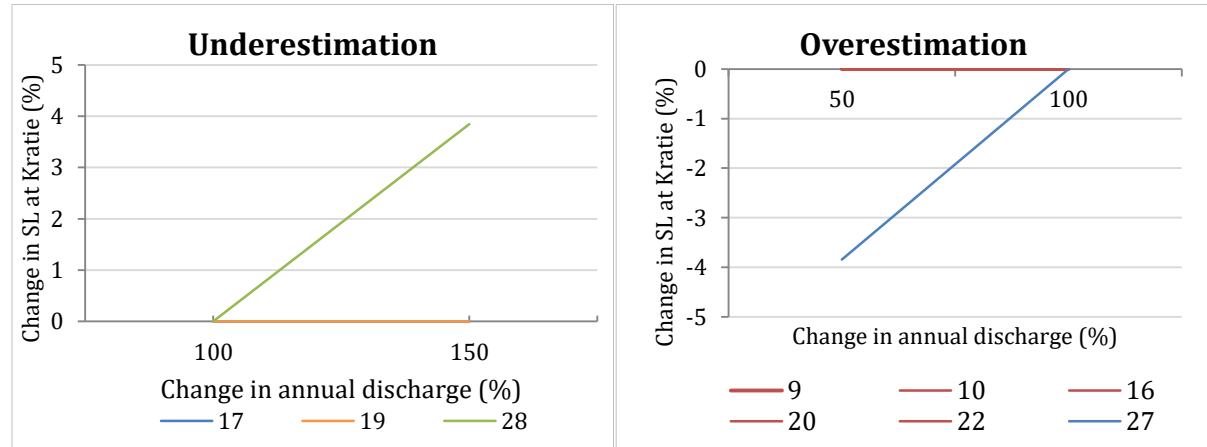


Figure 61: Sensitivity analysis of under- and overestimated discharges for the Brune model in 2020. This is done for the sub-basins for which the discharge was under- or overestimated.

2040

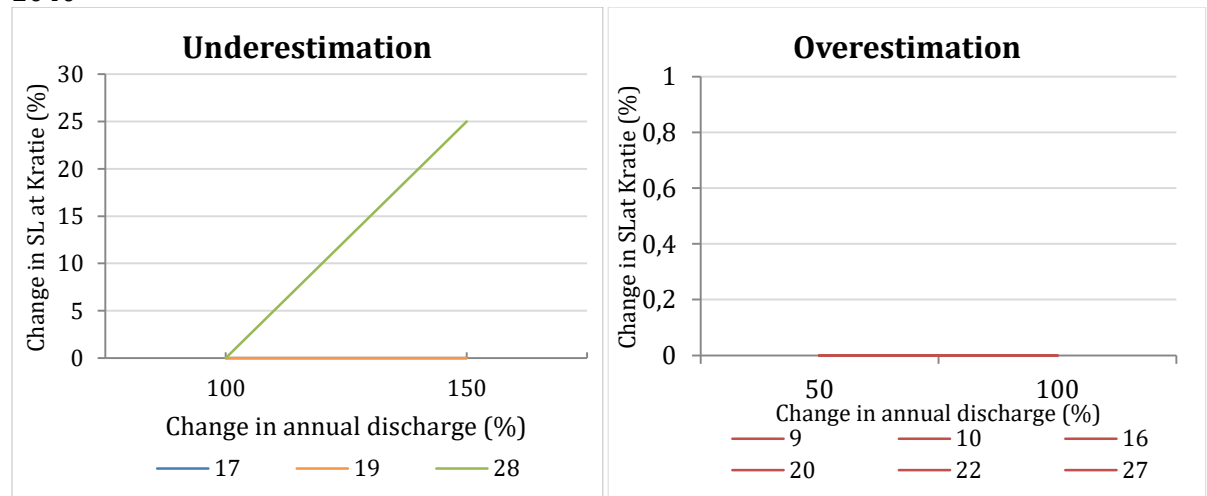


Figure 62: Sensitivity analysis of under- and overestimated discharges for the Brune model in 2040. This is done for the sub-basins for which the discharge was under- or overestimated.

Appendix E.3.1 Defined TE Model

2004

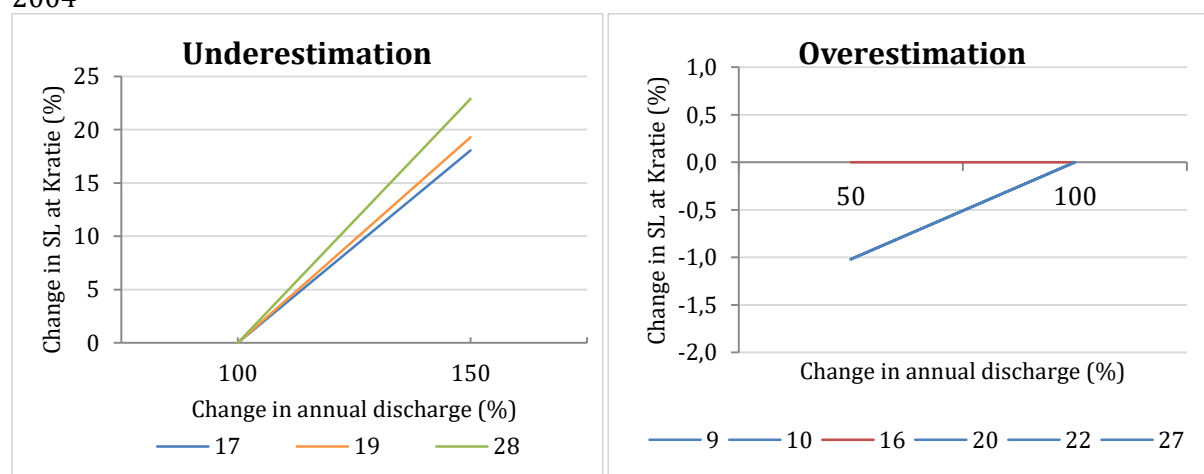


Figure 63: Sensitivity analysis of under- and overestimated discharges for the Defined TE model in 2004. This is done for the sub-basins for which the discharge was under- or overestimated.

2020

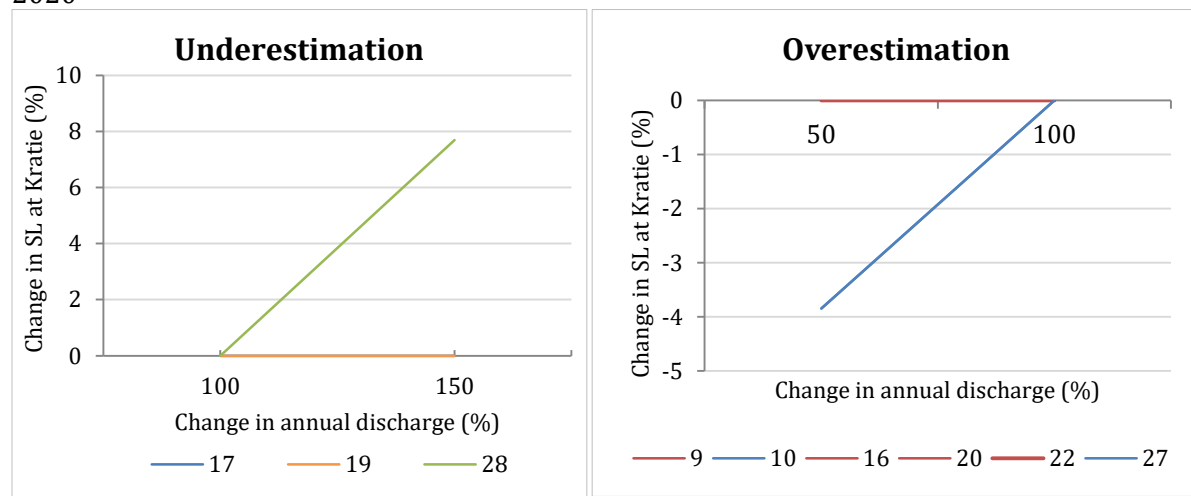


Figure 64: Sensitivity analysis of under- and overestimated discharges for the Defined TE model in 2020. This is done for the sub-basins for which the discharge was under- or overestimated.

2040

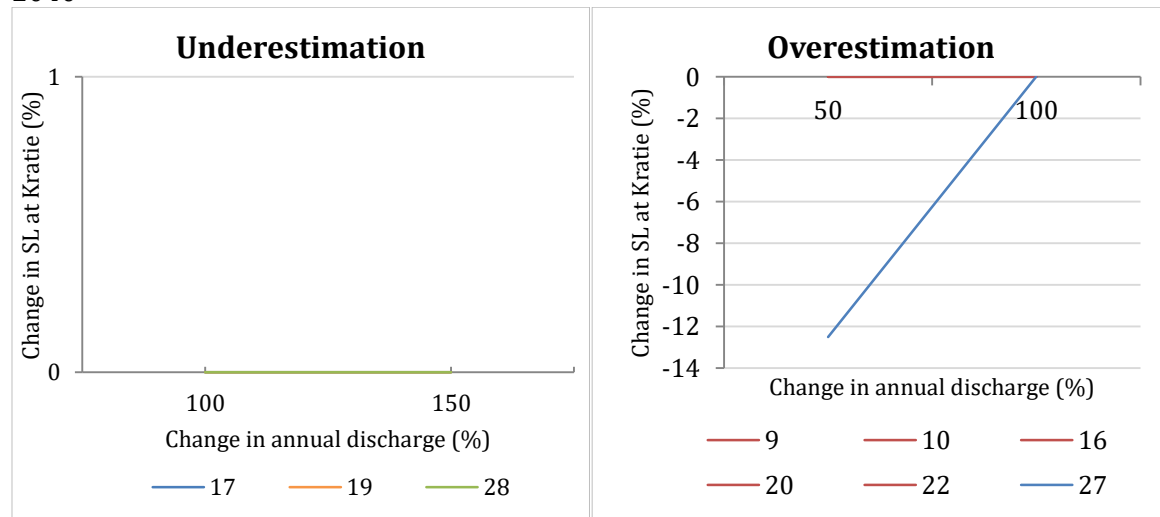


Figure 65: Sensitivity analysis of under- and overestimated discharges for the Defined TE model in 2040. This is done for the sub-basins for which the discharge was under- or overestimated

Appendix E.4 Sensitivity analysis of Glacier Melting

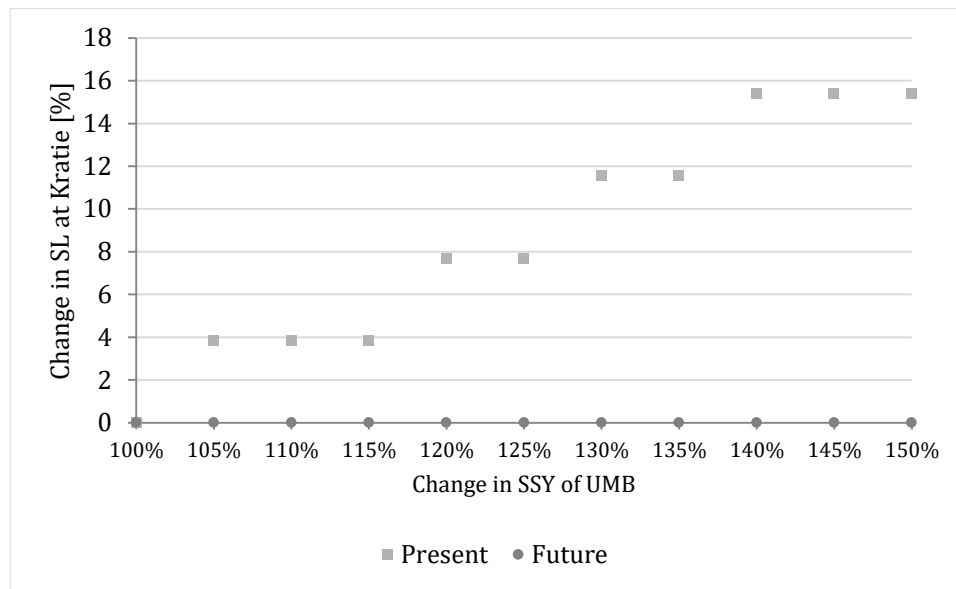


Figure 66: Sensitivity analysis of glacier melting for Present and Future scenario

Appendix F. Strategy analyses

Appendix F.1 Cancelling dams

Appendix F.1.1 Brune Model

In Table 12, an overview is given of all possible cancellation options of planned dams in the Mekong Basin for the Brune model. In the first row the dam names are stated and in the last two columns the SL at Kratie is given. If a 0 is assigned to a dam, this means that the dam is not constructed. All other values are the active volumes (km^3) of the dams.

The optimum is indicated with green: option 185.

Table 12: Overview of all cancellation options for the Brune model and their corresponding SL at Kratie. The optimum is given in green.

124	0,31	0,0558	2,01	0,03	0,005	0,0048	0,68	1,174	0	0,288	1,477	0,56148	0,51795	0,01931	0,0195	0,41341	4
125	0,31	0,0558	2,01	0,03	0,005	0,0048	0,68	1,174	0	0	1,477	0,56148	0,51795	0,01931	0,0195	0,41341	4
126	0,31	0,0558	2,01	0,03	0,005	0,0048	0,68	1,174	0	0	0	0,56148	0,51795	0,01931	0,0195	0,41341	4
127	0,31	0,0558	2,01	0,03	0,005	0,0048	0,68	1,174	0	0	0	0	0,51795	0,01931	0,0195	0,41341	4
128	0,31	0,0558	2,01	0,03	0,005	0,0048	0,68	1,174	0	0	0	0	0	0,01931	0,0195	0,41341	5
129	0,31	0,0558	2,01	0,03	0,005	0,0048	0,68	1,174	0	0	0	0	0	0	0,0195	0,41341	5
130	0,31	0,0558	2,01	0,03	0,005	0,0048	0,68	1,174	0	0	0	0	0	0	0	0,41341	5
131	0,31	0,0558	2,01	0,03	0,005	0,0048	0,68	1,174	0	0	0	0	0	0	0	0	5
132	0	0,0558	2,01	0,03	0,005	0,0048	0,68	1,174	0	0	0	0	0	0	0	0	5
133	0	0	2,01	0,03	0,005	0,0048	0,68	1,174	0	0	0	0	0	0	0	0	5
134	0	0	0	0,03	0,005	0,0048	0,68	1,174	0	0	0	0	0	0	0	0	5
135	0	0	0	0	0,005	0,0048	0,68	1,174	0	0	0	0	0	0	0	0	5
136	0	0	0	0	0	0,0048	0,68	1,174	0	0	0	0	0	0	0	0	5
137	0	0	0	0	0	0	0,68	1,174	0	0	0	0	0	0	0	0	5
138	0	0	0	0	0	0	0	1,174	0	0	0	0	0	0	0	0	5
139	0,31	0,0558	2,01	0,03	0,005	0,0048	0,68	1,174	1,5651	0	1,477	0,56148	0,51795	0,01931	0,0195	0,41341	4
140	0,31	0,0558	2,01	0,03	0,005	0,0048	0,68	1,174	1,5651	0	0	0,56148	0,51795	0,01931	0,0195	0,41341	4
141	0,31	0,0558	2,01	0,03	0,005	0,0048	0,68	1,174	1,5651	0	0	0	0,51795	0,01931	0,0195	0,41341	4
142	0,31	0,0558	2,01	0,03	0,005	0,0048	0,68	1,174	1,5651	0	0	0	0	0,01931	0,0195	0,41341	5
143	0,31	0,0558	2,01	0,03	0,005	0,0048	0,68	1,174	1,5651	0	0	0	0	0	0,0195	0,41341	5
144	0,31	0,0558	2,01	0,03	0,005	0,0048	0,68	1,174	1,5651	0	0	0	0	0	0	0,41341	5
145	0,31	0,0558	2,01	0,03	0,005	0,0048	0,68	1,174	1,5651	0	0	0	0	0	0	0	5
146	0	0,0558	2,01	0,03	0,005	0,0048	0,68	1,174	1,5651	0	0	0	0	0	0	0	5
147	0	0	2,01	0,03	0,005	0,0048	0,68	1,174	1,5651	0	0	0	0	0	0	0	5
148	0	0	0	0,03	0,005	0,0048	0,68	1,174	1,5651	0	0	0	0	0	0	0	5
149	0	0	0	0	0,005	0,0048	0,68	1,174	1,5651	0	0	0	0	0	0	0	5
150	0	0	0	0	0	0,0048	0,68	1,174	1,5651	0	0	0	0	0	0	0	5
151	0	0	0	0	0	0	0,68	1,174	1,5651	0	0	0	0	0	0	0	5
152	0	0	0	0	0	0	0	1,174	1,5651	0	0	0	0	0	0	0	5
153	0	0	0	0	0	0	0	0	1,5651	0	0	0	0	0	0	0	5
154	0,31	0,0558	2,01	0,03	0,005	0,0048	0,68	1,174	1,5651	0,288	0	0,56148	0,51795	0,01931	0,0195	0,41341	4
155	0,31	0,0558	2,01	0,03	0,005	0,0048	0,68	1,174	1,5651	0,288	0	0	0,51795	0,01931	0,0195	0,41341	4
156	0,31	0,0558	2,01	0,03	0,005	0,0048	0,68	1,174	1,5651	0,288	0	0	0	0,01931	0,0195	0,41341	5
157	0,31	0,0558	2,01	0,03	0,005	0,0048	0,68	1,174	1,5651	0,288	0	0	0	0	0,0195	0,41341	5
158	0,31	0,0558	2,01	0,03	0,005	0,0048	0,68	1,174	1,5651	0,288	0	0	0	0	0	0,41341	5
159	0,31	0,0558	2,01	0,03	0,005	0,0048	0,68	1,174	1,5651	0,288	0	0	0	0	0	0	5
160	0	0,0558	2,01	0,03	0,005	0,0048	0,68	1,174	1,5651	0,288	0	0	0	0	0	0	5
161	0	0	2,01	0,03	0,005	0,0048	0,68	1,174	1,5651	0,288	0	0	0	0	0	0	5
162	0	0	0	0,03	0,005	0,0048	0,68	1,174	1,5651	0,288	0	0	0	0	0	0	5
163	0	0	0	0	0,005	0,0048	0,68	1,174	1,5651	0,288	0	0	0	0	0	0	5
164	0	0	0	0	0	0,0048	0,68	1,174	1,5651	0,288	0	0	0	0	0	0	5
165	0	0	0	0	0	0	0,68	1,174	1,5651	0,288	0	0	0	0	0	0	5
166	0	0	0	0	0	0	0	1,174	1,5651	0,288	0	0	0	0	0	0	5
167	0	0	0	0	0	0	0	0	1,5651	0,288	0	0	0	0	0	0	5
168	0	0	0	0	0	0	0	0	0	0,288	0	0	0	0	0	0	5

169	0,31	0,0558	2,01	0,03	0,005	0,0048	0,68	1,174	1,5651	0,288	1,477	0	0,51795	0,01931	0,0195	0,41341	4
170	0,31	0,0558	2,01	0,03	0,005	0,0048	0,68	1,174	1,5651	0,288	1,477	0	0	0,01931	0,0195	0,41341	5
171	0,31	0,0558	2,01	0,03	0,005	0,0048	0,68	1,174	1,5651	0,288	1,477	0	0	0	0,0195	0,41341	5
172	0,31	0,0558	2,01	0,03	0,005	0,0048	0,68	1,174	1,5651	0,288	1,477	0	0	0	0	0,41341	5
173	0,31	0,0558	2,01	0,03	0,005	0,0048	0,68	1,174	1,5651	0,288	1,477	0	0	0	0	0	5
174	0	0,0558	2,01	0,03	0,005	0,0048	0,68	1,174	1,5651	0,288	1,477	0	0	0	0	0	5
175	0	0	2,01	0,03	0,005	0,0048	0,68	1,174	1,5651	0,288	1,477	0	0	0	0	0	5
176	0	0	0	0,03	0,005	0,0048	0,68	1,174	1,5651	0,288	1,477	0	0	0	0	0	5
177	0	0	0	0,03	0,005	0,0048	0,68	1,174	1,5651	0,288	1,477	0	0	0	0	0	5
178	0	0	0	0	0,005	0,0048	0,68	1,174	1,5651	0,288	1,477	0	0	0	0	0	5
179	0	0	0	0	0	0,0048	0,68	1,174	1,5651	0,288	1,477	0	0	0	0	0	5
180	0	0	0	0	0	0	0,68	1,174	1,5651	0,288	1,477	0	0	0	0	0	5
181	0	0	0	0	0	0	0	1,174	1,5651	0,288	1,477	0	0	0	0	0	5
182	0	0	0	0	0	0	0	0	1,5651	0,288	1,477	0	0	0	0	0	5
183	0	0	0	0	0	0	0	0	0	0,288	1,477	0	0	0	0	0	5
184	0	0	0	0	0	0	0	0	0	0	1,477	0	0	0	0	0	5
185	0,31	0,0558	2,01	0,03	0,005	0,0048	0,68	1,174	1,5651	0,288	1,477	0,56148	0	0,01931	0,0195	0,41341	5
186	0,31	0,0558	2,01	0,03	0,005	0,0048	0,68	1,174	1,5651	0,288	1,477	0,56148	0	0	0,0195	0,41341	5
187	0,31	0,0558	2,01	0,03	0,005	0,0048	0,68	1,174	1,5651	0,288	1,477	0,56148	0	0	0	0,41341	5
188	0,31	0,0558	2,01	0,03	0,005	0,0048	0,68	1,174	1,5651	0,288	1,477	0,56148	0	0	0	0	5
189	0	0,0558	2,01	0,03	0,005	0,0048	0,68	1,174	1,5651	0,288	1,477	0,56148	0	0	0	0	5
190	0	0	2,01	0,03	0,005	0,0048	0,68	1,174	1,5651	0,288	1,477	0,56148	0	0	0	0	5
191	0	0	0	0,03	0,005	0,0048	0,68	1,174	1,5651	0,288	1,477	0,56148	0	0	0	0	5
192	0	0	0	0	0,005	0,0048	0,68	1,174	1,5651	0,288	1,477	0,56148	0	0	0	0	5
193	0	0	0	0	0	0,0048	0,68	1,174	1,5651	0,288	1,477	0,56148	0	0	0	0	5
194	0	0	0	0	0	0	0,68	1,174	1,5651	0,288	1,477	0,56148	0	0	0	0	5
195	0	0	0	0	0	0	0	1,174	1,5651	0,288	1,477	0,56148	0	0	0	0	5
196	0	0	0	0	0	0	0	0	1,5651	0,288	1,477	0,56148	0	0	0	0	5
197	0	0	0	0	0	0	0	0	0	0,288	1,477	0,56148	0	0	0	0	5
198	0	0	0	0	0	0	0	0	0	0	1,477	0,56148	0	0	0	0	5
199	0	0	0	0	0	0	0	0	0	0	0	0,56148	0	0	0	0	5
200	0,31	0,0558	2,01	0,03	0,005	0,0048	0,68	1,174	1,5651	0,288	1,477	0,56148	0,51795	0	0,0195	0,41341	4
201	0,31	0,0558	2,01	0,03	0,005	0,0048	0,68	1,174	1,5651	0,288	1,477	0,56148	0,51795	0	0	0,41341	4
202	0,31	0,0558	2,01	0,03	0,005	0,0048	0,68	1,174	1,5651	0,288	1,477	0,56148	0,51795	0	0	0	4
203	0	0,0558	2,01	0,03	0,005	0,0048	0,68	1,174	1,5651	0,288	1,477	0,56148	0,51795	0	0	0	4
204	0	0	2,01	0,03	0,005	0,0048	0,68	1,174	1,5651	0,288	1,477	0,56148	0,51795	0	0	0	4
205	0	0	0	0,03	0,005	0,0048	0,68	1,174	1,5651	0,288	1,477	0,56148	0,51795	0	0	0	4
206	0	0	0	0	0,005	0,0048	0,68	1,174	1,5651	0,288	1,477	0,56148	0,51795	0	0	0	4
207	0	0	0	0	0	0,0048	0,68	1,174	1,5651	0,288	1,477	0,56148	0,51795	0	0	0	4
208	0	0	0	0	0	0	0,68	1,174	1,5651	0,288	1,477	0,56148	0,51795	0	0	0	4
209	0	0	0	0	0	0	0	1,174	1,5651	0,288	1,477	0,56148	0,51795	0	0	0	4
210	0	0	0	0	0	0	0	0	1,5651	0,288	1,477	0,56148	0,51795	0	0	0	4
211	0	0	0	0	0	0	0	0	0	0,288	1,477	0,56148	0,51795	0	0	0	4
212	0	0	0	0	0	0	0	0	0	0	1,477	0,56148	0,51795	0	0	0	4
213	0	0	0	0	0	0	0	0	0	0	0	0,56148	0,51795	0	0	0	4
214	0	0	0	0	0	0	0	0	0	0	0	0,51795	0	0	0	0	4

215	0,31	0,0558	2,01	0,03	0,005	0,0048	0,68	1,174	1,5651	0,288	1,477	0,56148	0,51795	0,01931	0	0,41341	4	
216	0,31	0,0558	2,01	0,03	0,005	0,0048	0,68	1,174	1,5651	0,288	1,477	0,56148	0,51795	0,01931	0	0	4	
217	0	0,0558	2,01	0,03	0,005	0,0048	0,68	1,174	1,5651	0,288	1,477	0,56148	0,51795	0,01931	0	0	4	
218	0	0	2,01	0,03	0,005	0,0048	0,68	1,174	1,5651	0,288	1,477	0,56148	0,51795	0,01931	0	0	4	
219	0	0	0	0,03	0,005	0,0048	0,68	1,174	1,5651	0,288	1,477	0,56148	0,51795	0,01931	0	0	4	
220	0	0	0	0	0,005	0,0048	0,68	1,174	1,5651	0,288	1,477	0,56148	0,51795	0,01931	0	0	4	
221	0	0	0	0	0	0,0048	0,68	1,174	1,5651	0,288	1,477	0,56148	0,51795	0,01931	0	0	4	
222	0	0	0	0	0	0	0,68	1,174	1,5651	0,288	1,477	0,56148	0,51795	0,01931	0	0	4	
223	0	0	0	0	0	0	0	1,174	1,5651	0,288	1,477	0,56148	0,51795	0,01931	0	0	4	
224	0	0	0	0	0	0	0	0	1,5651	0,288	1,477	0,56148	0,51795	0,01931	0	0	4	
225	0	0	0	0	0	0	0	0	0	0,288	1,477	0,56148	0,51795	0,01931	0	0	4	
226	0	0	0	0	0	0	0	0	0	0	0	1,477	0,56148	0,51795	0,01931	0	0	4
227	0	0	0	0	0	0	0	0	0	0	0	0	0,56148	0,51795	0,01931	0	0	4
228	0	0	0	0	0	0	0	0	0	0	0	0	0	0,51795	0,01931	0	0	4
229	0	0	0	0	0	0	0	0	0	0	0	0	0	0	0,01931	0	0	5
230	0,31	0,0558	2,01	0,03	0,005	0,0048	0,68	1,174	1,5651	0,288	1,477	0,56148	0,51795	0,01931	0,0195	0	4	
231	0	0,0558	2,01	0,03	0,005	0,0048	0,68	1,174	1,5651	0,288	1,477	0,56148	0,51795	0,01931	0,0195	0	4	
232	0	0	2,01	0,03	0,005	0,0048	0,68	1,174	1,5651	0,288	1,477	0,56148	0,51795	0,01931	0,0195	0	4	
233	0	0	0	0,03	0,005	0,0048	0,68	1,174	1,5651	0,288	1,477	0,56148	0,51795	0,01931	0,0195	0	4	
234	0	0	0	0	0	0,005	0,0048	0,68	1,174	1,5651	0,288	1,477	0,56148	0,51795	0,01931	0,0195	0	4
235	0	0	0	0	0	0	0,0048	0,68	1,174	1,5651	0,288	1,477	0,56148	0,51795	0,01931	0,0195	0	4
236	0	0	0	0	0	0	0	0,68	1,174	1,5651	0,288	1,477	0,56148	0,51795	0,01931	0,0195	0	4
237	0	0	0	0	0	0	0	0	1,174	1,5651	0,288	1,477	0,56148	0,51795	0,01931	0,0195	0	4
238	0	0	0	0	0	0	0	0	0	1,5651	0,288	1,477	0,56148	0,51795	0,01931	0,0195	0	4
239	0	0	0	0	0	0	0	0	0	0	0,288	1,477	0,56148	0,51795	0,01931	0,0195	0	4
240	0	0	0	0	0	0	0	0	0	0	0	1,477	0,56148	0,51795	0,01931	0,0195	0	4
241	0	0	0	0	0	0	0	0	0	0	0	0	0,56148	0,51795	0,01931	0,0195	0	4
242	0	0	0	0	0	0	0	0	0	0	0	0	0	0,51795	0,01931	0,0195	0	4
243	0	0	0	0	0	0	0	0	0	0	0	0	0	0	0,01931	0,0195	0	5
244	0	0	0	0	0	0	0	0	0	0	0	0	0	0	0	0,0195	0	5

Appendix F.1.2 Defined TE Model

In Table 13 an overview is given of all possible cancellation options of planned dams in the Mekong Basin for the Defined TE model. For explanation see Appendix F.1.1. The optimum is indicated with green: option 170.

Table 13: Overview of all cancellation options for the Defined TE model and their corresponding SL at Kratie. The optimum is given in green.

139	0,31	0,0558	2,01	0,03	0,005	0,0048	0,68	1,174	1,5651	0	1,477	0,56148	0,51795	0,01931	0,0195	0,41341	8	
140	0,31	0,0558	2,01	0,03	0,005	0,0048	0,68	1,174	1,5651	0	0	0,56148	0,51795	0,01931	0,0195	0,41341	8	
141	0,31	0,0558	2,01	0,03	0,005	0,0048	0,68	1,174	1,5651	0	0	0	0,51795	0,01931	0,0195	0,41341	9	
142	0,31	0,0558	2,01	0,03	0,005	0,0048	0,68	1,174	1,5651	0	0	0	0	0,01931	0,0195	0,41341	11	
143	0,31	0,0558	2,01	0,03	0,005	0,0048	0,68	1,174	1,5651	0	0	0	0	0	0,0195	0,41341	11	
144	0,31	0,0558	2,01	0,03	0,005	0,0048	0,68	1,174	1,5651	0	0	0	0	0	0	0,41341	11	
145	0,31	0,0558	2,01	0,03	0,005	0,0048	0,68	1,174	1,5651	0	0	0	0	0	0	0	11	
146	0	0,0558	2,01	0,03	0,005	0,0048	0,68	1,174	1,5651	0	0	0	0	0	0	0	11	
147	0	0	2,01	0,03	0,005	0,0048	0,68	1,174	1,5651	0	0	0	0	0	0	0	11	
148	0	0	0	0,03	0,005	0,0048	0,68	1,174	1,5651	0	0	0	0	0	0	0	11	
149	0	0	0	0	0,005	0,0048	0,68	1,174	1,5651	0	0	0	0	0	0	0	11	
150	0	0	0	0	0	0,0048	0,68	1,174	1,5651	0	0	0	0	0	0	0	11	
151	0	0	0	0	0	0	0,68	1,174	1,5651	0	0	0	0	0	0	0	11	
152	0	0	0	0	0	0	0	1,174	1,5651	0	0	0	0	0	0	0	11	
153	0	0	0	0	0	0	0	0	1,5651	0	0	0	0	0	0	0	11	
154	0,31	0,0558	2,01	0,03	0,005	0,0048	0,68	1,174	1,5651	0,288	0	0,56148	0,51795	0,01931	0,0195	0,41341	8	
155	0,31	0,0558	2,01	0,03	0,005	0,0048	0,68	1,174	1,5651	0,288	0	0	0,51795	0,01931	0,0195	0,41341	9	
156	0,31	0,0558	2,01	0,03	0,005	0,0048	0,68	1,174	1,5651	0,288	0	0	0	0,01931	0,0195	0,41341	11	
157	0,31	0,0558	2,01	0,03	0,005	0,0048	0,68	1,174	1,5651	0,288	0	0	0	0	0,0195	0,41341	11	
158	0,31	0,0558	2,01	0,03	0,005	0,0048	0,68	1,174	1,5651	0,288	0	0	0	0	0	0,41341	11	
159	0,31	0,0558	2,01	0,03	0,005	0,0048	0,68	1,174	1,5651	0,288	0	0	0	0	0	0	11	
160	0	0,0558	2,01	0,03	0,005	0,0048	0,68	1,174	1,5651	0,288	0	0	0	0	0	0	11	
161	0	0	2,01	0,03	0,005	0,0048	0,68	1,174	1,5651	0,288	0	0	0	0	0	0	11	
162	0	0	0	0,03	0,005	0,0048	0,68	1,174	1,5651	0,288	0	0	0	0	0	0	11	
163	0	0	0	0	0	0,005	0,0048	0,68	1,174	1,5651	0,288	0	0	0	0	0	11	
164	0	0	0	0	0	0	0,0048	0,68	1,174	1,5651	0,288	0	0	0	0	0	11	
165	0	0	0	0	0	0	0,68	1,174	1,5651	0,288	0	0	0	0	0	0	11	
166	0	0	0	0	0	0	0	0	1,174	1,5651	0,288	0	0	0	0	0	11	
167	0	0	0	0	0	0	0	0	0	1,5651	0,288	0	0	0	0	0	11	
168	0	0	0	0	0	0	0	0	0	0	0,288	0	0	0	0	0	11	
169	0,31	0,0558	2,01	0,03	0,005	0,0048	0,68	1,174	1,5651	0,288	1,477	0	0,51795	0,01931	0,0195	0,41341	9	
170	0,31	0,0558	2,01	0,03	0,005	0,0048	0,68	1,174	1,5651	0,288	1,477	0	0	0,01931	0,0195	0,41341	11	
171	0,31	0,0558	2,01	0,03	0,005	0,0048	0,68	1,174	1,5651	0,288	1,477	0	0	0	0,0195	0,41341	11	
172	0,31	0,0558	2,01	0,03	0,005	0,0048	0,68	1,174	1,5651	0,288	1,477	0	0	0	0	0,41341	11	
173	0,31	0,0558	2,01	0,03	0,005	0,0048	0,68	1,174	1,5651	0,288	1,477	0	0	0	0	0	11	
174	0	0,0558	2,01	0,03	0,005	0,0048	0,68	1,174	1,5651	0,288	1,477	0	0	0	0	0	11	
175	0	0	2,01	0,03	0,005	0,0048	0,68	1,174	1,5651	0,288	1,477	0	0	0	0	0	11	
176	0	0	0	0,03	0,005	0,0048	0,68	1,174	1,5651	0,288	1,477	0	0	0	0	0	11	
177	0	0	0	0	0	0,005	0,0048	0,68	1,174	1,5651	0,288	1,477	0	0	0	0	0	11
178	0	0	0	0	0	0	0,0048	0,68	1,174	1,5651	0,288	1,477	0	0	0	0	0	11
179	0	0	0	0	0	0	0,68	1,174	1,5651	0,288	1,477	0	0	0	0	0	11	
180	0	0	0	0	0	0	0	0	1,174	1,5651	0,288	1,477	0	0	0	0	0	11
181	0	0	0	0	0	0	0	0	0	1,5651	0,288	1,477	0	0	0	0	0	11
182	0	0	0	0	0	0	0	0	0	0	0,288	1,477	0	0	0	0	0	11
183	0	0	0	0	0	0	0	0	0	0	0	1,477	0	0	0	0	0	11

184	0,31	0,0558	2,01	0,03	0,005	0,0048	0,68	1,174	1,5651	0,288	1,477	0,56148	0	0,01931	0,0195	0,41341	9	
185	0,31	0,0558	2,01	0,03	0,005	0,0048	0,68	1,174	1,5651	0,288	1,477	0,56148	0	0	0,0195	0,41341	9	
186	0,31	0,0558	2,01	0,03	0,005	0,0048	0,68	1,174	1,5651	0,288	1,477	0,56148	0	0	0	0,41341	9	
187	0,31	0,0558	2,01	0,03	0,005	0,0048	0,68	1,174	1,5651	0,288	1,477	0,56148	0	0	0	0	9	
188	0	0,0558	2,01	0,03	0,005	0,0048	0,68	1,174	1,5651	0,288	1,477	0,56148	0	0	0	0	10	
189	0	0	2,01	0,03	0,005	0,0048	0,68	1,174	1,5651	0,288	1,477	0,56148	0	0	0	0	10	
190	0	0	0	0,03	0,005	0,0048	0,68	1,174	1,5651	0,288	1,477	0,56148	0	0	0	0	10	
191	0	0	0	0	0,005	0,0048	0,68	1,174	1,5651	0,288	1,477	0,56148	0	0	0	0	9,51769	
192	0	0	0	0	0	0,0048	0,68	1,174	1,5651	0,288	1,477	0,56148	0	0	0	0	9,51769	
193	0	0	0	0	0	0	0,68	1,174	1,5651	0,288	1,477	0,56148	0	0	0	0	9,51769	
194	0	0	0	0	0	0	0	0,174	1,5651	0,288	1,477	0,56148	0	0	0	0	9,51769	
195	0	0	0	0	0	0	0	0	0,174	1,5651	0,288	1,477	0,56148	0	0	0	0	9,51769
196	0	0	0	0	0	0	0	0	0	0,288	1,477	0,56148	0	0	0	0	9,51769	
197	0	0	0	0	0	0	0	0	0	0	1,477	0,56148	0	0	0	0	9,51769	
198	0	0	0	0	0	0	0	0	0	0	0	0,56148	0	0	0	0	9,51769	
199	0,31	0,0558	2,01	0,03	0,005	0,0048	0,68	1,174	1,5651	0,288	1,477	0,56148	0,51795	0	0,0195	0,41341	8	
200	0,31	0,0558	2,01	0,03	0,005	0,0048	0,68	1,174	1,5651	0,288	1,477	0,56148	0,51795	0	0	0,41341	8	
201	0,31	0,0558	2,01	0,03	0,005	0,0048	0,68	1,174	1,5651	0,288	1,477	0,56148	0,51795	0	0	0	0	8
202	0	0,0558	2,01	0,03	0,005	0,0048	0,68	1,174	1,5651	0,288	1,477	0,56148	0,51795	0	0	0	0	8
203	0	0	2,01	0,03	0,005	0,0048	0,68	1,174	1,5651	0,288	1,477	0,56148	0,51795	0	0	0	0	8
204	0	0	0	0,03	0,005	0,0048	0,68	1,174	1,5651	0,288	1,477	0,56148	0,51795	0	0	0	0	8
205	0	0	0	0	0,005	0,0048	0,68	1,174	1,5651	0,288	1,477	0,56148	0,51795	0	0	0	0	8
206	0	0	0	0	0	0,0048	0,68	1,174	1,5651	0,288	1,477	0,56148	0,51795	0	0	0	0	8
207	0	0	0	0	0	0	0,68	1,174	1,5651	0,288	1,477	0,56148	0,51795	0	0	0	0	8
208	0	0	0	0	0	0	0	1,174	1,5651	0,288	1,477	0,56148	0,51795	0	0	0	0	8
209	0	0	0	0	0	0	0	0	1,5651	0,288	1,477	0,56148	0,51795	0	0	0	0	8
210	0	0	0	0	0	0	0	0	0	0,288	1,477	0,56148	0,51795	0	0	0	0	8
211	0	0	0	0	0	0	0	0	0	0	1,477	0,56148	0,51795	0	0	0	0	8
212	0	0	0	0	0	0	0	0	0	0	0	0,56148	0,51795	0	0	0	0	8
213	0	0	0	0	0	0	0	0	0	0	0	0	0,51795	0	0	0	0	9
214	0,31	0,0558	2,01	0,03	0,005	0,0048	0,68	1,174	1,5651	0,288	1,477	0,56148	0,51795	0,01931	0	0,41341	8	
215	0,31	0,0558	2,01	0,03	0,005	0,0048	0,68	1,174	1,5651	0,288	1,477	0,56148	0,51795	0,01931	0	0	0	8
216	0	0,0558	2,01	0,03	0,005	0,0048	0,68	1,174	1,5651	0,288	1,477	0,56148	0,51795	0,01931	0	0	0	8
217	0	0	2,01	0,03	0,005	0,0048	0,68	1,174	1,5651	0,288	1,477	0,56148	0,51795	0,01931	0	0	0	8
218	0	0	0	0,03	0,005	0,0048	0,68	1,174	1,5651	0,288	1,477	0,56148	0,51795	0,01931	0	0	0	8
219	0	0	0	0	0,005	0,0048	0,68	1,174	1,5651	0,288	1,477	0,56148	0,51795	0,01931	0	0	0	8
220	0	0	0	0	0	0,0048	0,68	1,174	1,5651	0,288	1,477	0,56148	0,51795	0,01931	0	0	0	8
221	0	0	0	0	0	0	0,68	1,174	1,5651	0,288	1,477	0,56148	0,51795	0,01931	0	0	0	8
222	0	0	0	0	0	0	0	1,174	1,5651	0,288	1,477	0,56148	0,51795	0,01931	0	0	0	8
223	0	0	0	0	0	0	0	0	1,5651	0,288	1,477	0,56148	0,51795	0,01931	0	0	0	8
224	0	0	0	0	0	0	0	0	0	0,288	1,477	0,56148	0,51795	0,01931	0	0	0	8
225	0	0	0	0	0	0	0	0	0	0	1,477	0,56148	0,51795	0,01931	0	0	0	8
226	0	0	0	0	0	0	0	0	0	0	0	0,56148	0,51795	0,01931	0	0	0	8
227	0	0	0	0	0	0	0	0	0	0	0	0	0,51795	0,01931	0	0	0	9
228	0	0	0	0	0	0	0	0	0	0	0	0	0	0,01931	0	0	0	11

229	0,31	0,0558	2,01	0,03	0,005	0,0048	0,68	1,174	1,5651	0,288	1,477	0,56148	0,51795	0,01931	0,0195	0	8
230	0	0,0558	2,01	0,03	0,005	0,0048	0,68	1,174	1,5651	0,288	1,477	0,56148	0,51795	0,01931	0,0195	0	8
231	0	0	2,01	0,03	0,005	0,0048	0,68	1,174	1,5651	0,288	1,477	0,56148	0,51795	0,01931	0,0195	0	8
232	0	0	0	0,03	0,005	0,0048	0,68	1,174	1,5651	0,288	1,477	0,56148	0,51795	0,01931	0,0195	0	8
233	0	0	0	0	0,005	0,0048	0,68	1,174	1,5651	0,288	1,477	0,56148	0,51795	0,01931	0,0195	0	8
234	0	0	0	0	0	0,0048	0,68	1,174	1,5651	0,288	1,477	0,56148	0,51795	0,01931	0,0195	0	8
235	0	0	0	0	0	0	0,68	1,174	1,5651	0,288	1,477	0,56148	0,51795	0,01931	0,0195	0	8
236	0	0	0	0	0	0	0	1,174	1,5651	0,288	1,477	0,56148	0,51795	0,01931	0,0195	0	8
237	0	0	0	0	0	0	0	0	1,5651	0,288	1,477	0,56148	0,51795	0,01931	0,0195	0	8
238	0	0	0	0	0	0	0	0	0	0,288	1,477	0,56148	0,51795	0,01931	0,0195	0	8
239	0	0	0	0	0	0	0	0	0	0	1,477	0,56148	0,51795	0,01931	0,0195	0	8
240	0	0	0	0	0	0	0	0	0	0	0	0,56148	0,51795	0,01931	0,0195	0	8
241	0	0	0	0	0	0	0	0	0	0	0	0	0,51795	0,01931	0,0195	0	9
242	0	0	0	0	0	0	0	0	0	0	0	0	0	0,01931	0,0195	0	11
243	0	0	0	0	0	0	0	0	0	0	0	0	0	0	0,0195	0	11

Appendix F.1.3 Effect on energy generation

When the optimum is executed, it has an effect on the annual energy generation in the Mekong Basin. In Figure 67 is shown that the reduction in energy generation is less in the Brune Model than in the Defined TE model due to less dams being cancelled.

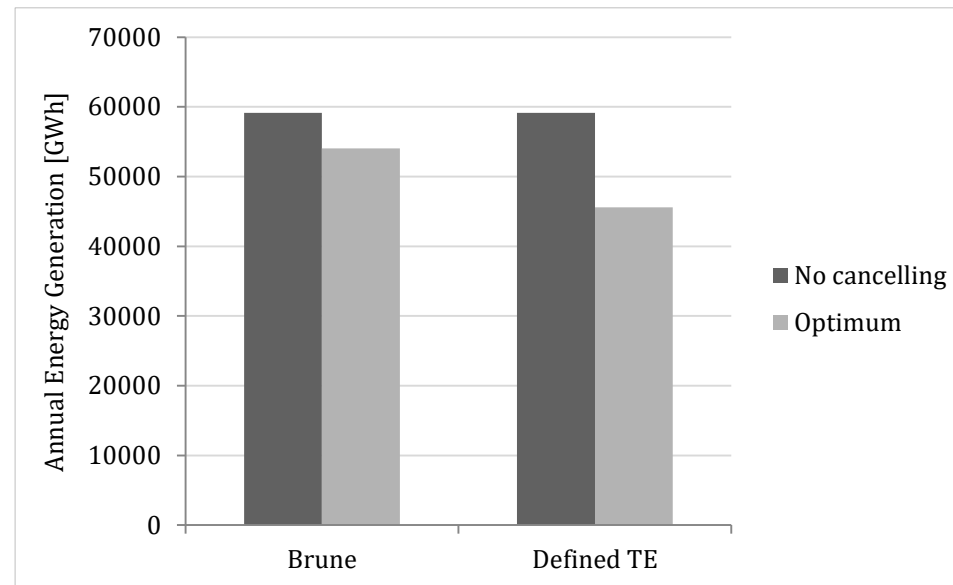


Figure 67: Change in annual energy generation caused by the cancelling of the dams (optimum)

Appendix F.2 Sluicing dams

Appendix F.2.1 Effectiveness of sluicing

The general information of the dams with a higher trapping efficiency for both models is given in Table 14 and Table 15.

Table 14: Overview of dams in which more than 1% of the SL is trapped for the Brune model

Dam Project	Trapped sediment [%]	Volume [km3]	Area [km2]	Depth [m]	Length [km]	Average width [m]	Cross section area [km2]
Nam Tha 1	1	1	64	15	100	75	1118
Mekong at Pakbeng	9	2	87	20	145	250	4993
Mekong at Luangprabang	6	2	90	18	140	465	8212
Mekong at Xayabuly	1	1	49	15	150	460	6816
Mekong at Ban Kum	3	2	133	16	100	560	8884
Mekong at Don sahong	1	0	3	86	5	245	21121
Mekong at Latsua (Phou Ngoy)	4	0	13	14	12	1000	13846
Lower Se San 2	1	2	75	24	30	600	14340
Lower Sre Pok 3 (3A)	2	6	721	8	55	350	2846

Table 15: Overview of dams in which more than 1% of the SL is trapped for the Defined TE model

Dam Project	Trapped sediment [%]	Volume [km3]	Area [km2]	Depth [m]	Length [km]	Average width [m]	Cross section area [km2]
Mekong at Pakbeng	9	2	87	20	145	250	4993
Mekong at Luangprabang	5	2	90	18	140	465	8212
Mekong at Xayabuly	4	1	49	15	150	460	6816
Mekong at Paklay	2	1	108	13	130	450	5630
Mekong at Sanakham	2	0	94	3	150	400	1200
Pak Mun	1	0	60	4	150	400	1500
Mekong at Ban Kum	3	2	133	16	100	560	8884
Mekong at Don sahong	2	0	3	86	5	245	21121
Mekong at Latsua (Phou Ngoy)	2	0	13	14	12	1000	13846
Stung Treng	1	1	211	3	13	1000	3169
Lower Se San 2	2	2	75	24	30	600	14340
Lower Sre Pok 3 (3A)	2	6	721	8	55	350	2846

The data for the calculation of the Stokes Settling Velocity and its outcomes for silt and clay are given in Table 16.

Table 16: Information for calculation of Stokes Settling Velocity

Mass density silt [kg/m3]	1400
Mass density water [kg/m3]	997
Dynamic viscosity water [kg/(m*s)]	0,001
Gravitational field strength [m/s2]	9,81
Radius clay [mm]	0,00195
Radius silt [mm]	0,0166
Stokes Settling velocity clay [m/s]	3,33E-06
Stokes Settling velocity silt [m/s]	0,00024

Clay

The settling lengths [m] of clay for different months in the different reservoirs are depicted in Table 17 for the Brune model and in Table 18 for the Defined TE model. If the number is in green, this indicates that sluicing can be useful.

Table 17: Settling lengths [m] for clay in different months in the Brune Model. Green means that sluicing can be effective

Dam Project	January	February	March	April	May	June	July	August	September	October	November	December
Nam Tha 1	190755	33459	130278	519281	525682	1197888	1997691	2359252	915676	648954	204569	115275
Mekong at Pakbeng	373554	110134	322820	1330060	1542269	3162855	5587204	6951729	2875649	1680044	423848	243957
Mekong at Luangprabang	12671	3736	10950	45117	52315	107287	189523	235809	97544	56989	14377	8275
Mekong at Xayabuly	7245	8841	24196	52380	99815	211926	287419	351071	193136	92933	12891	6604
Mekong at Ban Kum	30388	70906	293242	379256	1081476	2221433	4687892	3714641	3448423	1414104	280896	79410
Mekong at Don sahong	17001	4313	53435	85726	285348	550887	1019587	866566	886778	358792	110749	15587
Mekong at Latsua (Phou Ngoy)	3648	926	11467	18396	61233	118214	218792	185955	190293	76993	23766	3345
Lower Se San 2	5831	2450	8023	18542	51548	106823	123453	142202	137472	88821	76332	11848
Lower Sre Pok 3 (3A)	31878	13396	43866	101374	281831	584038	674962	777469	751609	485616	417336	64776

Table 18: Settling lengths [m] for clay in different months in the Defined TE Model. Green means that sluicing can be effective

Dam Project	January	February	March	April	May	June	July	August	September	October	November	December
Mekong at Pakbeng	373554	110134	322820	1330060	1542269	3162855	5587204	6951729	2875649	1680044	423848	243957
Mekong at Luangprabang	12671	3736	10950	45117	52315	107287	189523	235809	97544	56989	14377	8275
Mekong at Xayabuly	7245	8841	24196	52380	99815	211926	287419	351071	193136	92933	12891	6604
Mekong at Paklay	6000	7322	20038	43379	82662	175506	238026	290739	159946	76962	10675	5469
Mekong at Sanakham	10440	12740	34866	75479	143832	305382	414167	505889	278307	133915	18575	9517
Pak Mun	65667	82642	490450	697107	1817507	2829479	4371963	4510066	4926958	2191426	313417	59676
Mekong at Ban Kum	30388	70906	293242	379256	1081476	2221433	4687892	3714641	3448423	1414104	280896	79410
Mekong at Don sahong	17001	4313	53435	85726	285348	550887	1019587	866566	886778	358792	110749	15587
Mekong at Latsua (Phou Ngoy)	3648	926	11467	18396	61233	118214	218792	185955	190293	76993	23766	3345
Stung Treng	1164	295	3659	5870	19539	37723	69817	59339	60723	24569	7584	1067
Lower Se San 2	5831	2450	8023	18542	51548	106823	123453	142202	137472	88821	76332	11848
Lower Sre Pok 3 (3A)	31878	13396	43866	101374	281831	584038	674962	777469	751609	485616	417336	64776

Silt

The settling lengths [m] of silt for different months in the different reservoirs are depicted in Table 19 for the Brune model and in Table 20 for the Defined TE model. If the number is in green, this indicates that sluicing can be useful.

Table 19: Settling lengths [m] for silt in different months in the Brune Model. Green means that sluicing can be effective

Dam Project	January	February	March	April	May	June	July	August	September	October	November	December
Nam Tha 1	2632	462	1798	7166	7254	16530	27566	32556	12636	8955	2823	1591
Mekong at Pakbeng	5155	1520	4455	18354	21282	43645	77099	95928	39682	23183	5849	3366
Mekong at Luangprabang	175	52	151	623	722	1480	2615	3254	1346	786	198	114
Mekong at Xayabuly	100	122	334	723	1377	2924	3966	4844	2665	1282	178	91
Mekong at Ban Kum	419	978	4046	5233	14923	30654	64689	51259	47585	19513	3876	1096
Mekong at Don sahong	235	60	737	1183	3938	7602	14069	11958	12237	4951	1528	215
Mekong at Latsua (Phou Ngoy)	50	13	158	254	845	1631	3019	2566	2626	1062	328	46
Lower Se San 2	80	34	111	256	711	1474	1704	1962	1897	1226	1053	163
Lower Sre Pok 3 (3A)	440	185	605	1399	3889	8059	9314	10728	10372	6701	5759	894

Table 20: Settling lengths [m] for silt in different months in the Brune Model. Green means that sluicing can be effective

Dam Project	January	February	March	April	May	June	July	August	September	October	November	December
Mekong at Pakbeng	5155	1520	4455	18354	21282	43645	77099	95928	39682	23183	5849	3366
Mekong at Luangprabang	175	52	151	623	722	1480	2615	3254	1346	786	198	114
Mekong at Xayabuly	100	122	334	723	1377	2924	3966	4844	2665	1282	178	91
Mekong at Paklay	83	101	277	599	1141	2422	3285	4012	2207	1062	147	75
Mekong at Sanakham	144	176	481	1042	1985	4214	5715	6981	3840	1848	256	131
Pak Mun	906	1140	6768	9620	25080	39044	60329	62235	67988	30240	4325	823
Mekong at Ban Kum	419	978	4046	5233	14923	30654	64689	51259	47585	19513	3876	1096
Mekong at Don sahong	235	60	737	1183	3938	7602	14069	11958	12237	4951	1528	215
Mekong at Latsua (Phou Ngoy)	50	13	158	254	845	1631	3019	2566	2626	1062	328	46
Stung Treng	16	4	50	81	270	521	963	819	838	339	105	15
Lower Se San 2	80	34	111	256	711	1474	1704	1962	1897	1226	1053	163
Lower Sre Pok 3 (3A)	440	185	605	1399	3889	8059	9314	10728	10372	6701	5759	894

It was decided that sluicing can only be effect for clay. Therefore, all combinations of dams are tested for sluicing only in June and also the combination of June and May.

F.2.2. Outcomes of analysis

In the tables an overview is given of all possible sluicing options in the Mekong Basin for both models. In the first row the dam names are stated and in the last column the SL at Kratie is given. If a 0 is assigned to a dam, this means that the dam is being sluiced in that particular month. All other values are the active volumes (km^3) of the dams. The optimum is indicated with green.

Brune model

June

Table 21: All sluicing options in June for the Brune model and their corresponding SL at Kratie. The optimum is given in green

Option	Nam Tha 1	Mekong at Ban Kum	Mekong at Don sahong	Mekong at Latsua (Phou Ngoy)	Lower Se San 2	Lower Sre Pok 3 (3A)	SL [Mt]
1	0,94	0,65	0,77	0,94	0,93	0,94	4
2	0,00	0,00	0,00	0,00	0,00	0,00	5
3	0,00	0,65	0,77	0,94	0,93	0,94	4
4	0,00	0,00	0,77	0,94	0,93	0,94	4
5	0,00	0,00	0,00	0,94	0,93	0,94	4
6	0,00	0,00	0,00	0,00	0,93	0,94	5
7	0,00	0,00	0,00	0,00	0,00	0,94	5
8	0,94	0,00	0,77	0,94	0,93	0,94	4
9	0,94	0,00	0,00	0,94	0,93	0,94	4
10	0,94	0,00	0,00	0,00	0,93	0,94	5
11	0,94	0,00	0,00	0,00	0,00	0,94	5
12	0,94	0,00	0,00	0,00	0,00	0,00	5
13	0,94	0,65	0,00	0,94	0,93	0,94	4
14	0,94	0,65	0,00	0,00	0,93	0,94	5
15	0,94	0,65	0,00	0,00	0,00	0,94	5
16	0,94	0,65	0,00	0,00	0,00	0,00	5
17	0,00	0,65	0,00	0,00	0,00	0,00	5
18	0,94	0,65	0,77	0,00	0,93	0,94	4
19	0,94	0,65	0,77	0,00	0,00	0,94	5
20	0,94	0,65	0,77	0,00	0,00	0,00	5
21	0,00	0,65	0,77	0,00	0,00	0,00	5
22	0,00	0,00	0,77	0,00	0,00	0,00	5
23	0,94	0,65	0,77	0,94	0,00	0,94	5
24	0,94	0,65	0,77	0,94	0,00	0,00	5
25	0,00	0,65	0,77	0,94	0,00	0,00	5
26	0,00	0,00	0,77	0,94	0,00	0,00	5
27	0,00	0,00	0,00	0,94	0,00	0,00	5
28	0,94	0,65	0,77	0,94	0,93	0,00	4
29	0,00	0,65	0,77	0,94	0,93	0,00	4
30	0,00	0,00	0,77	0,94	0,93	0,00	4
31	0,00	0,00	0,00	0,94	0,93	0,00	5
32	0,00	0,00	0,00	0,00	0,93	0,00	5

May and June

Table 22: All sluicing options in May and June for the Brune model and their corresponding SL at Kratie. The optimum is given in green.

39	0,94	0,85	0,94	0,94	0,00	0,65	0,77	0,94	0,93	0,94	4
40	0,94	0,85	0,94	0,94	0,00	0,00	0,77	0,94	0,93	0,94	4
41	0,94	0,85	0,94	0,94	0,00	0,00	0,00	0,94	0,93	0,94	4
42	0,94	0,85	0,94	0,94	0,00	0,00	0,00	0,00	0,93	0,94	5
43	0,94	0,85	0,94	0,94	0,00	0,00	0,00	0,00	0,00	0,94	5
44	0,94	0,85	0,94	0,94	0,00	0,00	0,00	0,00	0,00	0,00	5
45	0,00	0,85	0,94	0,94	0,00	0,00	0,00	0,00	0,00	0,00	5
46	0,00	0,00	0,94	0,94	0,00	0,00	0,00	0,00	0,00	0,00	5
47	0,00	0,00	0,00	0,94	0,00	0,00	0,00	0,00	0,00	0,00	5
48	0,94	0,85	0,94	0,94	0,94	0,00	0,77	0,94	0,93	0,94	4
49	0,94	0,85	0,94	0,94	0,94	0,00	0,00	0,94	0,93	0,94	4
50	0,94	0,85	0,94	0,94	0,94	0,00	0,00	0,00	0,93	0,94	5
51	0,94	0,85	0,94	0,94	0,94	0,00	0,00	0,00	0,00	0,94	5
52	0,94	0,85	0,94	0,94	0,94	0,00	0,00	0,00	0,00	0,00	5
53	0,00	0,85	0,94	0,94	0,94	0,00	0,00	0,00	0,00	0,00	5
54	0,00	0,00	0,94	0,94	0,94	0,00	0,00	0,00	0,00	0,00	5
55	0,00	0,00	0,00	0,94	0,94	0,00	0,00	0,00	0,00	0,00	5
56	0,00	0,00	0,00	0,00	0,94	0,00	0,00	0,00	0,00	0,00	6
57	0,94	0,85	0,94	0,94	0,94	0,65	0,00	0,94	0,93	0,94	4
58	0,94	0,85	0,94	0,94	0,94	0,65	0,00	0,00	0,93	0,94	5
59	0,94	0,85	0,94	0,94	0,94	0,65	0,00	0,00	0,00	0,94	5
60	0,94	0,85	0,94	0,94	0,94	0,65	0,00	0,00	0,00	0,00	5
61	0,00	0,85	0,94	0,94	0,94	0,65	0,00	0,00	0,00	0,00	5
62	0,00	0,00	0,94	0,94	0,94	0,65	0,00	0,00	0,00	0,00	5
63	0,00	0,00	0,00	0,94	0,94	0,65	0,00	0,00	0,00	0,00	5
64	0,00	0,00	0,00	0,00	0,94	0,65	0,00	0,00	0,00	0,00	5
65	0,00	0,00	0,00	0,00	0,00	0,65	0,00	0,00	0,00	0,00	5
66	0,94	0,85	0,94	0,94	0,94	0,65	0,77	0,00	0,93	0,94	4
67	0,94	0,85	0,94	0,94	0,94	0,65	0,77	0,00	0,00	0,94	5
68	0,94	0,85	0,94	0,94	0,94	0,65	0,77	0,00	0,00	0,00	5
69	0,00	0,85	0,94	0,94	0,94	0,65	0,77	0,00	0,00	0,00	5
70	0,00	0,00	0,94	0,94	0,94	0,65	0,77	0,00	0,00	0,00	5
71	0,00	0,00	0,00	0,94	0,94	0,65	0,77	0,00	0,00	0,00	5
72	0,00	0,00	0,00	0,00	0,94	0,65	0,77	0,00	0,00	0,00	5
73	0,00	0,00	0,00	0,00	0,00	0,65	0,77	0,00	0,00	0,00	5
74	0,00	0,00	0,00	0,00	0,00	0,00	0,00	0,77	0,00	0,00	5

75	0,94	0,85	0,94	0,94	0,94	0,65	0,77	0,94	0,00	0,94	5
76	0,94	0,85	0,94	0,94	0,94	0,65	0,77	0,94	0,00	0,00	5
77	0,00	0,85	0,94	0,94	0,94	0,65	0,77	0,94	0,00	0,00	5
78	0,00	0,00	0,94	0,94	0,94	0,65	0,77	0,94	0,00	0,00	5
79	0,00	0,00	0,00	0,94	0,94	0,65	0,77	0,94	0,00	0,00	5
80	0,00	0,00	0,00	0,00	0,94	0,65	0,77	0,94	0,00	0,00	5
81	0,00	0,00	0,00	0,00	0,00	0,65	0,77	0,94	0,00	0,00	5
82	0,00	0,00	0,00	0,00	0,00	0,00	0,77	0,94	0,00	0,00	5
83	0,00	0,00	0,00	0,00	0,00	0,00	0,00	0,94	0,00	0,00	5
84	0,94	0,85	0,94	0,94	0,94	0,65	0,77	0,94	0,93	0,00	4
85	0,94	0,85	0,94	0,94	0,94	0,65	0,77	0,94	0,93	0,00	4
86	0,94	0,00	0,94	0,94	0,94	0,65	0,77	0,94	0,93	0,00	4
87	0,94	0,00	0,00	0,94	0,94	0,65	0,77	0,94	0,93	0,00	5
88	0,94	0,00	0,00	0,00	0,94	0,65	0,77	0,94	0,93	0,00	5
89	0,94	0,00	0,00	0,00	0,00	0,65	0,77	0,94	0,93	0,00	5
90	0,94	0,00	0,00	0,00	0,00	0,00	0,77	0,94	0,93	0,00	5
91	0,94	0,00	0,00	0,00	0,00	0,00	0,00	0,94	0,93	0,00	5
92	0,00	0,00	0,00	0,00	0,00	0,00	0,00	0,00	0,93	0,00	5

Defined TE model

June

Table 23: All sluicing options in June for the Defined TE model and their corresponding SL at Kratie. The optima are given in green

Option	Mekong at Paklay	Pak Mun	Mekong at Ban Kum	Mekong at Don sahong	Mekong at Latsua (Phou Ngoy)	Stung Treng	Lower Se San 2	Lower Sre Pok 3 (3A)	SL [Mt]
1		0,4	0,6		0,4		0,4	0,6	0,6 8
2		0	0	0	0	0	0	0	0 10
3		0	0,6	0,4	0,4	0,4	0,6	0,6	8
4		0	0	0,4	0,4	0,4	0,6	0,6	8
5		0	0	0	0,4	0,4	0,6	0,6	8
6		0	0	0	0	0,4	0,6	0,6	8
7		0	0	0	0	0	0,4	0,6	0,6 9
8		0	0	0	0	0	0	0,6	0,6 10
9		0	0	0	0	0	0	0	0,6 10
10	0,4	0		0,4	0,4	0,4	0,6	0,6	0,6 8
11	0,4	0		0	0,4	0,4	0,6	0,6	0,6 8
12	0,4	0		0	0	0,4	0,6	0,6	0,6 8
13	0,4	0		0	0	0	0,6	0,6	0,6 9
14	0,4	0	0	0	0	0	0,6	0,6	0,6 10
15	0,4	0		0	0	0	0	0	0,6 10
16	0,4	0		0	0	0	0	0	0 10
17	0,4	0,6	0		0,4	0,4	0,6	0,6	0,6 8
18	0,4	0,6	0		0	0,4	0,6	0,6	0,6 8
19	0,4	0,6	0		0	0	0,6	0,6	0,6 9
20	0,4	0,6	0		0	0	0	0,6	0,6 9
21	0,4	0,6	0		0	0	0	0	0,6 10
22	0,4	0,6	0		0	0	0	0	0 10
23	0	0,6	0		0	0	0	0	0 10
24	0,4	0,6	0,4		0	0,4	0,6	0,6	0,6 8
25	0,4	0,6	0,4		0	0	0,6	0,6	0,6 9
26	0,4	0,6	0,4		0	0	0	0,6	0,6 9
27	0,4	0,6	0,4		0	0	0	0	0,6 9
28	0,4	0,6	0,4		0	0	0	0	0 10
29	0	0,6	0,4		0	0	0	0	0 10
30	0	0	0,4		0	0	0	0	0 10
31	0,4	0,6	0,4		0,4	0	0,6	0,6	0,6 8
32	0,4	0,6	0,4		0,4	0	0	0,6	0,6 8
33	0,4	0,6	0,4		0,4	0	0	0	0,6 9
34	0,4	0,6	0,4		0,4	0	0	0	0 9
35	0	0,6	0,4		0,4	0	0	0	0 9
36	0	0	0,4		0,4	0	0	0	0 9
37	0	0	0		0,4	0	0	0	0 10
38	0,4	0,6	0,4		0,4	0,4	0,6	0,6	0,6 8
39	0,4	0,6	0,4		0,4	0,4	0	0	0,6 8
40	0,4	0,6	0,4		0,4	0,4	0	0	0 9
41	0	0,6	0,4		0,4	0,4	0	0	0 9
42	0	0	0,4		0,4	0,4	0	0	0 9
43	0	0	0		0,4	0,4	0	0	0 9
44	0	0	0		0	0,4	0	0	0 10

45	0,4	0,6	0,4	0,4		0,4	0,4	0		0,6	8
46	0,4	0,6	0,4	0,4		0,4	0,4	0		0	9
47	0	0,6	0,4	0,4		0,4	0,4	0		0	9
48	0	0	0,4	0,4		0,4	0,4	0		0	9
49	0	0	0	0,4		0,4	0,4	0		0	9
50	0	0	0	0		0,4	0,4	0		0	9
51	0	0	0	0		0	0,4	0		0	10
52	0,4	0,6	0,4	0,4		0,4	0,4	0,6		0	8
53	0	0,6	0,4	0,4		0,4	0,4	0,6		0	8
54	0	0	0,4	0,4		0,4	0,4	0,6		0	8
55	0	0	0	0,4		0,4	0,4	0,6		0	8
56	0	0	0	0		0,4	0,4	0,6		0	9
57	0	0	0	0		0	0,4	0,6		0	9
58	0	0	0	0		0	0	0,6		0	10

May and June

Table 24: All sluicing options in May and June for the Defined TE model and their corresponding SL at Kratie. The optimum is given in green.

51	0,9	0,7	0,7	0,9	0,9	0	0,6	0,4	0,4	0,4	0,4	0,4	0,6	0,6	8
52	0,9	0,7	0,7	0,9	0,9	0	0	0,4	0,4	0,4	0,4	0,4	0,6	0,6	8
53	0,9	0,7	0,7	0,9	0,9	0	0	0	0,4	0,4	0,4	0,4	0,6	0,6	8
54	0,9	0,7	0,7	0,9	0,9	0	0	0	0	0,4	0,4	0,4	0,6	0,6	8
55	0,9	0,7	0,7	0,9	0,9	0	0	0	0	0	0,4	0,4	0,6	0,6	9
56	0,9	0,7	0,7	0,9	0,9	0	0	0	0	0	0	0	0,6	0,6	10
57	0,9	0,7	0,7	0,9	0,9	0	0	0	0	0	0	0	0	0,6	10
58	0,9	0,7	0,7	0,9	0,9	0	0	0	0	0	0	0	0	0	10
59	0	0,7	0,7	0,9	0,9	0	0	0	0	0	0	0	0	0	10
60	0	0	0,7	0,9	0,9	0	0	0	0	0	0	0	0	0	11
61	0	0	0	0,9	0,9	0	0	0	0	0	0	0	0	0	11
62	0	0	0	0	0,9	0	0	0	0	0	0	0	0	0	11
63	0,9	0,7	0,7	0,9	0,9	0,4	0	0,4	0,4	0,4	0,4	0,4	0,6	0,6	8
64	0,9	0,7	0,7	0,9	0,9	0,4	0	0	0,4	0,4	0,4	0,4	0,6	0,6	8
65	0,9	0,7	0,7	0,9	0,9	0,4	0	0	0	0,4	0,4	0,4	0,6	0,6	8
66	0,9	0,7	0,7	0,9	0,9	0,4	0	0	0	0	0	0,4	0,6	0,6	9
67	0,9	0,7	0,7	0,9	0,9	0,4	0	0	0	0	0	0	0,6	0,6	9
68	0,9	0,7	0,7	0,9	0,9	0,4	0	0	0	0	0	0	0	0,6	9
69	0,9	0,7	0,7	0,9	0,9	0,4	0	0	0	0	0	0	0	0	9
70	0	0,7	0,7	0,9	0,9	0,4	0	0	0	0	0	0	0	0	10
71	0	0	0,7	0,9	0,9	0,4	0	0	0	0	0	0	0	0	10
72	0	0	0	0,9	0,9	0,4	0	0	0	0	0	0	0	0	11
73	0	0	0	0	0,9	0,4	0	0	0	0	0	0	0	0	11
74	0	0	0	0	0	0,4	0	0	0	0	0	0	0	0	11
75	0,9	0,7	0,7	0,9	0,9	0,4	0,6	0	0,4	0,4	0,4	0,4	0,6	0,6	8
76	0,9	0,7	0,7	0,9	0,9	0,4	0,6	0	0	0,4	0,4	0,4	0,6	0,6	8
77	0,9	0,7	0,7	0,9	0,9	0,4	0,6	0	0	0	0	0,4	0,6	0,6	9
78	0,9	0,7	0,7	0,9	0,9	0,4	0,6	0	0	0	0	0	0,6	0,6	9
79	0,9	0,7	0,7	0,9	0,9	0,4	0,6	0	0	0	0	0	0	0,6	10
80	0,9	0,7	0,7	0,9	0,9	0,4	0,6	0	0	0	0	0	0	0	10
81	0	0,7	0,7	0,9	0,9	0,4	0,6	0	0	0	0	0	0	0	10
82	0	0	0,7	0,9	0,9	0,4	0,6	0	0	0	0	0	0	0	10
83	0	0	0	0,9	0,9	0,4	0,6	0	0	0	0	0	0	0	10
84	0	0	0	0	0,9	0,4	0,6	0	0	0	0	0	0	0	10
85	0	0	0	0	0	0,4	0,6	0	0	0	0	0	0	0	11
86	0	0	0	0	0	0	0,6	0	0	0	0	0	0	0	11
87	0,9	0,7	0,7	0,9	0,9	0,4	0,6	0,4	0	0,4	0,4	0,4	0,6	0,6	8
88	0,9	0,7	0,7	0,9	0,9	0,4	0,6	0,4	0	0	0,4	0,4	0,6	0,6	8
89	0,9	0,7	0,7	0,9	0,9	0,4	0,6	0,4	0	0	0	0	0,6	0,6	9
90	0,9	0,7	0,7	0,9	0,9	0,4	0,6	0,4	0	0	0	0	0	0,6	9
91	0,9	0,7	0,7	0,9	0,9	0,4	0,6	0,4	0	0	0	0	0	0	10
92	0	0,7	0,7	0,9	0,9	0,4	0,6	0,4	0	0	0	0	0	0	10
93	0	0	0,7	0,9	0,9	0,4	0,6	0,4	0	0	0	0	0	0	10
94	0	0	0	0,9	0,9	0,4	0,6	0,4	0	0	0	0	0	0	10
95	0	0	0	0	0,9	0,4	0,6	0,4	0	0	0	0	0	0	10
96	0	0	0	0	0	0,4	0,6	0,4	0	0	0	0	0	0	10
97	0	0	0	0	0	0	0,6	0,4	0	0	0	0	0	0	10
98	0	0	0	0	0	0	0	0,4	0	0	0	0	0	0	11

99	0,9	0,7	0,7	0,9	0,9	0,4	0,6	0,4	0,4	0	0,4	0,6	0,6	8	
100	0,9	0,7	0,7	0,9	0,9	0,4	0,6	0,4	0,4	0	0	0,6	0,6	8	
101	0,9	0,7	0,7	0,9	0,9	0,4	0,6	0,4	0,4	0	0	0	0,6	9	
102	0,9	0,7	0,7	0,9	0,9	0,4	0,6	0,4	0,4	0	0	0	0	9	
103	0	0,7	0,7	0,9	0,9	0,4	0,6	0,4	0,4	0	0	0	0	9	
104	0	0	0,7	0,9	0,9	0,4	0,6	0,4	0,4	0	0	0	0	9	
105	0	0	0	0,9	0,9	0,4	0,6	0,4	0,4	0	0	0	0	9	
106	0	0	0	0	0,9	0,4	0,6	0,4	0,4	0	0	0	0	9	
107	0	0	0	0	0	0,4	0,6	0,4	0,4	0	0	0	0	10	
108	0	0	0	0	0	0	0,6	0,4	0,4	0	0	0	0	10	
109	0	0	0	0	0	0	0	0,4	0,4	0	0	0	0	10	
110	0	0	0	0	0	0	0	0	0,4	0	0	0	0	11	
111	0,9	0,7	0,7	0,9	0,9	0,4	0,6	0,4	0,4	0,4	0	0,6	0,6	8	
112	0,9	0,7	0,7	0,9	0,9	0,4	0,6	0,4	0,4	0,4	0	0	0,6	8	
113	0,9	0,7	0,7	0,9	0,9	0,4	0,6	0,4	0,4	0,4	0	0	0	9	
114	0	0,7	0,7	0,9	0,9	0,4	0,6	0,4	0,4	0,4	0	0	0	9	
115	0	0	0,7	0,9	0,9	0,4	0,6	0,4	0,4	0,4	0	0	0	9	
116	0	0	0	0,9	0,9	0,4	0,6	0,4	0,4	0,4	0	0	0	9	
117	0	0	0	0	0,9	0,4	0,6	0,4	0,4	0,4	0	0	0	9	
118	0	0	0	0	0	0,4	0,6	0,4	0,4	0,4	0	0	0	9	
119	0	0	0	0	0	0	0,6	0,4	0,4	0,4	0	0	0	9	
120	0	0	0	0	0	0	0	0	0,4	0,4	0	0	0	10	
121	0	0	0	0	0	0	0	0	0	0,4	0,4	0	0	10	
122	0	0	0	0	0	0	0	0	0	0	0,4	0	0	11	
123	0,9	0,7	0,7	0,9	0,9	0,4	0,6	0,4	0,4	0,4	0,4	0	0,6	8	
124	0,9	0,7	0,7	0,9	0,9	0,4	0,6	0,4	0,4	0,4	0,4	0	0	9	
125	0	0,7	0,7	0,9	0,9	0,4	0,6	0,4	0,4	0,4	0,4	0	0	9	
126	0	0	0,7	0,9	0,9	0,4	0,6	0,4	0,4	0,4	0,4	0	0	9	
127	0	0	0	0,9	0,9	0,4	0,6	0,4	0,4	0,4	0,4	0	0	9	
128	0	0	0	0	0,9	0,4	0,6	0,4	0,4	0,4	0,4	0	0	9	
129	0	0	0	0	0	0,4	0,6	0,4	0,4	0,4	0,4	0	0	9	
130	0	0	0	0	0	0	0,6	0,4	0,4	0,4	0,4	0	0	9	
131	0	0	0	0	0	0	0	0	0,4	0,4	0,4	0	0	9	
132	0	0	0	0	0	0	0	0	0	0,4	0,4	0	0	9	
133	0	0	0	0	0	0	0	0	0	0	0,4	0,4	0	10	
134	0	0	0	0	0	0	0	0	0	0	0,4	0	0	11	
135	0,9	0,7	0,7	0,9	0,9	0,4	0,6	0,4	0,4	0,4	0,4	0,6	0	8	
136	0	0,7	0,7	0,9	0,9	0,4	0,6	0,4	0,4	0,4	0,4	0,6	0	8	
137	0	0	0,7	0,9	0,9	0,4	0,6	0,4	0,4	0,4	0,4	0,6	0	8	
138	0	0	0	0,9	0,9	0,4	0,6	0,4	0,4	0,4	0,4	0,6	0	8	
139	0	0	0	0	0,9	0,4	0,6	0,4	0,4	0,4	0,4	0,6	0	8	
140	0	0	0	0	0	0,4	0,6	0,4	0,4	0,4	0,4	0,6	0	9	
141	0	0	0	0	0	0	0,6	0,4	0,4	0,4	0,4	0,6	0	9	
142	0	0	0	0	0	0	0	0,4	0,4	0,4	0,4	0,6	0	9	
143	0	0	0	0	0	0	0	0	0,4	0,4	0,4	0,6	0	9	
144	0	0	0	0	0	0	0	0	0	0	0,4	0,4	0,6	0	9
145	0	0	0	0	0	0	0	0	0	0	0,4	0,6	0	10	
146	0	0	0	0	0	0	0	0	0	0	0	0,6	0	11	

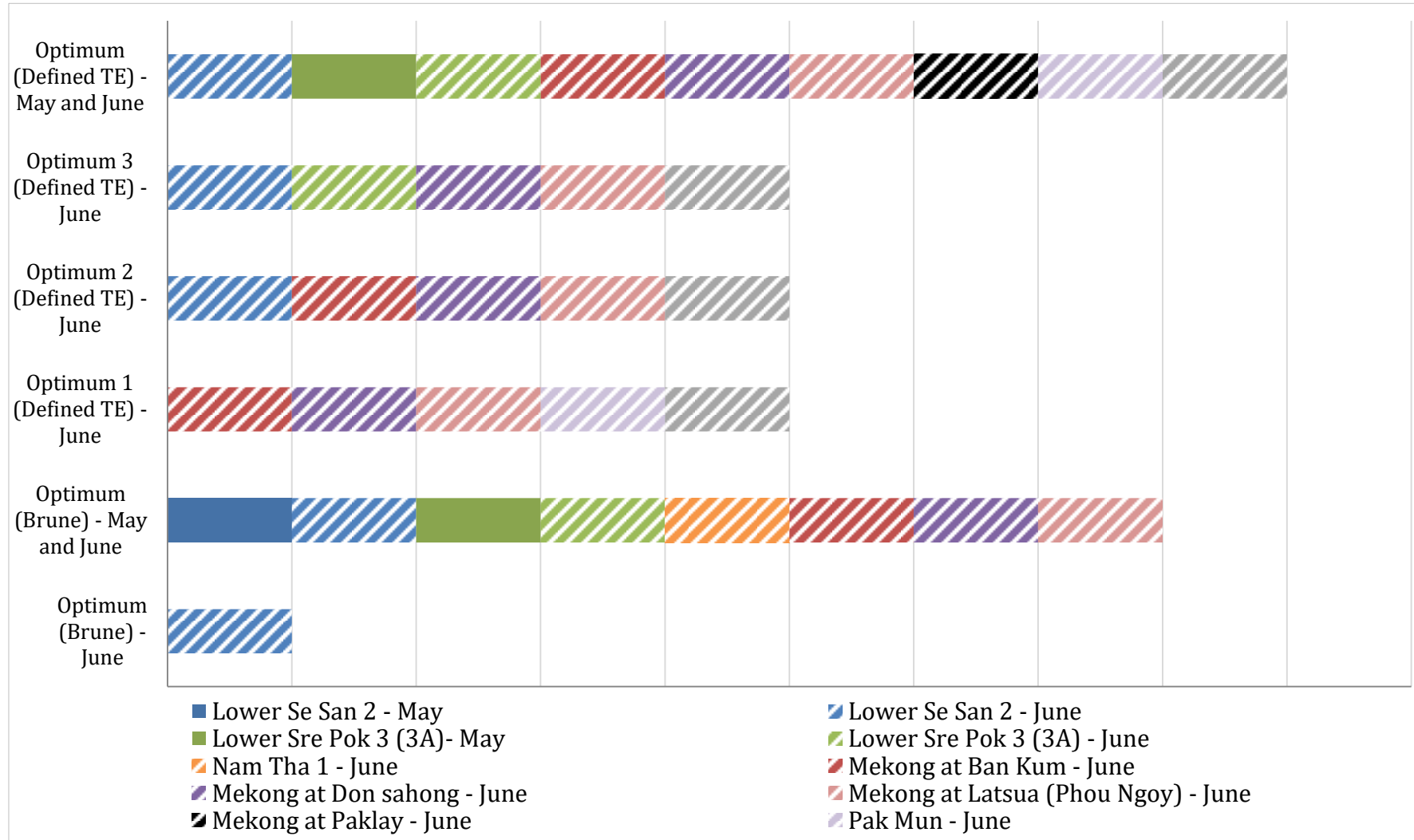


Figure 69: Overview of all optima for the different sluicing months and models

Appendix G. Threshold of motion

The forces acting on a sediment grain are gravity force (G), net flow force (F) resulting from drag (F_{drag}) and lift forces (F_{lift}) and reaction forces of surrounding grains (Figure 70) (Blom, 2021). The initiation of motion of a particle can be calculated by the non-dimensional Shields stress number (θ) which is related to the flow force and the gravity force.

$$F = \tau_b D^2 \quad (\text{G.1})$$

$$G = (\rho_s - \rho)gD^3 \quad (\text{G.2})$$

$$\theta = \frac{\tau_b}{(\rho_s - \rho)gD} \quad (\text{G.3})$$

$$\tau_{bc} = (\rho_s - \rho)gD\theta_c \quad (\text{G.4})$$

F	Net flow force [N]	ρ_s	Density of particle [kg/m^3]
τ_b	Bed shear stress [N/m^2]	ρ	Density of water [kg/m^3]
τ_{bc}	Critical bed shear stress [N/m^2]	g	Gravitational acceleration [m/s^2]
D	Diameter of sediment [m]	θ	Shields stress number [-]
G	Gravitational force [N]	θ_c	Critical Shields stress number [-]

A minimum Shields stress, also known as the critical Shields stress (θ_c), is required to move a particle. This means that for $\theta < \theta_c$ there will be no sediment transport and for $\theta > \theta_c$ there will be (Blom, 2021). When $\theta = \theta_c$, the channel will likely be in equilibrium (VT Agency of Natural Resources, 2004). The critical Shields stress can be assumed to be constant, so the critical bed shear stress increases linearly with the sediment diameter (Figure 70). In other words, coarser grains are harder to move as they have more mass.

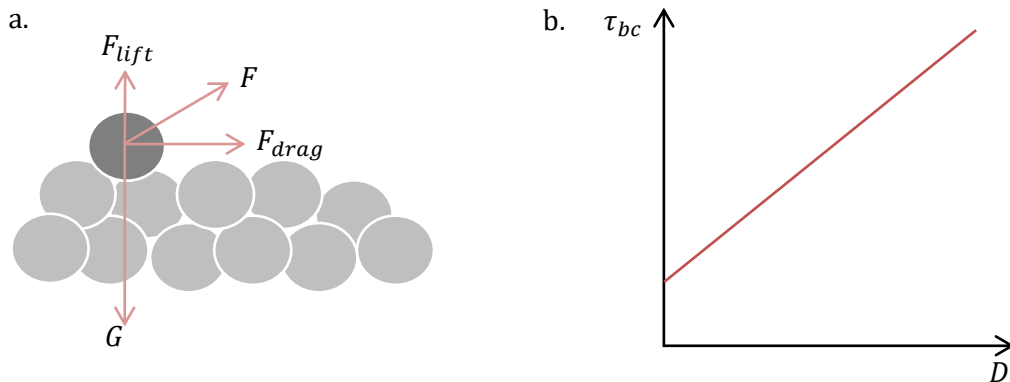


Figure 70: a. Forces acting on a soil particle and b. Relation critical shear stress (τ_{bc}) and sediment diameter (D) (Blom, 2021)